Numerical simulation of forming processes : the use of the Arbitrary-Eulerian-Lagrangian (AEL) formulation and the finite element method

NUMERICAL SIMULATION OF FORMING PROCESSES

The use of the Arbitrary-Eulerian-Lagrangian (AEL) formulation and the finite element method

PIET SCHREURS

DISSERTATIE DRUKKERIJ
wibro
HELMOND
TELEFOON 04920-23981

NUMERICAL SIMULATION OF FORMING PROCESSES

The use of the Arbitrary-Eulerian-Lagrangian (AEL) formulation and the finite element method

NUMERICAL SIMULATION OF FORMING PROCESSES

The use of the Arbitrary-Eulerian-Lagrangian (AEL) formulation and the finite element method

PROEFSCHRIFT

TER VERKRIJGING VAN DE GRAAD VAN DOCTOR IN DE TECHNISCHE WETENSCHAPPEN AAN DE TECHNISCHE HOGESCHOOL EINDHOVEN, OP GEZAG VAN DE RECTOR MAGNIFICUS, PROF. DR. S. T. M. ACKERMANS, VOOR EEN COMMISSIE AANGEWEZEN DOOR HET COLLEGE VAN DEKANEN IN HET OPENBAAR TE VERDEDIGEN OP DINSDAG 25 OKTOBER 1983 TE 14.00 UUR

DOOR

PETRUS JOHANNES GERARDUS SCHREURS

GEBOREN TE MAASTRICHT

Dit proefschrift is goedgekeurd
door de promotoren :

Prof. Dr. Ir. J.D. Janssen
en
Prof. Dr. Ir. D.H. van Campen

Co-promotor : Dr. Ir. F.E. Veldpaus

At first it seemed to them that although they walked and stumbled until they were weary, they were creeping forward like snails, and getting nowhere. Each day the land looked much the same as it had the day before. About the feet of the mountains there was tumbled an ever wider land of bleak hills, and deep valleys filled with turbulent waters. Paths were few and winding, and led them often only to the edge of some sheer fall, or down into treacherous swamps.

(J.R.R. Tolkien, *The Lord of the Rings*)

Index

Abstract

The finite element method is frequently used to simulate forming processes for the purpose of predicting the quality of the final product and the load on the tool. Until recently, the mathematical model which underlies the simulation was based on either the Eulerian or the Lagrangian formulation. The consequences are that some simulations are arduous or even impossible. This is not the case if the Arbitrary-Eulerian-Lagrangian (AEL) formulation is used. In this thesis the theoretical background of this formulation is described. It is employed in some numerical simulations.

The basis of the AEL formulation is the use of a reference coordinate system which is not associated with the material to be deformed (Lagrangian formulation) and has no fixed spatial position (Eulerian formulation). The relevant quantities are understood to be a function of the coordinates, defined in this reference system. The quantities are discussed and the mathematical model is formulated using the principle of weighted residuals.

To make the mathematical model suitable for numerical analysis, it is discretised, both with respect to the progress of the process (the incremental method) and to the reference system (the element method). A special technique is used to determine material-associated quantities.

The current position of the reference system, that is, the current position and geometry of the elements, is understood to be the result of the deformation of a fictitious material associated with the reference system. The load which causes this deformation and its kinematic boundary conditions are determined so as to satisfy certain requirements of the geometry of the elements and to provide the possibility to account for certain boundary conditions in a straightforward manner. The deformation of the real and the fictitious material is a simultaneous process.

The discretised mathematical model consists of a system of nonlinear algebraic equations. The unknown quantities are determined by an

iterative method. In that case a number of approximations for the final solution is determined by repeatedly solving a linearised version of the above system of equations.

The AEL formulation is succesfully employed in the simulation of some axisymmetric forming processes.

Symbols and notation

* an upper-right index denotes the state in which the quantity is considered.
* an asterix * denotes that the quantity is considered at a boundary point.
* a cap ˆ denotes that the quantity is co-rotational.
* an under-right index e denotes that the quantity is used to describe the state of one element.
* an over-lined symbol is used for a quantity, describing the state of the fictitious material.
* the number in brackets denotes the page where the symbol occurs for the first time.

$\vec{a}$	vector
$\mathbb{A}$	second-order tensor
$\|\|\vec{a}\|\|$	length of $\vec{a}$
$\|\|\mathbb{A}\|\|$	norm of $\mathbb{A}$
$\mathbb{A}^c$	conjugate of $\mathbb{A}$
$\mathbb{A}^{-1}$	inverse of $\mathbb{A}$
$\hat{\mathbb{A}}$	co-rotational tensor
$\mathbb{A}^d$	deviatoric part of $\mathbb{A}$
$\mathbb{A}^h$	hydrostatic part of $\mathbb{A}$
$^4\mathbb{A}$	fourth-order tensor
$\vec{a}.\vec{a}$	dot product of two vectors
$\vec{a}.\mathbb{A}$	dot product of a vector and a second-order tensor
$\vec{a} * \vec{b}$	cross product of two vectors
$\vec{a}\,\vec{b}$	dyadic product of two vectors
$\mathbb{A}.\mathbb{B}$	dot product of two second-order tensors
$\mathbb{A}:\mathbb{B}$	dubble dot product of two second-order tensors
$\mathbb{A}\,\mathbb{B}$	tensor product of two second-order tensors
$tr(\mathbb{A})$	trace of $\mathbb{A}$

$\det(\mathbf{A})$	determinant of $\mathbf{A}$
$\underset{\sim}{a}$	scalar column (= column with scalars)
$\underset{\sim}{\vec{a}}$	vector column
$\underline{a}$	scalar matrix
$\underline{\mathbf{A}}$	tensor matrix
$\underset{\sim}{a}^{T}$	transposed column
$\underline{a}^{T}$	transposed matrix
$\underset{\sim}{\vec{b}}$	MRS vector basis [II.4]
$\underset{\sim}{\vec{b}}^{*}$	tangent vectors [II.9]
$\underset{\sim}{\vec{\beta}}$	CRS vector basis [II.18]
$\underset{\sim}{\vec{\beta}}^{*}$	tangent vectors [II.20]
$\underset{\sim}{\vec{c}}$	reciprocal MRS vector basis [II.6]
$\underset{\sim}{\vec{c}}^{*}$	reciprocal tangent vectors [II.10]
$\underset{\sim}{\vec{\gamma}}$	reciprocal CRS vector basis [II.19]
$\underset{\sim}{\vec{\gamma}}^{*}$	reciprocal tangent vectors [II.21]
$\mathbf{C}$	logarithmic strain tensor [II.17]
$^{4}\hat{\mathbf{C}}$	elastic material tensor [II.29]
$\mathbf{D}$	deformation rate tensor [II.8]
δ	volume-change factor [II.13]
δ^{*}	surface-change factor [II.15]
$\Delta_{m}( )$	MRS change [II.7]
$\Delta_{g}( )$	CRS change [II.19]
$d_{m}( )$	iterative MRS change [V.2]
$d_{g}( )$	iterative CRS change [V.2]
$\mathbf{E}$	Green-Lagrange strain tensor [II.15]
E	Young's modulus [V.8]
$\tilde{\varepsilon}^{p}$	effective plastic strain [V.8]
$\underset{\sim}{\vec{e}}$	Cartesian vector basis [VI.1]
$\underset{\sim}{\vec{\varepsilon}}$	cilindrical vector basis [VI.1]

$\mathbb{F}$	deformation tensor [II.12]
$\underset{\sim}{g}$, $\underset{\sim}{g}^*$	CRS coordinates [II.18, II.20]
G, G^*	set CRS coordinates [II.18, II.20]
G	shear modulus [V.8]
$\tilde{G}$	material parameter [V.16]
H	set history parameters [II.30]
h	hardening parameter [V.11]
$\underline{I}$	unit matrix [II.6]
$\mathbb{I}$	unit tensor [II.6]
J, J^*	Jacobian [II.5, II.9]
$\mathfrak{J}$, $\mathfrak{J}^*$	Jacobian [II.18, II.21]
J_1, J_2, J_3	invariants of a second-order tensor [A3.1]
K	bulk modulus [V.8]
λ	lenght-change factor [II.14]; scaling factor [V.12]
$^4\hat{\mathbb{L}}$	elasto-plastic material tensor [II.30]
ℓ	length of an element side [VI.13]
$\underset{\sim}{m}$, $\underset{\sim}{m}^*$	MRS coordinates [II.3, II.8]
M, M^*	set MRS coordinates [II.3, II.8]
$\tilde{\mu}$	material parameter [V.16]
$^4\mathbb{M}$	iterative elasto-plastic material tensor [V.16]
$\vec{n}$	unit outward normal vector at MRS boundary point [II.10]
$\vec{v}$	unit outward normal vector at CRS boundary point [II.21]
n	number of elements [III.5]
ν	Poisson's ratio [V.8]
$\vec{p}$	position vector [II.3]
$\vec{\underline{p}}$	boundary force vector [IV.4]
$\vec{q}$, $\vec{\underline{q}}$	body force vector [II.27, IV.4]
$\mathbb{R}$	rotation tensor [II.15]

$\underset{\sim}{\vec{\varrho}}$, $\underset{\sim}{\vec{\varrho}}_e$, $\underset{\sim}{\vec{r}}^k$	nodal point force vectors [IV.5, IV.5, VII.9]
r, φ, z	cilindrical coordinates [VI.1]
$\mathbb{\sigma}$	Cauchy stress tensor [II.25]
σ_v	yield stress [V.8]
τ	state [I.1]
$\mathbb{T}$	rotation tensor [II.16]
$\vec{t}$, $\vec{t}^*$	stress vector [II.25, II.28]
t_n	normal stress [II.25]
t_s	shearing stress [II.25]
$\mathbb{U}$	stretch tensor [II.14]
$\vec{u}$	velocity of a CRS point [II.19]
V, dV	volume [II.3, II.13]
V^*, dV^*	surface [II.9, II.15]
$\vec{v}$	velocity of an MRS point [II.7]
$\vec{w}$	weighting function [II.28]
$\underset{\sim}{\psi}$	column with interpolation functions [III.6]
$\vec{x}$, $\vec{x}^*$	mapping [II.3, II.8]
$\vec{\chi}$, $\vec{\chi}^*$	mapping [II.18, II.20]
$d\vec{x}$	material line element [II.13]
$\Delta_m\vec{x}$	incremental MRS point displacement [III.4]
$\Delta_g\vec{\chi}$	incremental CRS point displacement [III.3]
$d_m\vec{x}$	iterative MRS point displacement [V.2]
$d_g\vec{\chi}$	iterative CRS point displacement [V.2]
x, y, z	Cartesian coordinates [VI.1]
$\mathbb{\Omega}$	rotation rate tensor [II.8]
$\underset{\sim m}{\nabla}$, $\underset{\sim m}{\nabla^*}$	column operator [II.4, II.9]
$\underset{\sim g}{\nabla}$, $\underset{\sim g}{\nabla^*}$	column operator [II.18, II.21]
$\vec{\nabla}$, $\vec{\nabla}^*$	gradient operator [II.7, II.11]

I Introduction

The mathematical model

Necessary for the simulation of a metal forming process is the formulation of a mathematical model of it. Analysis of this model by means of a computer provides numerical data on the forming process.

The state variable

When formulating the mathematical model, a state variable is used to identify discrete states of the forming process. The state variable, which is a scalar quantity denoted by τ, is found to increase in value, when succeeding states of this process are considered.

The reference system

A set of independent variables, coordinates within a reference system, is used to identify either points of the body undergoing the deformation or points of space. Several reference systems can be used, all resulting in different formulations of the mathematical model. The Eulerian and Lagrangian formulations are frequently used.

The Eulerian formulation

With the Eulerian formulation the reference system is fixed in space, as is shown in figure I.1 for two states - τ_1 and τ_2 - of the process. This space-associated reference system is called the Spatial Reference System (SRS). Every spatial point of the SRS is unambiguously identified by an invariable set of independent SRS coordinates.

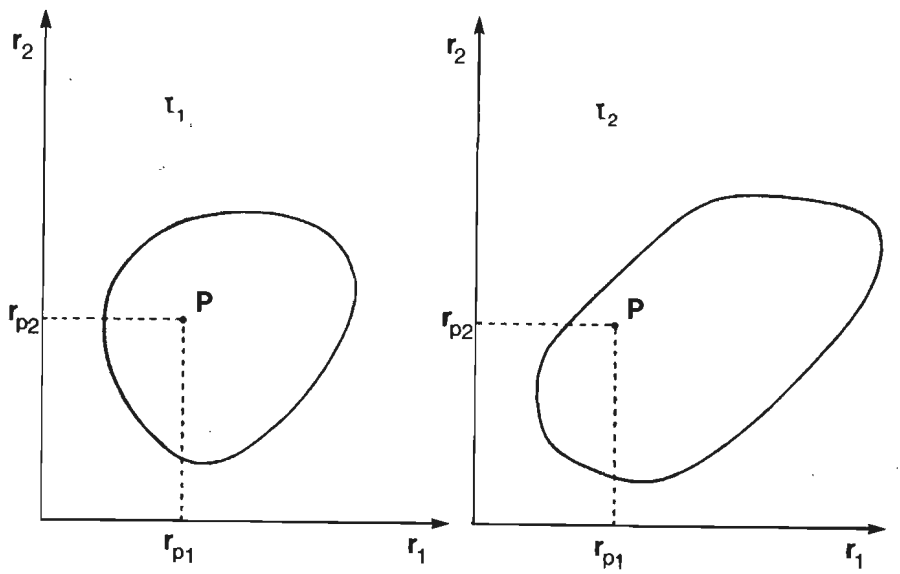

Fig. I.1
SRS point P *with SRS coordinates* (r_{p1}, r_{p2})

The Lagrangian formulation

In the case of the Lagrangian formulation the reference system is attached to the body, as is shown in figure I.2. This material-associated reference system is called the Material Reference System (MRS). Every point of the MRS and thus every material point of the body is unambiguously identified by an invariable set of independent MRS coordinates.

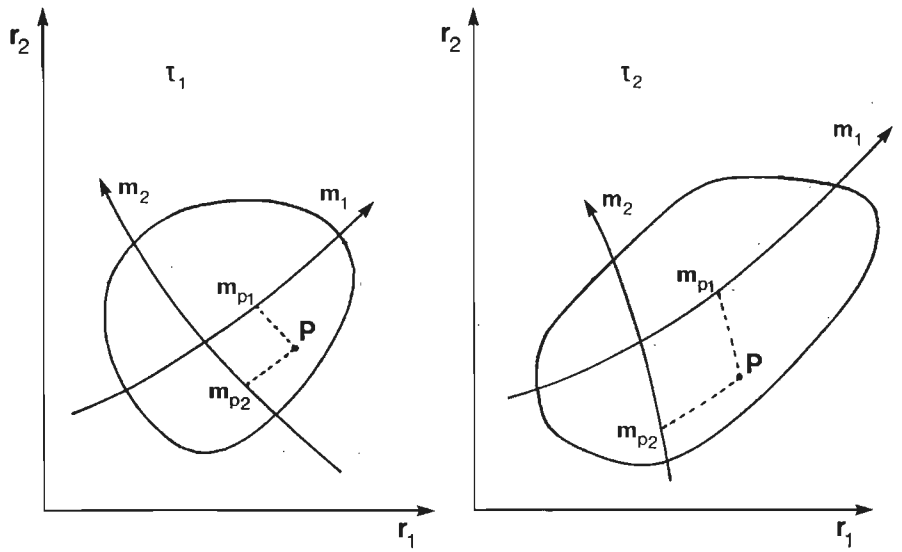

Fig. I.2
MRS point P *with MRS coordinates* (m_{p1}, m_{p2})

The finite element method

The merits and demerits of the foregoing formulations become clear when the finite element method is used to analyse the mathematical model. Following this method the state of the forming process is described at a limited number of points of the used reference system, the nodal points. To determine the state at these points it is necessary to subdivide the reference system or part of it in a limited number of subregions, the finite elements.

Using the Eulerian formulation the boundary of the body does not coincide everywhere with an element side, as can be perceived from figure I.3a. This makes it rather arduous to take material-associated boundary conditions into account. Using the Lagrangian formulation, elements may distort excessively on account of the deformation of the body, as is shown in figure I.3b. This may cause numerical difficulties during the analysis of the model. By using the Arbitrary-Eulerian-Lagrangian (AEL) formulation the above-mentioned difficulties can be overcome.

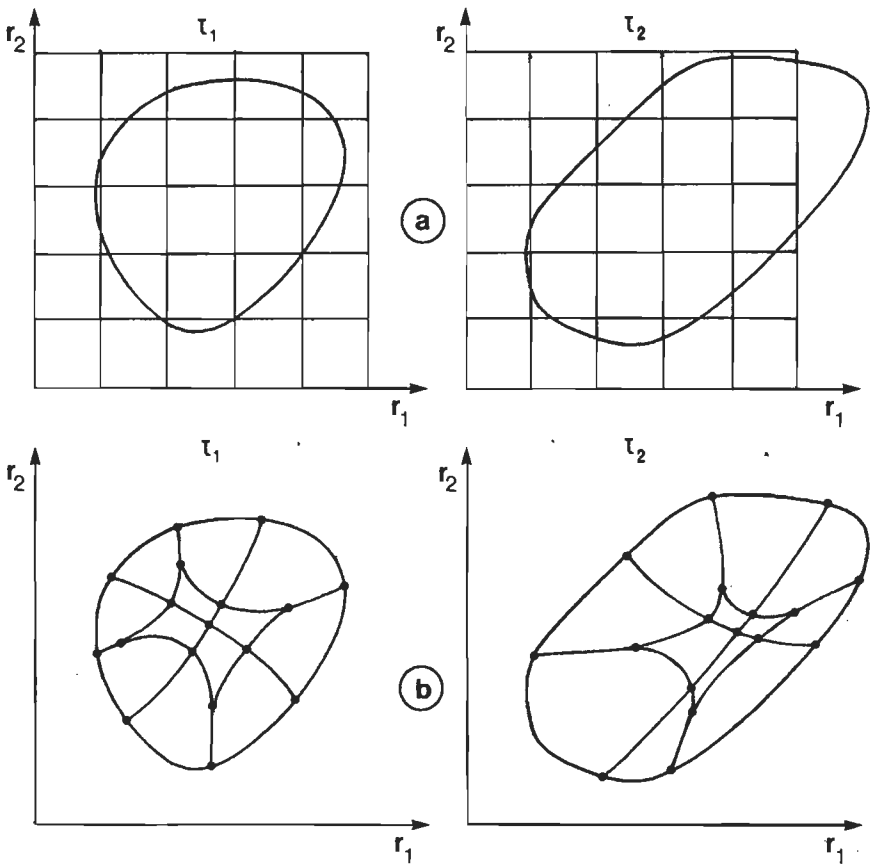

Fig. I.3
Element mesh, using the Eulerian (a) *and the Lagrangian* (b) *formulation*

The Arbitrary-Eulerian-Lagrangian formulation

The reference system used in the AEL formulation is not fixed in space nor attached to the body, as is shown in figure I.4. This non-associated reference system is called the Computational Reference System (CRS). Every point of the CRS is unambiguously identified by an invariable set of independent CRS coordinates.

The fact that the position of the CRS points is not given, yet can

be freely determined provides much freedom in formulating the mathematical model. The CRS can be fixed in space, which leads to an Eulerian formulation, or can be attached to the body, thus leading to a Lagrangian formulation. The position of the CRS points can also be changed continuously and in a prescribed manner during the simulation of the forming process. The CRS point positions can also occur in the mathematical model as unknown variables. In that case the model has to be extended by considering a so-called CRS determination process simultaneously with the forming process.

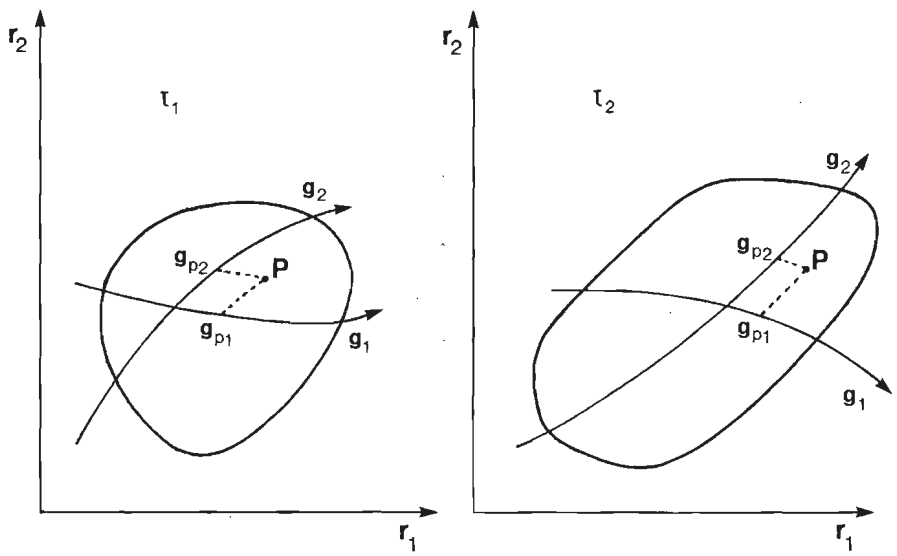

Fig. I.4
CRS point P *with CRS coordinates* (g_{p1}, g_{p2})

In the mathematical model of a forming process according to the AEL formulation, both the CRS and the MRS are used. The AEL formulation requires that there is an unambiguous connection between these two reference systems in every state. The freedom to choose the position of the CRS points is thus limited in the sense that each CRS point always coincides with one and only one, though not always the same MRS point and vice versa. This means that the boundary of the CRS always coincides with the boundary of the body to be deformed. Thus, when using the finite element method, all sorts of boundary

conditions can easily be taken into account. At the same time the nodal point positions can be prescribed or determined in a CRS determination process, in such a way that the dimension and the geometry of the elements is appropriate (see figure I.5).

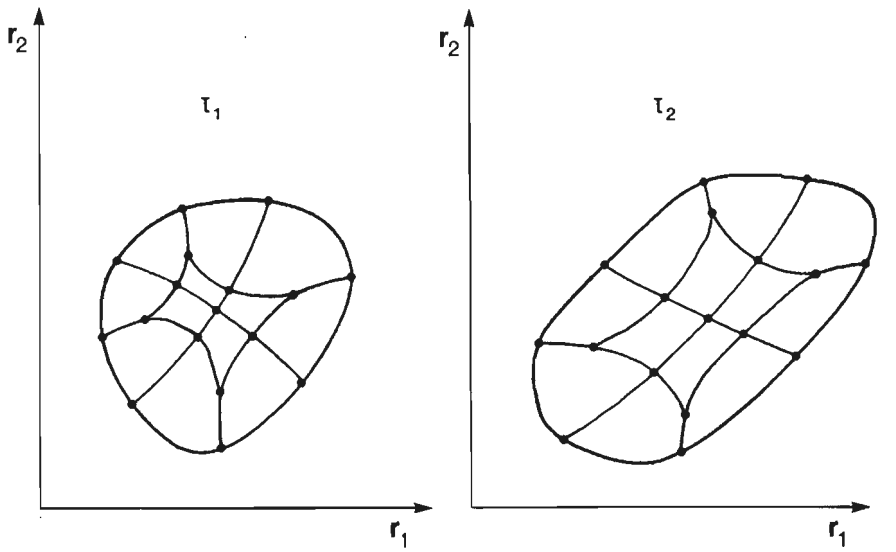

Fig. I.5
Element mesh, using the AEL formulation

The AEL formulation in literature

The AEL formulation, together with the finite difference or the finite element method, is frequently employed to simulate processes in gasses and fluids and processes with fluid-structure interaction. - Hirt et al. (1972), Pracht (1974), Stein et al. (1976), Belytschko & Kennedy (1978), Donea (1978), Dwyer et al. (1980), Hughes et al. (1981), Kennedy & Belytschko (1981), Donea et al. (1982) -. Very recently the AEL formulation, together with the finite element method, has been used to simulate forming processes - Huetink (1982) -. As well in the Eulerian as in the Lagrangian formulation, so-called rezoning methods are used, where the nodal point positions are adjusted, if necessary, in a rather ad hoc manner - Gelten & De Jong (1981), Roll & Neitzert (1982) -.

II An AEL formulation for continuum mechanics

II.1 Introduction

When employing the Arbitrary-Eulerian-Lagrangian (AEL) formulation to the simulation of metal forming processes, two sets of independent variables are used: the coordinates in the Computational Reference System (CRS) and the coordinates in the Material Reference System (MRS), respectively, the so-called CRS and MRS coordinates. Various geometric quantities can be defined at every point of these reference systems. Considering the change of these geometric quantities during a state transition leads to the definition of various kinematic quantities. The kinematic quantities which refer to a point of the MRS describe the deformation of the material. In every state there is an unambiguous relation between the CRS and MRS coordinates. Section II.2 deals with the geometric and kinematic quantities and the relation between CRS and MRS coordinates.

The deformation provokes stresses in the material. The stress state in an MRS point is represented by means of a stress tensor. In section II.3 two stress tensors are introduced.

If inertia effects are neglected the internal stresses and the external loads must constitute an equilibrium state. This means that

at every MRS point the stress tensor and the external load vector have to satisfy an equilibrium equation. This equation is presented in section II.4. Subsequently an integral formulation is introduced which is equivalent to the equilibrium equation and very suitable for determining an approximated solution.

The stresses in the material and the deformation which causes them must satisfy a constitutive equation. In section II.5 a constitutive equation for time independent, elasto-plastic material behaviour is presented.

II.2 Geometric and kinematic quantities

The MRS coordinates

Each particle of a three-dimensional body can be identified unambiguously by a set of three independent MRS coordinates m_1, m_2 and m_3, which can be taken as elements of a column $\underset{\sim}{m}$. The columns $\underset{\sim}{m}$ of all MRS points are the elements of an invariable set M. In state τ the position vector $\vec{p}$ of MRS point $\underset{\sim}{m}$ with respect to a fixed spatial point, the origin, is

$$\vec{p} = \vec{x}(\underset{\sim}{m},\tau) \qquad \text{(II.2.1)}$$

In state τ the function $\vec{x}$, which is unique, continuous and sufficiently differentiable, can be considered as a mapping $\vec{x} : M \rightarrow V(\tau)$, where $V(\tau)$ is the set of end points of the position vectors $\vec{p}$ of the MRS points. A subset of $V(\tau)$, containing the end points of the position vectors $\vec{p} = \vec{x}(\underset{\sim}{m},\tau)$, with $\underset{\sim}{m} \in M$ and m_j is constant for $j \neq i$, is called the m_i-parametric curve in state τ. The end point of every position vector $\vec{p}$ is situated on three different parametric curves (see figure II.2.1).

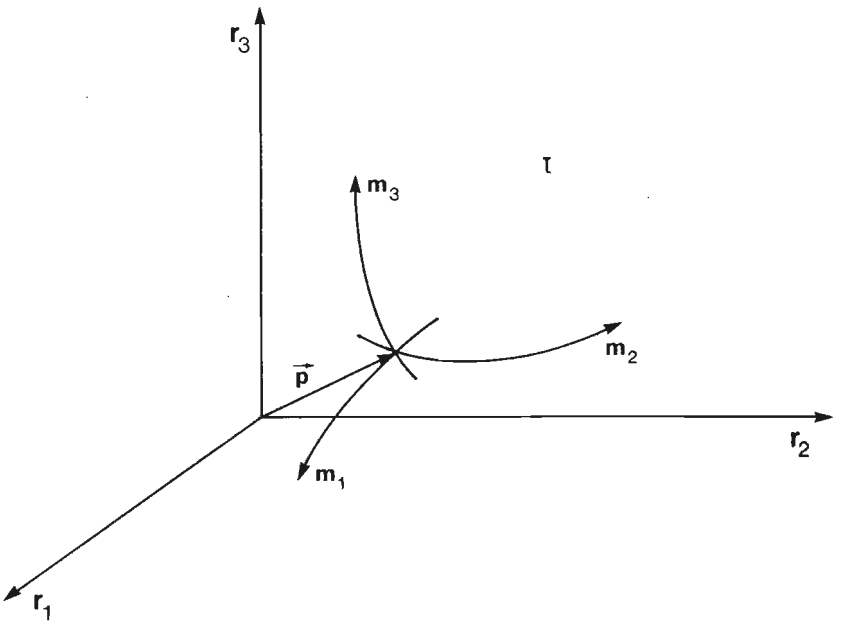

Fig. II.2.1
Position vector $\vec{p} = \vec{x}(\underset{\sim}{m},\tau)$ *and the three parametric curves through MRS point* $\underset{\sim}{m}$

Geometric quantities

The tangent vectors to the three parametric curves in every MRS point $\underset{\sim}{m}$, are mutually independent and constitute the local MRS vector basis $\vec{\underset{\sim}{b}}(\underset{\sim}{m},\tau)$ which is considered to be always right-handed and is defined by

$$\vec{\underset{\sim}{b}}^{T} = [\vec{b}_1\ \vec{b}_2\ \vec{b}_3] \quad ; \quad \vec{b}_i = \frac{\partial \vec{x}}{\partial m_i} \qquad (i \in \{1, 2, 3\}) \qquad \text{(II.2.2)}$$

In shortened form this can be written as

$$\vec{\underset{\sim}{b}} = \underset{\sim}{\nabla}_{m} \vec{x} \qquad \text{(II.2.3)}$$

where $\nabla_{\underset{\sim}{m}}$ is a column operator which, in transposed form, is given by

$$\nabla^T_{\underset{\sim}{m}} = [\frac{\partial}{\partial m_1} \frac{\partial}{\partial m_2} \frac{\partial}{\partial m_3}] \qquad \text{(II.2.4)}$$

The basis vectors are shown in figure II.2.2.

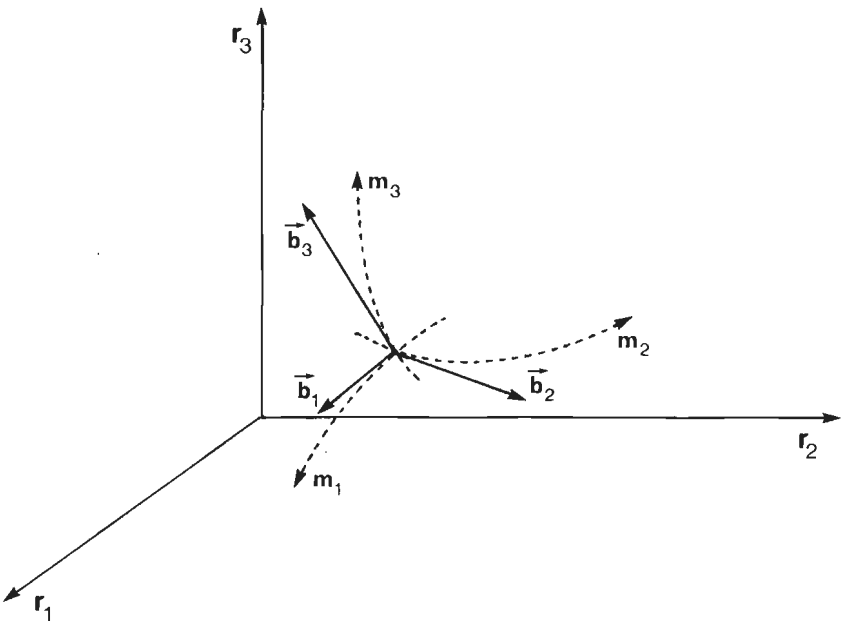

Fig. II.2.2
Basis vectors $\vec{b}_1$, $\vec{b}_2$ *and* $\vec{b}_3$ *at MRS point* $\underset{\sim}{m}$

The Jacobian $J(\underset{\sim}{m},\tau)$ of the mapping $\vec{x} : M \rightarrow V(\tau)$ equals the triple product of the basis vectors $\vec{b}_1$, $\vec{b}_2$ and $\vec{b}_3$

$$J = \vec{b}_1 . \vec{b}_2 * \vec{b}_3 \qquad \text{(II.2.5)}$$

On account of the properties of $\vec{x} : M \rightarrow V(\tau)$, it is obvious that J is never equal to zero.

The reciprocal MRS vector basis is denoted by $\vec{\underset{\sim}{c}}(\underset{\sim}{m},\tau)$ and can be determined from the requirement

$$\vec{\underset{\sim}{b}}.\vec{\underset{\sim}{c}}^{T} = \underline{I} \quad ; \quad \vec{\underset{\sim}{c}}^{T} = [\vec{c}_1\ \vec{c}_2\ \vec{c}_3] \qquad \text{(II.2.6)}$$

where $\underline{I}$ is the 3x3 unit matrix. It is easily shown that

$$\vec{\underset{\sim}{b}}^{T}\vec{\underset{\sim}{c}} = \mathbb{I} \qquad \text{(II.2.7)}$$

where $\mathbb{I}$ is the second-order unit tensor. From this relation it can be shown that $\vec{c}_1$, $\vec{c}_2$ and $\vec{c}_3$ must satisfy

$$\vec{c}_1 = \frac{1}{J}\vec{b}_2 * \vec{b}_3 \; ; \quad \vec{c}_2 = \frac{1}{J}\vec{b}_3 * \vec{b}_1 \; ; \quad \vec{c}_3 = \frac{1}{J}\vec{b}_1 * \vec{b}_2 \qquad \text{(II.2.8)}$$

The reciprocal basis vectors are shown in figure II.2.3.

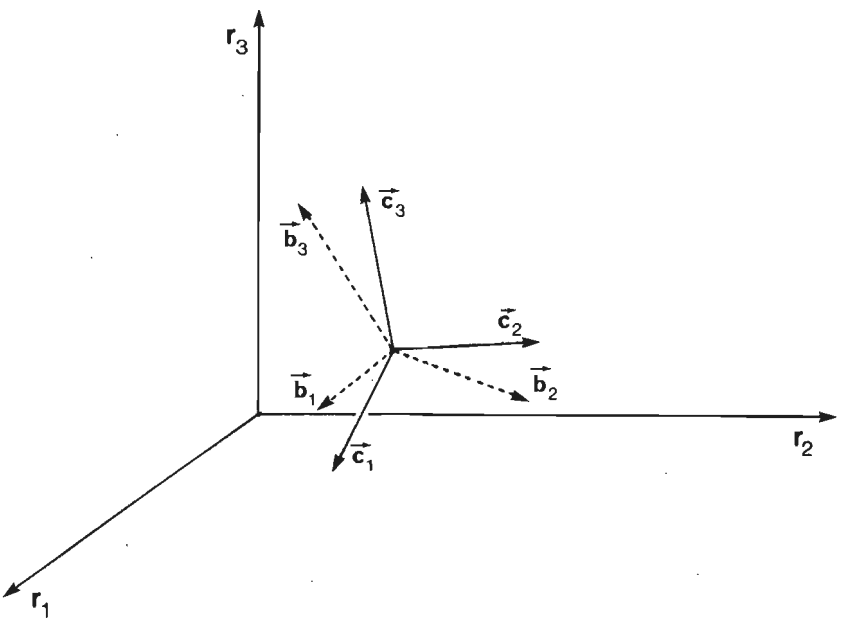

Fig. II.2.3
Reciprocal basis vectors $\vec{c}_1$, $\vec{c}_2$ *and* $\vec{c}_3$ *at MRS point* $\underset{\sim}{m}$

Using the local reciprocal vector basis, the gradient operator can be expressed in the column operator $\underset{\sim}{\nabla}_m$

$$\vec{\nabla} = \vec{\underset{\sim}{c}}^T \underset{\sim}{\nabla}_m \quad ; \quad \underset{\sim}{\nabla}_m = \vec{\underset{\sim}{b}} . \vec{\nabla} \tag{II.2.9}$$

Kinematic quantities

In every state and at every MRS point the quantity A is defined and given by $A = a(\underset{\sim}{m},\tau)$. The change of A at MRS point $\underset{\sim}{m}$ during a state transition $\Delta\tau$ is called the MRS change of A and denoted by $\Delta_m A$

$$\Delta_m A = a(\underset{\sim}{m},\tau+\Delta\tau) - a(\underset{\sim}{m},\tau) \tag{II.2.10}$$

The MRS derivative of A is denoted by $\dot{A}$ and defined by

$$\dot{A} = \lim_{\Delta\tau \to 0} \frac{\Delta_m A}{\Delta\tau} \tag{II.2.11}$$

The velocity $\vec{v}$ of an MRS point is defined as the MRS derivative of the position vector of that point

$$\vec{v} = \dot{\vec{x}}(\underset{\sim}{m},\tau) = \dot{\vec{p}} = \lim_{\Delta\tau \to 0} \frac{\Delta_m \vec{p}}{\Delta\tau} \tag{II.2.12}$$

Using (II.2.3) and (II.2.9) it is easily shown that for the MRS derivate of $\vec{\underset{\sim}{b}}$ the following expression holds

$$\dot{\vec{\underset{\sim}{b}}} = \vec{\underset{\sim}{b}} . (\vec{\nabla}\ \vec{v}) \tag{II.2.13}$$

With $\vec{\underset{\sim}{c}} . \vec{\underset{\sim}{b}}^T = \underline{I}$ we find for $\dot{\vec{\underset{\sim}{c}}}$ that

$$\dot{\vec{\underset{\sim}{c}}} = - \vec{\underset{\sim}{c}} . (\vec{\nabla}\ \vec{v})^C \tag{II.2.14}$$

The tensor $(\vec{\nabla}\ \vec{v})^C$ in the above expression can be decomposed into a symmetric part $\mathbb{D}$ and a skew-symmetric part $\mathbb{Q}$, so that

$$(\vec{v}\ \vec{v})^C = \mathbb{D} + \mathbb{Q} = \dot{\underset{\sim}{b}}^T \underset{\sim}{c} \quad ; \quad \mathbb{D} = \mathbb{D}^C \quad ; \quad \mathbb{Q} = -\mathbb{Q}^C \qquad \text{(II.2.15)}$$

For the tensors $\mathbb{D}$ and $\mathbb{Q}$, called the deformation and rotation rate tensor, the next expressions hold

$$\mathbb{D} = \frac{1}{2}\left(\dot{\underset{\sim}{b}}^T \underset{\sim}{c} + \underset{\sim}{c}^T \dot{\underset{\sim}{b}}\right) = \frac{1}{2}\left\{(\vec{v}\ \vec{v})^C + (\vec{v}\ \vec{v})\right\} \qquad \text{(II.2.16)}$$

$$\mathbb{Q} = \frac{1}{2}\left(\dot{\underset{\sim}{b}}^T \underset{\sim}{c} - \underset{\sim}{c}^T \dot{\underset{\sim}{b}}\right) = \frac{1}{2}\left\{(\vec{v}\ \vec{v})^C - (\vec{v}\ \vec{v})\right\} \qquad \text{(II.2.17)}$$

For the MRS derivative of the Jacobian J we find

$$\dot{J} = J\ \underset{\sim}{c}^T . \dot{\underset{\sim}{b}} = J(\vec{v}.\vec{v}) = J\ \mathrm{tr}(\mathbb{D}) \qquad \text{(II.2.18)}$$

The boundary

An MRS point on the boundary of a three-dimensional body can be identified both by the MRS coordinates $\underset{\sim}{m}$ and a set of two independent coordinates m_1^* and m_2^*, taken as the elements of a column $\underset{\sim}{m}^*$. The columns $\underset{\sim}{m}^*$ of the MRS points on the boundary are the elements of a set M^*. We assume that the boundary is always made up of the same MRS points and therefore the set M^* is invariable. In state τ the position vector $\vec{p}$ of MRS point $\underset{\sim}{m}^*$ is

$$\vec{p} = \vec{x}^*(\underset{\sim}{m}^*, \tau) \qquad \text{(II.2.19)}$$

In this state, the function $\vec{x}^*$, which is unique, continuous and sufficiently differentiable, can be considered as a mapping $\vec{x}^* : M^* \rightarrow V^*(\tau)$, where $V^*(\tau)$ is the set of the end points of the position vectors $\vec{p}$ of the MRS points on the boundary. A subset of $V^*(\tau)$, containing the end points of the position vectors $\vec{p} = \vec{x}^*(\underset{\sim}{m}^*, \tau)$, with $\underset{\sim}{m}^* \in M^*$ and m_j^* is constant for $j \neq i$, is called the m_i^*-parametric curve in state τ. The end point of every position vector $\vec{p}$ is situated on two different parametric curves (see figure II.2.4).

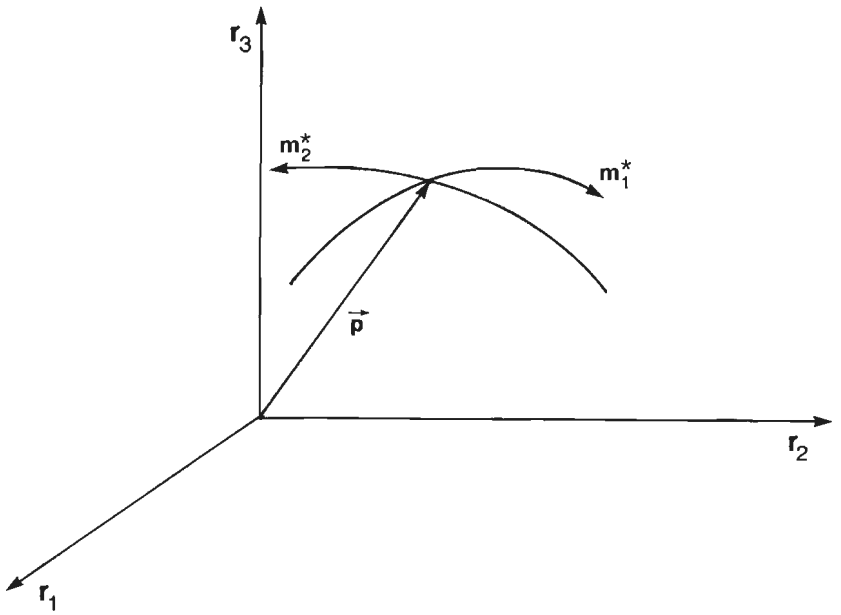

Fig. II.2.4

Position vector $\vec{p} = \vec{x}^*(\underset{\sim}{m}^*, \tau)$ *and the two parametric curves through MRS boundary point* $\underset{\sim}{m}^*$

Geometric quantities at the boundary

The tangent vectors to the m_1^*- and m_2^*-parametric curves at an MRS point are independent. They are understood to be the elements $\vec{b}_1^*$ and $\vec{b}_2^*$ of a column $\underset{\sim}{\vec{b}}^*$ defined by

$$\underset{\sim}{\vec{b}}^* = \underset{\sim m}{\nabla^*} \vec{x}^* \quad ; \quad \underset{\sim}{\vec{b}}^{*T} = [\vec{b}_1^* \; \vec{b}_2^*] \tag{II.2.20}$$

where $\underset{\sim m}{\nabla^*}$ is a column operator, which in transposed form is given by

$$\underset{\sim m}{\nabla^{*T}} = \left[\frac{\partial}{\partial m_1^*} \; \frac{\partial}{\partial m_2^*}\right] \tag{II.2.21}$$

The Jacobian $J^*(\underset{\sim}{m}^*, \tau)$ of the mapping $\vec{x}^* : M^* \to V^*(\tau)$ is defined by

$$J^* = ||\vec{b}_1^* * \vec{b}_2^*|| \tag{II.2.22}$$

On account of the properties of $\vec{x}^*: M^* \to V^*(\tau)$, J^* will never be zero.

The vector $\vec{b}_1^* * \vec{b}_2^*$ is perpendicular to the boundary and is of length J^*. In state τ the unit vector, outward and normal to the boundary at MRS point $\underset{\sim}{m}^*$ is denoted by $\vec{n}(\underset{\sim}{m}^*, \tau)$ and defined by

$$\vec{n} = s \frac{\vec{b}_1^* * \vec{b}_2^*}{||\vec{b}_1^* * \vec{b}_2^*||} = s \frac{\vec{b}_1^* * \vec{b}_2^*}{J^*} \quad ; \quad s^2 = 1 \qquad \text{(II.2.23)}$$

where s is chosen in such a way (s = +1 or s = -1) that the vector $\vec{n}$ is outward with respect to the body. The vectors $\vec{b}_1^*$, $\vec{b}_2^*$ and $\vec{n}$ are shown in figure II.2.5.

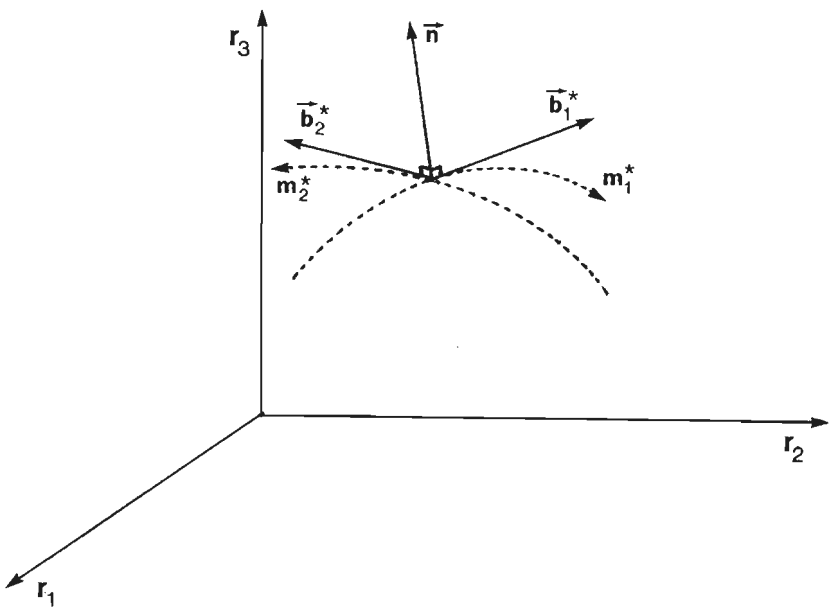

Fig. II.2.5
Basis vectors $\vec{b}_1^*$ *and* $\vec{b}_2^*$, *and the unit outward normal vector* $\vec{n}$ *at MRS boundary point* $\underset{\sim}{m}^*$

On the analogy of (II.2.6) the reciprocal vectors $\vec{c}_1^*$ and $\vec{c}_2^*$ at MRS

point $\underset{\sim}{m}^*$ can be determined from

$$\underset{\sim}{\vec{b}}^* . \underset{\sim}{\vec{c}}^{*T} = \underline{I} \quad ; \quad \underset{\sim}{\vec{c}}^{*T} = [\vec{c}_1^* \; \vec{c}_2^*] \tag{II.2.24}$$

and

$$\vec{c}_1^* . \vec{n} = \vec{c}_2^* . \vec{n} = 0 \tag{II.2.25}$$

where $\underline{I}$ is the 2x2 unit matrix. It can be shown not only that the expression

$$\underset{\sim}{\vec{b}}^{*T} \underset{\sim}{\vec{c}}^* = \mathbb{I} - \vec{n}\,\vec{n} \tag{II.2.26}$$

must apply, but also that $\vec{c}_1^*$ and $\vec{c}_2^*$ must satisfy

$$\vec{c}_1^* = \frac{s}{J^*} \vec{b}_2^* * \vec{n} \quad ; \quad \vec{c}_2^* = \frac{s}{J^*} \vec{n} * \vec{b}_1^* \tag{II.2.27}$$

The gradient operator $\vec{\nabla}^*$, used at MRS point $\underset{\sim}{m}^*$ to describe variations of quantities at adjacent points on the boundary in state τ, is defined by

$$\vec{\nabla}^* = \underset{\sim}{\vec{c}}^{*T} \underset{\sim m}{\nabla}^* = \{(\mathbb{I} - \vec{n}\,\vec{n}).\vec{\nabla}\} \tag{II.2.28}$$

Kinematic quantities at the boundary

Using (II.2.20), (II.2.28), (II.2.24) and (II.2.15), the next expression for the MRS derivative of $\underset{\sim}{\vec{b}}^*$ can be derived to give

$$\begin{aligned} \dot{\underset{\sim}{\vec{b}}}^* = \underset{\sim}{\vec{b}}^* . (\vec{\nabla}^* \dot{\vec{v}}^*) &= \underset{\sim}{\vec{b}}^* . \{(\mathbb{I} - \vec{n}\,\vec{n}).(\vec{\nabla}\,\dot{\vec{v}}^*)\} \\ &= \underset{\sim}{\vec{b}}^* . \{(\mathbb{I} - \vec{n}\,\vec{n}).(\mathbb{D} + \mathbb{Q})^C\} \end{aligned} \tag{II.2.29}$$

With $\underset{\sim}{\vec{c}}^* . \underset{\sim}{\vec{b}}^{*T} = \underline{I}$ we find for $\dot{\underset{\sim}{\vec{c}}}^*$

$$\begin{aligned} \dot{\underset{\sim}{\vec{c}}}^* = - \underset{\sim}{\vec{c}}^* . (\vec{\nabla}^* \dot{\vec{v}}^*)^C &= - \underset{\sim}{\vec{c}}^* . \{(\vec{\nabla}\,\dot{\vec{v}}^*)^C . (\mathbb{I} - \vec{n}\,\vec{n})\} \\ &= - \dot{\underset{\sim}{\vec{c}}}^* . \{(\mathbb{D} + \mathbb{Q}) . (\mathbb{I} - \vec{n}\,\vec{n})\} \end{aligned} \tag{II.2.30}$$

For the MRS derivative of the Jacobian J^* we find

$$\dot{J}^* = J^* \underset{\sim}{\overset{*}{C}}^{*T} . \underset{\sim}{\dot{b}}^* = J^* (\vec{\nabla}^* . \vec{v}^*) = J^* (\mathbb{I} - \vec{n}\,\vec{n}) : \mathbb{D} \qquad \text{(II.2.31)}$$

Deformation quantities

The deformation of the material at a point with MRS coordinates $\underset{\sim}{m}$ in state τ compared to state τ_o is described by means of the deformation tensor $\mathbb{F}(\underset{\sim}{m},\tau)$. As is shown in figure II.2.6 this tensor maps $\vec{b}^o = \vec{b}(\underset{\sim}{m},\tau_o)$, the vector basis in state τ_o, in $\vec{b} = \vec{b}(\underset{\sim}{m},\tau)$, the vector basis at the same MRS point in state τ

$$\vec{b} = \mathbb{F} . \vec{b}^o \qquad \text{(II.2.32)}$$

The deformation tensor is regular, in other words $\det(\mathbb{F}) \neq 0$.

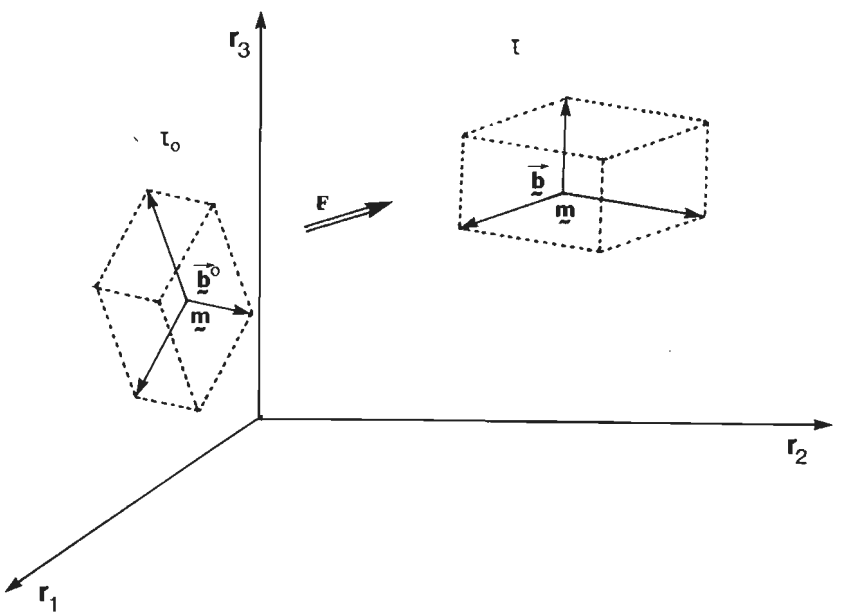

Fig. II.2.6
Vector basis at MRS point $\underset{\sim}{m}$ in state τ_o and state τ

The basis vectors $\vec{\underset{\sim}{b}}^{o}$ span a volume $\Delta V^{o} = |\vec{b}^{o}_{1}.\vec{b}^{o}_{2} * \vec{b}^{o}_{3}|$ and the basis vectors $\vec{\underset{\sim}{b}}$ span $\Delta V = |\vec{b}_{1}.\vec{b}_{2} * \vec{b}_{3}|$. It is easily shown that the next relation between the infinitesimal material volume elements dV and dV^{o} must apply

$$dV = \det(\mathbb{F})\, dV^{o} \tag{II.2.33}$$

From this relation we can conclude that $\det(\mathbb{F}) > 0$. The determinant of $\mathbb{F}$ is called the volume-change factor δ

$$\delta = \det(\mathbb{F}) = \frac{dV}{dV^{o}} \tag{II.2.34}$$

Using $\vec{\underset{\sim}{b}}^{T}\vec{\underset{\sim}{c}} = \mathbb{I}$, $\mathbb{F}$ can be written as

$$\mathbb{F} = \vec{\underset{\sim}{b}}^{T}\vec{\underset{\sim}{c}}^{o} = [\vec{\underset{\sim}{c}}^{oT}(\nabla_{\underset{\sim}{m}}\vec{x})]^{C} = (\vec{\nabla}^{o}\vec{x})^{C} \tag{II.2.35}$$

and $\mathbb{F}^{-1}$, the inverse of $\mathbb{F}$, as

$$\mathbb{F}^{-1} = \vec{\underset{\sim}{b}}^{oT}\vec{\underset{\sim}{c}} = [\vec{\underset{\sim}{c}}^{T}(\nabla_{\underset{\sim}{m}}\vec{x}^{o})]^{C} = (\vec{\nabla}\,\vec{x}^{o})^{C} \tag{II.2.36}$$

It can easily be shown that, for the MRS derivative of $\mathbb{F}$ and $\mathbb{F}^{-1}$, the next expressions apply

$$\dot{\mathbb{F}} = \dot{\vec{\underset{\sim}{b}}}^{T}\vec{\underset{\sim}{c}}^{o} = (\vec{\nabla}^{o}\vec{v})^{C} = (\vec{\nabla}\,\vec{v})^{C}.\mathbb{F} \tag{II.2.37}$$

$$\dot{\mathbb{F}}^{-1} = \vec{\underset{\sim}{b}}^{oT}\dot{\vec{\underset{\sim}{c}}} = -\,\mathbb{F}^{-1}.(\vec{\nabla}\,\vec{v})^{C} \tag{II.2.38}$$

On account of (II.2.35) the relation between the two infinitesimal material line elements $d\vec{x}^{o} = d\vec{x}(\underset{\sim}{m},\tau_{o})$ and $d\vec{x} = d\vec{x}(\underset{\sim}{m},\tau)$ is

$$d\vec{x} = \mathbb{F}.d\vec{x}^{o} \tag{II.2.39}$$

With $\vec{n}^{o}$ and $\vec{n}$ as the unit vectors in the direction of $d\vec{x}^{o}$ and $d\vec{x}$, and ds^{o} and ds, the lengths of these line elements, we can write, for the

length-change factor λ

$$\lambda = \frac{ds}{ds^o} = \frac{||d\vec{x}||}{ds^o} \qquad \text{(II.2.40)}$$

Using (II.2.39) we find

$$\lambda = ||\mathbf{F}.\vec{n}^o|| = (\vec{n}^o.\mathbf{F}^c.\mathbf{F}.\vec{n}^o)^{\frac{1}{2}} \qquad \text{(II.2.41)}$$

The above is illustrated in figure II.2.7.

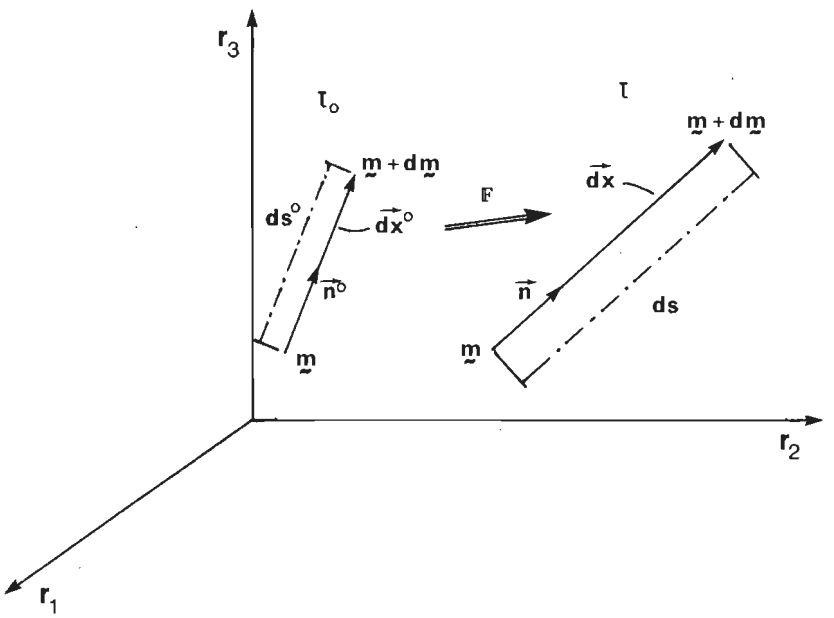

Fig. II.2.7

The infinitesimal material line elements:

$d\vec{x}^o = \vec{p}(\underset{\sim}{m}+d\underset{\sim}{m},\tau^o) - \vec{p}(\underset{\sim}{m},\tau^o) = ds^o\vec{n}^o$; $d\vec{x} = \vec{p}(\underset{\sim}{m}+d\underset{\sim}{m},\tau) - \vec{p}(\underset{\sim}{m},\tau) = ds\ \vec{n}$

According to (II.2.41) the total deformation of the material at an MRS point $\underset{\sim}{m}$ can be described by the so-called stretch tensor $\mathbf{U}$,

defined by

$$\mathbb{U} = (\mathbb{F}^C.\mathbb{F})^{\frac{1}{2}} \quad ; \quad \mathbb{U} = \mathbb{U}^C \tag{II.2.42}$$

On account of this definition of $\mathbb{U}$, a tensor $\mathbb{R}$ can be defined in such a way that the following decomposition of $\mathbb{F}$ applies

$$\mathbb{F} = \mathbb{R}.\mathbb{U} \quad ; \quad \mathbb{R}^C.\mathbb{R} = \mathbb{I} \quad ; \quad \det(\mathbb{R}) = +1 \tag{II.2.43}$$

Because of the requirements which $\mathbb{R}$ has to meet, we can conclude that $\mathbb{R}$ describes a rigid body rotation of the material at MRS point $\underset{\sim}{m}$. The above decomposition is called the polar decomposition of $\mathbb{F}$ and the tensor $\mathbb{R}$ the rotation tensor in the polar decomposition of $\mathbb{F}$.

The Green-Lagrange strain tensor $\mathbb{E}$ is defined by

$$\mathbb{E} = \frac{1}{2}(\mathbb{F}^C.\mathbb{F} - \mathbb{I}) = \frac{1}{2}(\mathbb{U}^2 - \mathbb{I}) \tag{II.2.44}$$

For the deformation rate tensor $\mathbb{D}$ and the rotation rate tensor $\mathbb{Q}$ we can write

$$\mathbb{D} + \mathbb{Q} = (\vec{\nabla}\ \vec{v})^C = \dot{\mathbb{F}}.\mathbb{F}^{-1} \quad ; \quad \mathbb{D} = \mathbb{D}^C \quad ; \quad \mathbb{Q} = -\mathbb{Q}^C \tag{II.2.45}$$

The MRS derivative of the volume-change factor δ can be expressed in $\mathbb{D}$ as

$$\dot{\delta} = \delta\ \mathrm{tr}(\dot{\mathbb{F}}.\mathbb{F}^{-1}) = \delta\ \mathrm{tr}(\mathbb{D}) \tag{II.2.46}$$

In state τ_o two independent vectors $\vec{b}_1^{*o}$ and $\vec{b}_2^{*o}$ on the boundary of a three dimensional body span a surface $\Delta V^{*o} = ||\vec{b}_1^{*o} * \vec{b}_2^{*o}||$. The corresponding vectors in state τ, $\vec{b}_1^{*}$ and $\vec{b}_2^{*}$, span a surface $\Delta V^{*} = ||\vec{b}_1^{*} * \vec{b}_2^{*}||$. The surface-change factor is defined as

$$\delta^* = \frac{dV^*}{dV^{*o}} = \frac{||\vec{b}_1^{*} * \vec{b}_2^{*}||}{||\vec{b}_1^{*o} * \vec{b}_2^{*o}||} \tag{II.2.47}$$

where dV^* and dV^{*o} are infinitesimal material surfaces. After some manipulations we arrive at the following expressions for δ^* and its MRS derivative $\dot{\delta}^*$

$$\delta^* = \det(\mathbb{F}) \; ||\mathbb{F}^{-c}.\vec{n}^o|| \tag{II.2.48}$$

$$\dot{\delta}^* = \det(\mathbb{F}) \; [(\vec{\nabla}\,\vec{v})||\mathbb{F}^{-c}.\vec{n}^o|| + \frac{\vec{n}^o.\dot{\mathbb{F}}^{-1}.\mathbb{F}.\mathbb{F}^{-c}.\vec{n}^o}{||\mathbb{F}^{-c}.\vec{n}^o||}] \tag{II.2.49}$$

Rigid body rotation and co-rotational quantities

Besides the rotation tensor $\mathbb{R}$ in the polar decomposition of $\mathbb{F}$ there are many tensors $\mathbb{T}$ which meet the requirements

$$\mathbb{T}^c.\mathbb{T} = \mathbb{I} \quad ; \quad \det(\mathbb{T}) = +1 \tag{II.2.50}$$

and also describe a rotation of the material in state τ compared to state τ_o. If we assume $\mathbb{D} = \mathbb{0}$, it is possible to introduce a rotation tensor, which unambiguously describes the rotation of a material line element $d\vec{x}$ in state τ compared to state τ_o, that is

$$d\vec{x}(\underset{\sim}{m},\tau) = \mathbb{T}(\underset{\sim}{m},\tau) \; . \; d\vec{x}(\underset{\sim}{m},\tau_o) \tag{II.2.51}$$

For the MRS derivative we obtain

$$\dot{d\vec{x}}(\underset{\sim}{m},\tau) = \dot{\mathbb{T}}(\underset{\sim}{m},\tau) \; . \; d\vec{x}(\underset{\sim}{m},\tau_o) \tag{II.2.52}$$

Using the deformation rate tensor $\mathbb{D}$ and the rotation rate tensor $\mathbb{Q}$, we write generally

$$\dot{d\vec{x}}(\underset{\sim}{m},\tau) = \{\mathbb{D}(\underset{\sim}{m},\tau) + \mathbb{Q}(\underset{\sim}{m},\tau)\} \; . \; d\vec{x}(\underset{\sim}{m},\tau) \tag{II.2.53}$$

In view of the assumption $\mathbb{D} = \mathbb{0}$, this expression becomes

$$\dot{d\vec{x}}(\underset{\sim}{m},\tau) = \mathbb{Q}(\underset{\sim}{m},\tau) \; . \; d\vec{x}(\underset{\sim}{m},\tau) \tag{II.2.54}$$

From (II.2.51), (II.2.52) and (II.2.54) the following differential equation results

$$\dot{\mathbb{T}} = \mathbb{Q}.\mathbb{T} \qquad \text{(II.2.55)}$$

with the initial conditions

$$\mathbb{T} = \mathbb{I} \quad \text{at} \quad \tau = \tau_o \qquad \text{(II.2.56)}$$

On the analogy of the polar decomposition, Nagtegaal & Veldpaus [21] decompose the deformation tensor $\mathbb{F}$ to give

$$\mathbb{F} = \mathbb{T}.\hat{\mathbb{F}} \qquad \text{(II.2.57)}$$

where $\hat{\mathbb{F}}$ is called the co-rotational deformation tensor which is invariant to the rotation described by $\mathbb{T}$. The co-rotational deformation rate tensor is defined by

$$\hat{\mathbb{D}} = \mathbb{T}^C.\mathbb{D}.\mathbb{T} \qquad \text{(II.2.58)}$$

If it is assumed that $\hat{\mathbb{D}}$ is constant during the state transition $\tau_o \rightarrow \tau$, it can be shown that $\mathbb{T} = \mathbb{R}$ and that the next expression for $\hat{\mathbb{D}}$ must hold

$$\hat{\mathbb{D}} = \frac{1}{\tau-\tau_o}\hat{\mathbb{C}} = \frac{1}{\tau-\tau_o}\ln(\hat{\mathbb{F}}) = \frac{1}{\tau-\tau_o}\frac{1}{2}\ln(\mathbb{I} + 2\mathbb{E}) \qquad \text{(II.2.59)}$$

The tensor $\hat{\mathbb{C}}$ is called the logarithmic strain tensor.

The CRS coordinates

Employing the Lagrangian formulation, the Material Reference System (MRS) is used, that is, every quantity is understood to be a function of the MRS coordinates $\underset{\sim}{m}$. The Computational Reference System (CRS), which can move independently of the material, is introduced into the AEL formulation in such a way that each MRS point coincides with only one CRS point and vice versa in every state.

Each CRS point can be identified unambiguously by a set of three independent CRS coordinates g_1, g_2 and g_3, which can be taken as elements of a column $\underset{\sim}{g}$. The columns $\underset{\sim}{g}$ of all CRS points are the elements of an invariable set G. In state τ the position vector $\vec{p}$ of CRS point $\underset{\sim}{g}$ is

$$\vec{p} = \vec{\chi}(\underset{\sim}{g},\tau) \qquad \text{(II.2.60)}$$

In state τ the function $\vec{\chi}$, which is unique, continuous and sufficiently differentiable, can be considered as a mapping $\vec{\chi} : G \rightarrow V(\tau)$, where $V(\tau)$ is the set of end points of the position vectors $\vec{p}$ of the CRS points in state τ. A subset of $V(\tau)$, containing the end points of the position vectors $\vec{p} = \vec{\chi}(\underset{\sim}{g},\tau)$, with $\underset{\sim}{g} \in G$ and g_j is constant for $j \neq i$, is called the g_i-parametric curve in state τ. The end point of every position vector $\vec{p}$ is situated on three different parametric curves.

In the preceding part of this section we introduced various quantities as a function of the MRS coordinates. In the succeeding part we introduce similar quantities as a function of the CRS coordinates.

Geometric quantities

The local CRS vector basis $\vec{\underset{\sim}{\beta}}(\underset{\sim}{g},\tau)$ is chosen right-handed and defined by

$$\vec{\underset{\sim}{\beta}} = \underset{\sim}{\nabla}_g \vec{\chi} \qquad \text{(II.2.61)}$$

where $\underset{\sim}{\nabla}_g$ is a column operator, given by

$$\underset{\sim}{\nabla}_g^T = [\frac{\partial}{\partial g_1} \frac{\partial}{\partial g_2} \frac{\partial}{\partial g_3}] \qquad \text{(II.2.62)}$$

The Jacobian $J(\underset{\sim}{g},\tau)$ of the mapping $\vec{\chi} : G \rightarrow V(\tau)$ equals the triple product of the basis vectors $\vec{\beta}_1$, $\vec{\beta}_2$ and $\vec{\beta}_3$, so that

$$J = \vec{\beta}_1 . \vec{\beta}_2 * \vec{\beta}_3 \qquad \text{(II.2.63)}$$

From the properties of $\vec{\chi} : G \to V(\tau)$ it follows that J is never equal to zero.

The reciprocal CRS vector basis $\vec{\underset{\sim}{\gamma}}(g,\tau)$ can be determined from

$$\vec{\underset{\sim}{\beta}} . \vec{\underset{\sim}{\gamma}}^T = \underline{I} \quad ; \quad \vec{\underset{\sim}{\gamma}}^T = [\vec{\gamma}_1 \; \vec{\gamma}_2 \; \vec{\gamma}_3] \tag{II.2.64}$$

It is easily shown that

$$\vec{\underset{\sim}{\beta}}^T \vec{\underset{\sim}{\gamma}} = \mathbb{I} \tag{II.2.65}$$

From this relation it follows that $\vec{\gamma}_1$, $\vec{\gamma}_2$ and $\vec{\gamma}_3$ must satisfy

$$\vec{\gamma}_1 = \frac{1}{J} \vec{\beta}_2 * \vec{\beta}_3 \; ; \quad \vec{\gamma}_2 = \frac{1}{J} \vec{\beta}_3 * \vec{\beta}_1 \; ; \quad \vec{\gamma}_3 = \frac{1}{J} \vec{\beta}_1 * \vec{\beta}_2 \tag{II.2.66}$$

Using the local reciprocal vector basis, the gradient operator can be expressed in the column operator $\underset{\sim}{\nabla}_g$ as

$$\vec{\nabla} = \vec{\underset{\sim}{\gamma}}^T \underset{\sim}{\nabla}_g \quad ; \quad \underset{\sim}{\nabla}_g = \vec{\underset{\sim}{\beta}} . \vec{\nabla} \tag{II.2.67}$$

Kinematic quantities

In every state and at each CRS point the quantity A is defined and given by $A = \alpha(g,\tau)$. The change of A at CRS point g during a state transition $\Delta\tau$ is called the CRS change of A and is denoted by $\Delta_g A$, hence

$$\Delta_g A = \alpha(g,\tau+\Delta\tau) - \alpha(g,\tau) \tag{II.2.68}$$

The CRS derivative of A is denoted by $\overset{\circ}{A}$ and defined by

$$\overset{\circ}{A} = \lim_{\Delta\tau \to 0} \frac{\Delta_g A}{\Delta\tau} \tag{II.2.69}$$

The velocity $\vec{u}$ of a CRS point is defined by

$$\vec{u} = \overset{\circ}{\vec{\chi}}(g,\tau) = \overset{\circ}{\vec{p}} = \lim_{\Delta\tau \to 0} \frac{\Delta_g \vec{p}}{\Delta\tau} \tag{II.2.70}$$

For the CRS derivatives of the vector basis, the reciprocal vector basis and the Jacobian, we find:

$$\overset{\circ}{\underset{\sim}{\vec{\beta}}} = \underset{\sim}{\vec{\beta}}.(\vec{v}\ \vec{u}) \qquad \text{(II.2.71)}$$

$$\overset{\circ}{\underset{\sim}{\vec{\gamma}}} = - \underset{\sim}{\vec{\gamma}}.(\vec{v}\ \vec{u})^{C} \qquad \text{(II.2.72)}$$

$$\overset{\circ}{J} = J\ \underset{\sim}{\vec{\gamma}}^{T}.\overset{\circ}{\underset{\sim}{\vec{\beta}}} = J\ (\vec{v}.\vec{u}) \qquad \text{(II.2.73)}$$

The boundary

A CRS point on the boundary of a three dimensional body can be identified both by the CRS coordinates $\underset{\sim}{g}$ and a set of two independent coordinates g^{*}_{1} and g^{*}_{2}, wich can be taken as the elements of a column $\underset{\sim}{g}^{*}$. The columns $\underset{\sim}{g}^{*}$ of the CRS points on the boundary are elements of a set G^{*}. We assume that the boundary is always made up of the same CRS points so that the set G^{*} is invariable. In state τ the position vector $\vec{p}$ of CRS point $\underset{\sim}{g}^{*}$ is

$$\vec{p} = \vec{\chi}^{*}(\underset{\sim}{g}^{*},\tau) \qquad \text{(II.2.74)}$$

In this state, the function $\vec{\chi}^{*}$, which is unique, continuous and sufficiently differentiable, can be considered as a mapping $\vec{\chi}^{*}: G^{*} \rightarrow V^{*}(\tau)$, where $V^{*}(\tau)$ is the set of the end points of the position vectors $\vec{p}$ of the CRS points on the boundary in state τ. A subset of $V^{*}(\tau)$, containing the end points of the position vectors $\vec{p} = \vec{\chi}^{*}(\underset{\sim}{g}^{*},\tau)$, with $\underset{\sim}{g}^{*} \in G^{*}$ and g^{*}_{j} is constant for $j \neq i$, is called the g^{*}_{i}-parametric curve in state τ. The end point of every position vector $\vec{p}$ is situated on two different parametric curves.

Geometric quantities at the boundary

At every CRS point $\underset{\sim}{g}^{*}$, the tangent vectors to the g^{*}_{1}- and g^{*}_{2}-parametric curves are independent. They are understood to be the elements $\vec{\beta}^{*}_{1}$ and $\vec{\beta}^{*}_{2}$ of a column $\underset{\sim}{\vec{\beta}}^{*}$, defined by

$$\underset{\sim}{\vec{\beta}}^{*} = \underset{\sim g}{\nabla}^{*} \vec{\chi}^{*} \quad ; \quad \underset{\sim}{\vec{\beta}}^{*T} = [\vec{\beta}_1^{*} \; \vec{\beta}_2^{*}] \tag{II.2.75}$$

where the column operator $\underset{\sim g}{\nabla}^{*}$ is given by

$$\underset{\sim g}{\nabla}^{*T} = [\frac{\partial}{\partial g_1^{*}} \; \frac{\partial}{\partial g_2^{*}}] \tag{II.2.76}$$

The Jacobian $J^{*}(\underset{\sim}{g}^{*}, \tau)$ of the mapping $\vec{\chi}^{*} : G^{*} \rightarrow V^{*}(\tau)$ is defined by

$$J^{*} = ||\vec{\beta}_1^{*} * \vec{\beta}_2^{*}|| \tag{II.2.77}$$

The unit vector, outward and normal to the boundary, $\vec{\nu}(\underset{\sim}{g}^{*}, \tau)$, can be defined by

$$\vec{\nu} = s^{*} \frac{\vec{\beta}_1^{*} * \vec{\beta}_2^{*}}{||\vec{\beta}_1^{*} * \vec{\beta}_2^{*}||} = s^{*} \frac{\vec{\beta}_1^{*} * \vec{\beta}_2^{*}}{J^{*}} \quad ; \quad s^{*2} = 1 \tag{II.2.78}$$

where s^{*} is chosen in such a way ($s^{*} = +1$ or $s^{*} = -1$) that the vector $\vec{\nu}$ is outward compared to the body.

The reciprocal vectors $\vec{\gamma}_1^{*}$ and $\vec{\gamma}_2^{*}$ can be determined from

$$\underset{\sim}{\vec{\beta}}^{*} . \underset{\sim}{\vec{\gamma}}^{*T} = \underline{I} \quad ; \quad \underset{\sim}{\vec{\gamma}}^{*T} = [\vec{\gamma}_1^{*} \; \vec{\gamma}_2^{*}] \tag{II.2.79}$$

and

$$\vec{\gamma}_1^{*} . \vec{\nu} = \vec{\gamma}_2^{*} . \vec{\nu} = 0 \tag{II.2.80}$$

The expression

$$\underset{\sim}{\vec{\beta}}^{*T} \underset{\sim}{\vec{\gamma}}^{*} = \mathbb{I} - \vec{\nu} \, \vec{\nu} \tag{II.2.81}$$

applies. The vectors $\vec{\gamma}_1^{*}$ and $\vec{\gamma}_2^{*}$ must satisfy

$$\vec{\gamma}_1^{*} = \frac{s^{*}}{J^{*}} \vec{\beta}_2 * \vec{\nu} \quad ; \quad \vec{\gamma}_2^{*} = \frac{s^{*}}{J^{*}} \vec{\nu} * \vec{\beta}_1 \tag{II.2.82}$$

The gradient operator $\vec{\nabla}^*$ at a CRS point $\underset{\sim}{g}^*$ describes variations of quantities at adjacent points on the boundary in state τ and is defined by

$$\vec{\nabla}^* = \underset{\sim}{\vec{\gamma}}^{*T} \underset{\sim}{\nabla}^*_g = \{(\mathbb{I} - \vec{\nu}\,\vec{\nu}).\vec{\nabla}\} \qquad \text{(II.2.83)}$$

Kinematic quantities at the boundary

The CRS derivatives of $\underset{\sim}{\vec{\beta}}^*$, $\underset{\sim}{\vec{\gamma}}^*$ and $\jmath^*$ are:

$$\overset{\circ}{\underset{\sim}{\vec{\beta}}}{}^* = \underset{\sim}{\vec{\beta}}^*.(\vec{\nabla}^*\vec{u}^*) = \underset{\sim}{\vec{\beta}}^*.\{(\mathbb{I} - \vec{\nu}\,\vec{\nu}).(\vec{\nabla}\,\vec{u}^*)\} \qquad \text{(II.2.84)}$$

$$\overset{\circ}{\underset{\sim}{\vec{\gamma}}}{}^* = -\underset{\sim}{\vec{\gamma}}^*.(\vec{\nabla}^*\vec{u}^*)^C = -\underset{\sim}{\vec{\gamma}}^*.\{(\vec{\nabla}\,\vec{u}^*)^C.(\mathbb{I} - \vec{\nu}\,\vec{\nu})\} \qquad \text{(II.2.85)}$$

$$\overset{\circ}{\jmath}{}^* = \jmath^*\underset{\sim}{\vec{\gamma}}^{*T}\overset{\circ}{\underset{\sim}{\vec{\beta}}}{}^* = \jmath^*(\vec{\nabla}^*.\vec{u}^*) \qquad \text{(II.2.86)}$$

The relation between MRS and CRS coordinates

In state τ, MRS point $\underset{\sim}{m}$ coincides with CRS point $\underset{\sim}{g}$. For the position vector $\vec{p}$ of these points we have

$$\vec{p} = \vec{x}(\underset{\sim}{m},\tau) = \vec{\chi}(\underset{\sim}{g},\tau) \qquad \text{(II.2.87)}$$

Since the functions $\vec{x}$ and $\vec{\chi}$ are unique, two unambiguous functions $\underset{\sim}{x}$ and $\underset{\sim}{\chi}$ exist, so that

$$\underset{\sim}{m} = \underset{\sim}{x}(\vec{p},\tau) \quad ; \quad \underset{\sim}{g} = \underset{\sim}{\chi}(\vec{p},\tau) \qquad \text{(II.2.88)}$$

Both functions are continuous and sufficiently differentiable. In state τ the coinciding MRS and CRS points are related to each other by the expressions

$$\underset{\sim}{m} = \underset{\sim}{x}(\vec{\chi}(\underset{\sim}{g},\tau),\tau) \quad ; \quad \underset{\sim}{g} = \underset{\sim}{\chi}(\vec{x}(\underset{\sim}{m},\tau),\tau) \qquad \text{(II.2.89)}$$

In state $\tau+\Delta\tau$ CRS point $\underset{\sim}{g}$ coincides with MRS point $\underset{\sim}{m}+\Delta\underset{\sim}{m}$ as is shown in figure II.2.8.

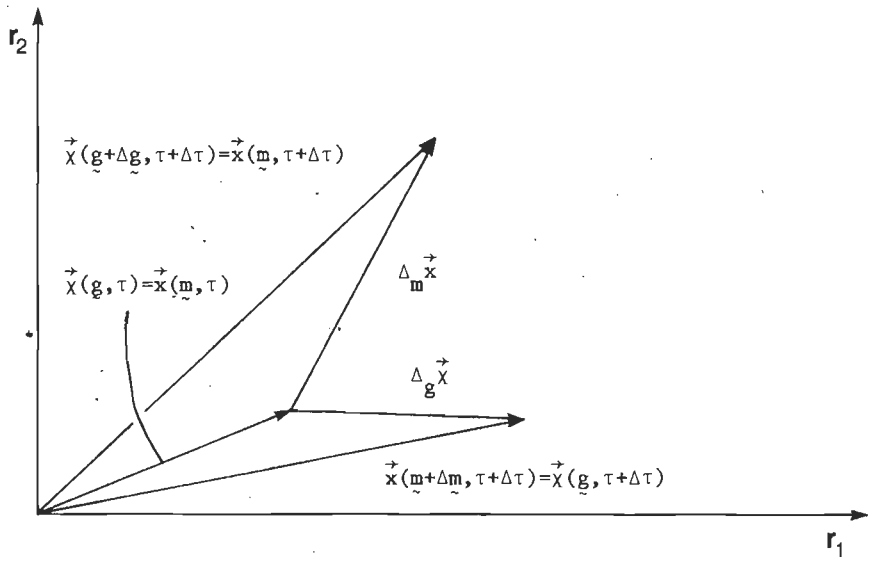

Fig. II.2.8
The position of MRS point $\underset{\sim}{m}$ *and CRS point* $\underset{\sim}{g}$ *in state* τ *and state* $\tau+\Delta\tau$

We can write

$$\vec{x}(\underset{\sim}{m}+\Delta\underset{\sim}{m},\tau+\Delta\tau) = \vec{\chi}(\underset{\sim}{g},\tau+\Delta\tau) \qquad \text{(II.2.90)}$$

Applying Taylor's theorem to expand the left-hand side, gives

$$(\underset{\sim}{\nabla}_m\vec{x})^T\Big|_{(\underset{\sim}{m},\tau+\Delta\tau)}\Delta\underset{\sim}{m} = \vec{\chi}(\underset{\sim}{g},\tau+\Delta\tau) - \vec{x}(\underset{\sim}{m},\tau+\Delta\tau) + O(\Delta\underset{\sim}{m}^2) \qquad \text{(II.2.91)}$$

where $O(\Delta\underset{\sim}{m}^2)$ represents a sum of terms which are at least quadratic in $\Delta\underset{\sim}{m}$. Using (II.2.3), (II.2.10), (II.2.68) and (II.2.87) we get

$$\vec{\underset{\sim}{b}}^T(\underset{\sim}{m},\tau+\Delta\tau)\ \Delta\underset{\sim}{m} = \Delta_g\vec{\chi} - \Delta_m\vec{x} + O(\Delta\underset{\sim}{m}^2) \qquad \text{(II.2.92)}$$

Since $\vec{\underset{\sim}{c}}.\vec{\underset{\sim}{b}}^T = \underline{I}$ we can write

$$\Delta\underset{\sim}{m} = \vec{\underset{\sim}{c}}.(\Delta_g\vec{\chi} - \Delta_m\vec{x}) + O(\Delta\underset{\sim}{m}^2) \qquad \text{(II.2.93)}$$

In state τ the value of the quantity A can be determined by employing either or both of the functions a or α, so that

$$A = a(\underset{\sim}{m},\tau) = \alpha(\underset{\sim}{g},\tau) \qquad \text{(II.2.94)}$$

The CRS change of A during the state transition $\Delta\tau$ is

$$\Delta_g A = \alpha(\underset{\sim}{g},\tau+\Delta\tau) - \alpha(\underset{\sim}{g},\tau) = a(\underset{\sim}{m}+\Delta\underset{\sim}{m},\tau+\Delta\tau) - a(\underset{\sim}{m},\tau) \qquad \text{(II.2.95)}$$

Expanding the first term of the right-hand side of the above expression by means of Taylor's theorem, we find

$$a(\underset{\sim}{m}+\Delta\underset{\sim}{m},\tau+\Delta\tau) = a(\underset{\sim}{m},\tau+\Delta\tau) + (\nabla_{\underset{\sim}{m}} a)^T\Big|_{(\underset{\sim}{m},\tau+\Delta\tau)} \Delta\underset{\sim}{m} + O(\Delta\underset{\sim}{m}^2) \qquad \text{(II.2.96)}$$

This results in the expression for $\Delta_g A$ given below,

$$\Delta_g A = a(\underset{\sim}{m},\tau+\Delta\tau) - a(\underset{\sim}{m},\tau) + (\nabla_{\underset{\sim}{m}} a)^T\Big|_{(\underset{\sim}{m},\tau+\Delta\tau)} \Delta\underset{\sim}{m} + O(\Delta\underset{\sim}{m}^2)$$

$$= \Delta_m A + (\nabla_{\underset{\sim}{m}} a)^T\Big|_{(\underset{\sim}{m},\tau+\Delta\tau)} \Delta\underset{\sim}{m} + O(\Delta\underset{\sim}{m}^2) \qquad \text{(II.2.97)}$$

Substitution of (II.2.93) gives

$$\Delta_g A = \Delta_m A + (\Delta_g\vec{\chi} - \Delta_m\vec{x}).(\vec{\nabla}\, A)\Big|_{(\underset{\sim}{m},\tau+\Delta\tau)} + O(\Delta\underset{\sim}{m}^2) \qquad \text{(II.2.98)}$$

If the state transition is small, we may assume that the last term in (II.2.98) can be neglected and that

$$(\vec{\nabla}\, A)\Big|_{(\underset{\sim}{m},\tau+\Delta\tau)} \approx (\vec{\nabla}\, A)\Big|_{(\underset{\sim}{m},\tau)} \qquad \text{(II.2.99)}$$

This leads to the following relationship between the CRS change $\Delta_g A$ and the MRS change $\Delta_m A$

$$\Delta_g A = \Delta_m A + (\Delta_g\vec{\chi} - \Delta_m\vec{x}).(\vec{\nabla}\, A) \qquad \text{(II.2.100)}$$

II.3 Stress tensors

The Cauchy stress tensor
The co-rotational Cauchy stress tensor

The Cauchy stress tensor

The stress vector $\vec{t}$ at MRS point $\vec{p} = \vec{x}(\underset{\sim}{m},\tau)$ on a plane passing through that point, is assigned to the unit vector $\vec{n}$, normal and outward to that plane at point $\vec{p}$, by a transformation $\underset{\sim}{\sigma}(\underset{\sim}{m},\tau)$. This transformation can be shown to be linear - Lai et al.(1978) - and is called the Cauchy stress tensor. We can write

$$\vec{t} = \underset{\sim}{\sigma}.\vec{n} \qquad \text{(II.3.1)}$$

In figure II.3.1 the stress vector on a plane S through point $\vec{p}$ is shown. The normal stress at $\vec{p}$ on the same plane is given by

$$t_n = \vec{n}.\vec{t} = \vec{n}.\underset{\sim}{\sigma}.\vec{n} \qquad \text{(II.3.2)}$$

The magnitude of the shearing stress at $\vec{p}$ on the plane is

$$t_s = \sqrt{||\vec{t}||^2 - t_n^2} \qquad \text{(II.3.3)}$$

The co-rotational Cauchy stress tensor

Following the introduction of co-rotational kinematic quantities in section II.2, the co-rotational Cauchy stress tensor $\hat{\underset{\sim}{\sigma}}(\underset{\sim}{m},\tau)$ is defined by

$$\hat{\underset{\sim}{\sigma}} = \underset{\sim}{\Gamma}^C.\underset{\sim}{\sigma}.\underset{\sim}{\Gamma} \qquad \text{(II.3.4)}$$

Using $\dot{\underset{\sim}{\Gamma}} = \underset{\sim}{\Omega}.\underset{\sim}{\Gamma}$ we find for the MRS derivative of $\hat{\underset{\sim}{\sigma}}$

$$\dot{\hat{\underset{\sim}{\sigma}}} = \underset{\sim}{\Gamma}^C.(\dot{\underset{\sim}{\sigma}} + \underset{\sim}{\sigma}.\underset{\sim}{\Omega} + \underset{\sim}{\Omega}^C.\underset{\sim}{\sigma}).\underset{\sim}{\Gamma} \qquad \text{(II.3.5)}$$

The sum of tensors in parenthesis is called the Jaumann derivative of the Cauchy stress tensor, and is widely used in elasto-plastic analysis.

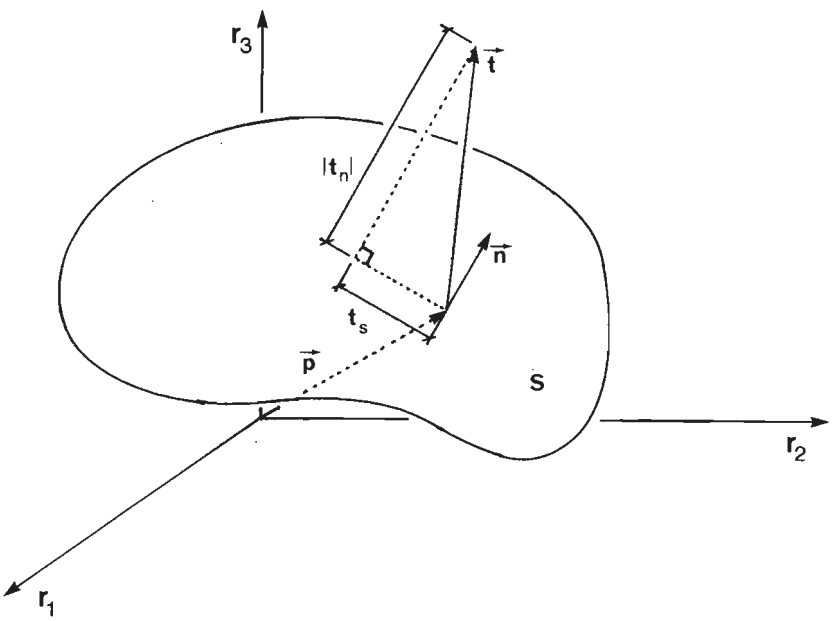

Fig. II.3.1
The stress vector on a plane S *through point* $\vec{p}$

II.4 The equilibrium equation and the principle of weighted residuals

The equilibrium equation: differential form
The equilibrium equation: integral form

The equilibrium equation: differential form

Assuming that inertia effects are negligible, it follows from the momentum and mass conservation laws that in every state and at each material point the next equilibrium equation must be satisfied

$$(\vec{\nabla}.\sigma) + \vec{q} = \vec{0} \qquad \forall\, \vec{x} \in V(\tau) \tag{II.4.1}$$

The vector $\vec{q}$ represents the body force per unit volume in state τ. From the moment of momentum conservation law it follows that the Cauchy stress tensor is symmetric, hence

$$\sigma = \sigma^{C} \qquad \forall\, \vec{x} \in V(\tau) \tag{II.4.2}$$

Since each material point and thus each MRS point always coincides with one single, yet not necessarily the same, CRS point, equations (II.4.1) and (II.4.2) have to be satisfied at each CRS point in every state τ. Simultaneously the stress distribution and the deformation have to satisfy the constitutive equation, the strain-displacement relationship, the kinematic boundary conditions at $V_r^* \subset V^*$ and the dynamic boundary conditions at $V_p^* \backslash V_r^*$, where V^* is the coincident boundary of CRS and MRS. Since, generally speaking, an exact solution of the above equations cannot be found, we shall try to determine an approximated solution. Equations (II.4.1) and (II.4.2) are not very suitable for this purpose and thus an integral formulation is introduced.

The equilibrium equation: integral form

According to the principle of weighted residuals, the equilibrium equation (II.4.1) is equivalent to the requirement that the integral equation given below is satisfied in every state τ for every allowable weighting function $\vec{w}(g,\tau)$

$$\int_{V(\tau)} \vec{w}.[(\vec{\nabla}.\sigma) + \vec{q}]\, dV = 0 \qquad \text{(II.4.3)}$$

The weighting functions $\vec{w}$ have to meet certain requirements, which will be the case, if these functions are piecewise continuous (see Zienkiewicz (1977)).

After choosing special weighting functions $\vec{w}$, equation (II.4.3) can be used to determine approximated solutions for the equilibrium equation. To relax the requirements as regards $\vec{\sigma}$, the term $\vec{w}.(\vec{\nabla}.\sigma)$ in (II.4.3) is integrated by parts. This requires the weighting function to be piecewise differentiable. Applying Gauss' law and using $\vec{t}^* = \vec{n}.\sigma$, we arrive at

$$\int_{V(t)} (\vec{\nabla}\,\vec{w})^C : \sigma\, dV = \int_{V(t)} \vec{w}.\vec{q}\, dV + \int_{V^*(t)} \vec{w}.\vec{t}^*\, dV^* \qquad \text{(II.4.4)}$$

Since the integrals over $V(t)$ and $V^*(t)$ are extremely difficult to evaluate, the integrations are carried out over the sets G and G^*. With $dV = \jmath\, dG$, $dV^* = \jmath^* dG^*$ and $\vec{\nabla} = \vec{\gamma}^T \nabla_g$ the above equation becomes

$$\int_G (\nabla_g \vec{w})^T \vec{\gamma} : \sigma\, \jmath\, dG = \int_G \vec{w}.\vec{q}\, \jmath\, dG + \int_{G^*} \vec{w}.\vec{t}^*\, \jmath^*\, dG^* \qquad \text{(II.4.5)}$$

where $\jmath = \vec{\beta}_1.\vec{\beta}_2 * \vec{\beta}_3$ is the Jacobian of the mapping $\vec{\chi} : G \to V(\tau)$ and $\jmath^* = ||\vec{\beta}_1^* * \vec{\beta}_2^*||$ the Jacobian of the mapping $\vec{\chi}^* : G^* \to V^*(\tau)$.

II.5 A constitutive equation for time independent elasto-plastic material behaviour

A constitutive equation for elastic material behaviour

If the material behaviour at an MRS point is purely elastic, the MRS derivative of the co-rotational Cauchy stress tensor and deformation rate tensor must satisfy the next constitutive equation

$$\mathring{\hat{\mathbf{\sigma}}} = {}^4\hat{\mathbf{C}} : \hat{\mathbf{D}} \qquad \text{(II.5.1)}$$

In general the fourth-order elastic material tensor ${}^4\hat{\mathbf{C}}$ is a function of the stretch tensor $\mathbf{U}$, compared to the stress-free state, and a set H, containing history parameters, which do not change during purely elastic deformation (for detailed discussion of ${}^4\hat{\mathbf{C}}$ see for instance Hutchinson (1978) and Nagtegaal & De Jong (1980)). In this report we assume, as is usually done, that ${}^4\hat{\mathbf{C}}$ is constant at an MRS point. This tensor is invertible and, owing to the symmetry of $\mathring{\hat{\mathbf{\sigma}}}$, left-symmetrical. On account of the symmetry of $\hat{\mathbf{D}}$, ${}^4\hat{\mathbf{C}}$ may be chosen right-symmetrical.

Elasto-plastic material behaviour

It is assumed that, if the material behaviour at an MRS point is elasto-plastic, the MRS derivative of the co-rotational Cauchy stress tensor and the co-rotational deformation rate tensor are related by a

constitutive equation similar to (II.5.1)

$$\dot{\hat{\sigma}} = {}^4\hat{\mathbb{L}}:\hat{\mathbb{D}} \qquad \text{(II.5.2)}$$

To determine the fourth-order tensor ${}^4\hat{\mathbb{L}}$, the first thing to do is to introduce a yield condition. After this the deformation rate tensor $\hat{\mathbb{D}}$ is written as the sum of a tensor $\hat{\mathbb{D}}^e$, representing the elastic deformation, and a tensor $\hat{\mathbb{D}}^p$, representing the plastic deformation. The next step is to write $\hat{\mathbb{D}}^p$ as a function of $\hat{\mathbb{D}}$. For this purpose an associated flow rule is assumed and assumptions are made concerning the MRS derivative of the history parameters. Because of the symmetry of $\dot{\hat{\sigma}}$ and $\hat{\mathbb{D}}$ the tensor ${}^4\hat{\mathbb{L}}$ is left-symmetrical and may be chosen right-symmetrical.

The yield condition

It is assumed that for plastic deformation to occur at a material point with MRS coordinates $\underset{\sim}{m}$, it is necessary that a scalar function of the co-rotational Cauchy stress tensor $\hat{\sigma}(\underset{\sim}{m})$ has reached a certain limit value. This value depends on the deformation history of the material at MRS point $\underset{\sim}{m}$, which is characterised by a set of history parameters H, which change during plastic deformation only. Hence, plastic deformation can occur only if the yield condition given below is satisfied

$$f(\hat{\sigma},H) = 0 \qquad \text{(II.5.3)}$$

The value of $f(\hat{\sigma},H)$ will never exceed zero, so that, during plastic deformation the consistency equation

$$\dot{f} = \frac{\partial f}{\partial \hat{\sigma}}:\dot{\hat{\sigma}} + \frac{\partial f}{\partial H}*\dot{H} = 0 \qquad \text{(II.5.4)}$$

must be satisfied. The symbol * denotes a multiplication if H is a scalar, a dot product if H is a vector and a double dot product if H is a second-order tensor. We will now discuss $\hat{\mathbb{D}}$ and $\dot{H}$.

The decomposition of the deformation rate tensor

Following Nagtegaal & De Jong (1980) the deformation rate tensor $\hat{\mathbb{D}}$ is written as the sum of a tensor $\hat{\mathbb{D}}^e$ representing the elastic deformation, and a tensor $\hat{\mathbb{D}}^p$ representing the plastic deformation. Tensor $\hat{\mathbb{D}}^e$ is defined by the following expression

$$\overset{\circ}{\hat{\boldsymbol{\sigma}}} = {}^4\hat{\mathbb{C}} : \hat{\mathbb{D}}^e \qquad \text{(II.5.5)}$$

The tensor $\hat{\mathbb{D}}^p$ is defined by

$$\hat{\mathbb{D}}^p = \hat{\mathbb{D}} - \hat{\mathbb{D}}^e \qquad \text{(II.5.6)}$$

Combination of (II.5.5) and (II.5.6) gives

$$\overset{\circ}{\hat{\boldsymbol{\sigma}}} = {}^4\hat{\mathbb{C}} : (\hat{\mathbb{D}} - \hat{\mathbb{D}}^p) \qquad \text{(II.5.7)}$$

It is assumed that the material behaviour during elasto-plastic deformation obeys an associated flow rule, that is

$$\hat{\mathbb{D}}^p = \alpha \frac{\partial f}{\partial \hat{\boldsymbol{\sigma}}} \qquad \text{(II.5.8)}$$

If the "length" of $\frac{\partial f}{\partial \hat{\boldsymbol{\sigma}}}$ is denoted by β and its "direction" by the normalized tensor $\mathbb{m}$, we get

$$\hat{\mathbb{D}}^p = \alpha \, \beta \, \mathbb{m} = \zeta \, \mathbb{m} \qquad \text{(II.5.9)}$$

Substitution in (II.5.7) results in

$$\overset{\circ}{\hat{\boldsymbol{\sigma}}} = {}^4\hat{\mathbb{C}} : \hat{\mathbb{D}} - \zeta \, {}^4\hat{\mathbb{C}} : \mathbb{m} \qquad \text{(II.5.10)}$$

The MRS derivative of the history parameters

It is assumed that the MRS derivative of the history parameters $\mathbb{H}$ is a function of the co-rotational plastic deformation rate tensor $\hat{\mathbb{D}}^p$,

so that

$$\dot{H} = k(\hat{\mathbb{D}}^P) = k(\zeta\ \mathbf{n}) \tag{II.5.11}$$

The function k is such that

$$\dot{H} = k(\zeta\ \mathbf{n}) = \zeta\ k(\mathbf{n}) \tag{II.5.12}$$

A constitutive equation for time independent elasto-plastic material behaviour

Applying $\frac{\partial f}{\partial \hat{\boldsymbol{\sigma}}} = \beta\ \mathbf{n}$ the consistency equation (II.5.4) becomes

$$\beta\ \mathbf{n}:\dot{\boldsymbol{\sigma}} + \frac{\partial f}{\partial H} * \dot{H} = 0 \tag{II.5.13}$$

Substituting (II.5.10) and (II.5.12) in (II.5.13) results in

$$\beta\ \mathbf{n}:\hat{\mathbb{C}}^4:\hat{\mathbb{D}} - \beta\ \zeta\ \mathbf{n}:\hat{\mathbb{C}}^4:\mathbf{n} + \zeta\ \frac{\partial f}{\partial H} * k(\mathbf{n}) = 0 \tag{II.5.14}$$

For ζ we can solve

$$\zeta = \frac{\mathbf{n}:\hat{\mathbb{C}}^4:\hat{\mathbb{D}}}{\mathbf{n}:\hat{\mathbb{C}}^4:\mathbf{n} - \frac{1}{\beta}\frac{\partial f}{\partial H} * k(\mathbf{n})} \tag{II.5.15}$$

Substituting in (II.5.9) results in the relation between $\hat{\mathbb{D}}^P$ and $\hat{\mathbb{D}}$ given below

$$\hat{\mathbb{D}}^P = \frac{\mathbf{n}\ \mathbf{n}:\hat{\mathbb{C}}^4}{\mathbf{n}:\hat{\mathbb{C}}^4:\mathbf{n} - \frac{1}{\beta}\frac{\partial f}{\partial H} * k(\mathbf{n})} :\hat{\mathbb{D}} \tag{II.5.16}$$

Substitution of (II.5.16) in (II.5.7) finally results in the constitutive equation

$$\dot{\hat{\boldsymbol{\sigma}}} = \left[\hat{\mathbb{C}}^4 - \frac{\hat{\mathbb{C}}^4:\mathbf{n}\ \mathbf{n}:\hat{\mathbb{C}}^4}{\mathbf{n}:\hat{\mathbb{C}}^4:\mathbf{n} - \frac{1}{\beta}\frac{\partial f}{\partial H} * k(\mathbf{n})}\right]:\hat{\mathbb{D}} = \hat{\mathbb{L}}^4:\hat{\mathbb{D}} \tag{II.5.17}$$

III Discretisation

III.1 Introduction

In order to determine the MRS change of the co-rotational Cauchy stress tensor during a state transition, the constitutive equation (II.5.17) has to be integrated. If, during the state transition $\Delta\tau$, the co-rotational deformation rate tensor $\hat{\mathbb{D}}$ is not a known, explicit function of the state parameter τ, integration can not be carried out. In that case an incremental method is employed, according to which the state transition is effected in a number of steps, the increments. The chosen size of an increment must allow the assumption that $\hat{\mathbb{D}}$ is constant during that increment. Starting from a known state τ_o, the beginning of an increment, the change of all relevant quantities should be determined in such a way that the weighted residual equation (II.4.5) is satisfied for every allowable weighting function, in state τ_e, the end of the increment. The change of a quantity ϕ during an increment is called the incremental change of ϕ and is denoted by $\Delta\phi$, where $\Delta\phi = \phi(\tau_e) - \phi(\tau_o) = \phi^e - \phi^o$. This incremental method, which in fact is a discretisation of a state transition, will be discussed in section III.2. In literature the method is also referred to as the incremental method of weighted residuals.

Though it is usually impossible to satisfy (II.4.5) in state τ_e for every allowable weighting function, this equation can be satisfied for every weighting function in a confined class. In this way an approximated solution for the equilibrium equation in state τ_e is

obtained. To handle integration over geometrical complex volumes and boundaries and to obtain a good approximated solution, despite the fact that a simple weighting function is used, the finite element method is employed. According to this method the CRS is subdivided into subregions of rather simple geometry: the elements. In every element the weighting function and the incremental change of some relevant quantities are interpolated between the values of these quantities at a limited number of CRS points belonging to this element, the element nodal points. Known and simple functions of the CRS coordinates $\underset{\sim}{g}$ are used for the interpolation. The finite element method is discussed in section III.3.

To determine whether the accuracy of the approximated solution is good enough and, if this is the case, to carry out the next incremental calculation, certain material-associated quantities must have a known value at various CRS points. Because the CRS is not material-associated, it is impossible to calculate these values directly. A special method which is discussed in section III.4 has to be used.

III.2 The incremental method

Starting from the known state τ_o, the beginning of the increment, the incremental changes of the reciprocal vector basis $\vec{\underset{\sim}{\gamma}}$, the Cauchy stress tensor $\underset{\sim}{\sigma}$, the boundary load $\vec{t}^*$, the Jacobians J of the mapping $\vec{\chi} : G \to V$ and J^* of the mapping $\vec{\chi}^* : G^* \to V^*$ have to be determined in such a way that in state τ_e, the end of the increment, the equation

$$\int_G (\underset{\sim}{\nabla}_g \vec{w})^{T\rightarrow} \vec{\underset{\sim}{\gamma}} : \underset{\sim}{\sigma}\, J\, dG = \int_G \vec{w}.\vec{q}\, J\, dG + \int_{G^*} \vec{w}.\vec{t}^*\, J^*\, dG^* \qquad \text{(III.2.1)}$$

is satisfied for every allowable weighting function $\vec{w}$. In addition to the above weighted residual equation, the constitutive equation, the strain-displacement relations and the kinematic and dynamic boundary conditions have also to be satisfied.

We assume the body force per unit volume, $\vec{q}$, to have a known value at every point. The quantities in (III.2.1) whose value is not known at every CRS point in state τ_e, are $\vec{\underset{\sim}{\gamma}}$, $\underset{\sim}{\sigma}$, $\vec{t}^*$, J and J^*. Each of these quantities can be written as a function of the incremental displacements of either the CRS points or the MRS points. In view of (II.2.72), (II.2.73) and (II.2.86) we can write:

$$\vec{\underset{\sim}{\gamma}} = \vec{\underset{\sim}{\gamma}}^o + \Delta_g \vec{\underset{\sim}{\gamma}} = \vec{\underset{\sim}{\gamma}}^o - \vec{\underset{\sim}{\gamma}}^o . (\underset{\sim}{\nabla}_g \Delta_g \vec{\chi})^{T\rightarrow o} \vec{\underset{\sim}{\gamma}}^o \qquad \text{(III.2.2)}$$

$$J = J^o + \Delta_g J = J^o + J^o \underset{\sim}{\gamma}^{o\rightarrow oT} . (\underset{\sim}{\nabla}_g \Delta_g \vec{\chi}) \qquad \text{(III.2.3)}$$

$$J^* = J^{*o} + \Delta_g J^* = J^{*o} + J^{*o} \underset{\sim}{\gamma}^{*o\rightarrow *oT} . (\underset{\sim}{\nabla}^*_g \Delta_g \vec{\chi}) \qquad \text{(III.2.4)}$$

Further we can write

$$\underset{\sim}{\sigma} = \underset{\sim}{\sigma}^o + \Delta_g \underset{\sim}{\sigma} \qquad \text{(III.2.5)}$$

Since the Cauchy stress tensor is a material-associated quantity, the CRS change $\Delta_g \underset{\sim}{\sigma}$ is expressed in the MRS change $\Delta_m \underset{\sim}{\sigma}$ in accordance with

expression (II.2.98)

$$\Delta_g \sigma = \Delta_m \sigma + (\Delta_g \vec{\chi} - \Delta_m \vec{x}).(\vec{\nabla}\ \sigma)\Big|_{(\underset{\sim}{m}, \tau_o + \Delta\tau)} + \mathcal{O}(\Delta \underset{\sim}{m}^2) \qquad \text{(III.2.6)}$$

where $\mathcal{O}(\Delta \underset{\sim}{m}^2)$ represents a sum of terms which are at least quadratic in

$$\Delta \underset{\sim}{m} = \underset{\sim}{x}(\vec{\chi}(\underset{\sim}{g}, \tau_e), \tau_e) - \underset{\sim}{x}(\vec{\chi}(\underset{\sim}{g}, \tau_o), \tau_o) \qquad \text{(III.2.7)}$$

this being the change of the MRS coordinates of the CRS point $\underset{\sim}{g}$ during the state transition $\Delta\tau$. We now assume the increment to be taken so small that $\mathcal{O}(\Delta \underset{\sim}{m}^2)$ in (III.2.6) can be neglected and $(\vec{\nabla}\ \sigma)$ determined in state τ_o. Thus we find for σ that

$$\sigma = \sigma^o + \Delta_m \sigma + \Delta_g \vec{\chi}.(\vec{\nabla}\ \sigma) - \Delta_m \vec{x}.(\vec{\nabla}\ \sigma) \qquad \text{(III.2.8)}$$

applies. After integrating the constitutive equation (II.5.17), $\Delta_m \sigma$ can be expressed in $\Delta_m \vec{x}$, formally: $\Delta_m \sigma = \mathfrak{f}(\Delta_m \vec{x})$, which results in

$$\sigma = \sigma^o + \mathfrak{f}(\Delta_m \vec{x}) + \Delta_g \vec{\chi}.(\vec{\nabla}\ \sigma) - \Delta_m \vec{x}.(\vec{\nabla}\ \sigma) \qquad \text{(III.2.9)}$$

For $\vec{t}^*$ we can write

$$\vec{t}^* = \vec{t}^{*o} + \Delta_g \vec{t}^* = \vec{t}^{*o} + f^*(\Delta_g \vec{\chi},\ \Delta_m \vec{x}) \qquad \text{(III.2.10)}$$

where we also use a formal relationship between $\Delta_g \vec{t}^*$, $\Delta_g \vec{\chi}$ and $\Delta_m \vec{x}$, which will not be discussed further. Substitution of (III.2.2-4), (III.2.9) and (III.2.10) in (III.2.1) leads to an expression in the unknown incremental changes $\Delta_g \vec{\chi}$, $\Delta_m \vec{x}$.

III.3 The finite element method

Discretisation of the CRS
Interpolation of various quantities
Assembly of the elements

Discretisation of the CRS

Employing the finite element method the CRS is subdivided into elements. In every state, element e ($e \in \{1,2,\ldots,n\}$) consists of the same CRS points, which can therefore be identified by local CRS coordinates $\underset{\sim}{g}$, defined per element. The set of local CRS coordinates of all CRS points of element e is called G_e. The CRS points of that element, pertaining to the boundary of the CRS, constitute the set G_e^*. The integrals in (III.2.1) are written as a summation of integrals evaluated for the individual elements

$$\sum_{e=1}^{n} \int_{G_e} (\nabla_{\underset{\sim}{g}} \vec{w}_e)^T \vec{\gamma}_e : \varpi_e J_e \, dG = \sum_{e=1}^{n} \int_{G_e} \vec{w}_e . \vec{q}_e J_e \, dG$$

$$+ \sum_{e=1}^{n} \int_{G_e^*} \vec{w}_e . \vec{t}_e^* J_e^* \, dG^* \qquad \text{(III.3.1)}$$

According to (III.2.2-4), (III.2.9) and (III.2.10), $\vec{\gamma}_e$, J_e, J_e^*, ϖ_e and $\vec{t}_e^*$ can be expressed in the incremental displacements $\Delta_g \vec{x}_e$ and $\Delta_m \vec{x}_e$.

Interpolation of various quantities

The second step in applying the finite element method is the interpolation of various quantities in every element. To interpolate a quantity ϕ is to write ϕ as a linear combination of a number of known functions of the local CRS coordinates, the interpolation functions. The parameters in this linear combination are the values of ϕ in a

limited number of CRS points, the element nodal points. The interpolation functions have to meet certain requirements as is discussed by Zienkiewicz (1977).

The interpolation of the position vector of CRS point $\underset{\sim}{g}$ of element e reads as

$$\vec{\underset{\sim}{x}}_e(\underset{\sim}{g},\tau) = \underset{\sim}{\psi}^T(\underset{\sim}{g})\ \vec{\underset{\sim}{x}}_e(\tau) \qquad \text{(III.3.2)}$$

Here, $\underset{\sim}{\psi}(\underset{\sim}{g})$ is a column containing the known interpolation functions and $\vec{\underset{\sim}{x}}_e(\tau)$ a column containing the position vectors of the element nodal points. The interpolation of the incremental CRS point displacement follows directly from (III.3.2)

$$\Delta_g\vec{\underset{\sim}{x}}_e(\underset{\sim}{g}) = \underset{\sim}{\psi}^T(\underset{\sim}{g})\ \Delta_g\vec{\underset{\sim}{x}}_e \qquad \text{(III.3.3)}$$

where $\Delta_g\vec{\underset{\sim}{x}}_e$ is a column containing the incremental nodal point displacements. The incremental MRS point displacement is also interpolated. In this interpolation, the interpolation functions and the element nodal points used are identical with those used when interpolating $\Delta_g\vec{x}_e$, thus

$$\Delta_m\vec{\underset{\sim}{x}}_e(\underset{\sim}{g}) = \underset{\sim}{\psi}^T(\underset{\sim}{g})\ \Delta_m\vec{\underset{\sim}{x}}_e \qquad \text{(III.3.4)}$$

where column $\Delta_m\vec{\underset{\sim}{x}}_e$ contains the incremental displacements of the MRS points that coincide with the element nodal points in state τ_o. The interpolation of $\Delta_m\vec{\underset{\sim}{x}}_e(\underset{\sim}{g})$ implies the introduction of an approximation. Finally, the weighting function $\vec{w}_e$ is interpolated similarly to $\Delta_g\vec{x}_e$ and $\Delta_m\vec{x}_e$

$$\vec{w}_e(\underset{\sim}{g}) = \underset{\sim}{\psi}^T(\underset{\sim}{g})\ \vec{\underset{\sim}{w}}_e \qquad \text{(III.3.5)}$$

where $\vec{\underset{\sim}{w}}_e$ is a column containing the values of the weighting function in the element nodal points.

Assembly of the elements

After substitution of (III.3.5) in (III.3.1) we find

$$\sum_{e=1}^{n} \vec{\underset{\sim}{w}}_e^T \cdot \int_{G_e} (\nabla_{\underset{\sim}{g}} \underset{\sim}{\psi}^T)^T \vec{\underset{\sim}{\gamma}}_e \cdot \sigma_e \rfloor_e \, dG = \sum_{e=1}^{n} \vec{\underset{\sim}{w}}_e^T \cdot \int_{G_e} \underset{\sim}{\psi} \, \vec{\underset{\sim}{q}}_e \rfloor_e \, dG$$

$$+ \sum_{e=1}^{n} \vec{\underset{\sim}{w}}_e^T \cdot \int_{G_e^*} \underset{\sim}{\psi} \, \vec{\underset{\sim}{t}}_e^* \rfloor_e^* \, dG^* \qquad \text{(III.3.6)}$$

With the introduction of the vector columns $\vec{\underset{\sim}{m}}_{1e}$ and $\vec{\underset{\sim}{r}}_{1e}$ according to

$$\vec{\underset{\sim}{m}}_{1e}(\Delta_g \vec{\underset{\sim}{\chi}}_e, \Delta_m \vec{\underset{\sim}{x}}_e) = \int_{G_e} (\nabla_{\underset{\sim}{g}} \underset{\sim}{\psi}^T)^T \vec{\underset{\sim}{\gamma}}_e \cdot \sigma_e \rfloor_e \, dG \quad \text{and} \qquad \text{(III.3.7)}$$

$$\vec{\underset{\sim}{r}}_{1e}(\Delta_g \vec{\underset{\sim}{\chi}}_e, \Delta_m \vec{\underset{\sim}{x}}_e) = \int_{G_e} \underset{\sim}{\psi} \, \vec{\underset{\sim}{q}}_e \rfloor_e \, dG + \int_{G_e^*} \underset{\sim}{\psi} \, \vec{\underset{\sim}{t}}_e^* \rfloor_e^* \, dG^* \qquad \text{(III.3.8)}$$

(III.3.6) becomes

$$\sum_{e=1}^{n} \vec{\underset{\sim}{w}}_e^T \cdot \vec{\underset{\sim}{m}}_{1e}(\Delta_g \vec{\underset{\sim}{\chi}}_e, \Delta_m \vec{\underset{\sim}{x}}_e) = \sum_{e=1}^{n} \vec{\underset{\sim}{w}}_e^T \cdot \vec{\underset{\sim}{r}}_{1e}(\Delta_g \vec{\underset{\sim}{\chi}}_e, \Delta_m \vec{\underset{\sim}{x}}_e) \qquad \text{(III.3.9)}$$

After assembling the elements in the usual way we find

$$\vec{\underset{\sim}{w}}^T \cdot \vec{\underset{\sim}{m}}_1(\Delta_g \vec{\underset{\sim}{\chi}}, \Delta_m \vec{\underset{\sim}{x}}) = \vec{\underset{\sim}{w}}^T \cdot \vec{\underset{\sim}{r}}_1(\Delta_g \vec{\underset{\sim}{\chi}}, \Delta_m \vec{\underset{\sim}{x}}) \qquad \text{(III.3.10)}$$

The columns in the above expression contain the values of the various quantities in all the nodal points of the element mesh. The elements of a column containing the element nodal point values, denoted by $\vec{\underset{\sim}{w}}_e$, constitute a subset of the elements of the corresponding column $\vec{\underset{\sim}{w}}$ containing all the nodal point values. The requirement that (III.2.1) is satisfied for all weighting functions, interpolated in every element according to (III.3.5), implies that (III.3.10) has to be satisfied for all possible nodal point values of $\vec{\underset{\sim}{w}}$, thus for every possible column $\vec{\underset{\sim}{w}}$. It is easily seen therefore that the incremental displacements $\Delta_g \vec{\underset{\sim}{\chi}}$ and $\Delta_m \vec{\underset{\sim}{x}}$ have to satisfy the set of vector equations

$$\vec{\underset{\sim}{m}}_1(\Delta_g \vec{\underset{\sim}{\chi}}, \Delta_m \vec{\underset{\sim}{x}}) = \vec{\underset{\sim}{r}}_1(\Delta_g \vec{\underset{\sim}{\chi}}, \Delta_m \vec{\underset{\sim}{x}}) \qquad \text{(III.3.11)}$$

III.4 Calculation of material-associated quantities

The necessary use of a special method
The follower points
Interpolation of material-associated quantities

The necessary use of a special method

The solution process used to solve the set of vector equations (III.3.11) will be discussed in chapter V. In this process a number of approximated solutions for (III.3.11) are determined. To establish the accuracy of an approximated solution, the extent to which this solution really satisfies the set of equations must be determined. This set as described in section III.3 results from the assembly of terms evaluated per element. To evaluate each of these terms, one has to integrate over the element domain. This integration is done numerically: the value of the integrand is calculated at the integration points of the element, after which a weighted summation of these values is carried out. Some of these integrands are a function of material-associated quantities, such as the Cauchy stress tensor and its gradient. Since the integration points are CRS points, which usually do not follow the material, it is not possible to determine the value of this material-associated quantities directly.

The follower points

In determining the value of material-associated quantities at the integration points of the elements, we make use of what are called follower points. These are MRS points, pertaining to a subset of M. This subset is defined at the beginning of each increment and does not change during that increment. In figure III.4.1a the element mesh is shown at the beginning of an increment. The follower points are defined as the vertices of the subregions into which each element is subdivided. Such a subregion is called a cell. In figure III.4.1b the element mesh in state τ of the same increment is shown. The follower points in that state are also shown. As both the deformation history

and the location of every follower point are known, the value of the material-associated quantities at that point can be calculated.

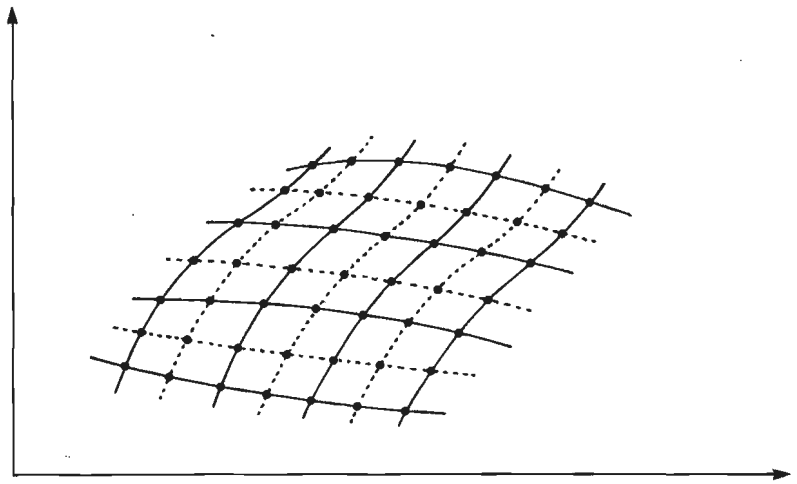

Fig. III.4.1a

Part of an element mesh with follower points (•) and cells (⬚) in state τ_o, the beginning of an increment

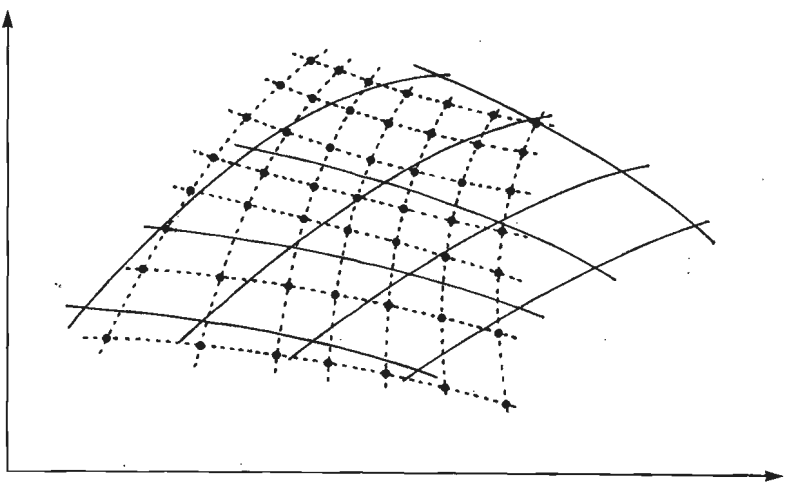

Fig. III.4.1b

Part of an element mesh with follower points (•) and cells (⬚) in state τ

Interpolation of material-associated quantities

After calculating the values of the material-associated quantities at the follower points, the values at the integration points of the elements have to be determined. This is done by interpolation between the values at the follower points of every cell in which one or more integration points are situated. An integration point within a cell is shown in figure III.4.2.

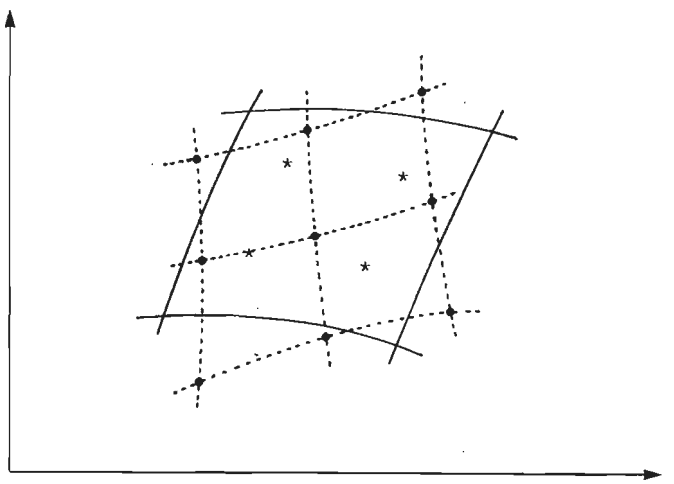

Fig. III.4.2
Part of an element mesh with follower points (•), cells (□) and integration points (*) in state τ

The value of the Cauchy stress tensor and the history parameters are determined at the nodal points as well, likewise by interpolation in the cells which contain these points. Then the gradient of the Cauchy stress tensor at every integration point is determined by interpolation between the values at the nodal points of the element in which the integration point is situated. The information at the nodal points is used also to determine the stresses and history parameters at the new follower points at the beginning of the next increment.

IV The CRS determination process

IV.1 Introduction

For every nodal point there is one vector equation in the set (III.3.11). The equation for a nodal point contains the incremental displacement vectors $\Delta_g\vec{x}$ and $\Delta_m\vec{x}$, which can both be unknown. The number of unknowns in the set of equations may be up to twice the number of equations which consequently cannot be solved. Specifying the nodal point displacements and the boundary conditions must lead to a solvable set of equations. The nodal point displacements must be such that there is always a unique relationship between CRS and MRS. Apart from this they may be chosen freely.

The freedom in specifying the nodal point displacements enables certain requirements concerning element shape and element size to be met. The shape affects the accuracy of the numerical integrations carried out over the element. A good shape can be indicated for every type of element. The element size affects the error which is possibly introduced by interpolating $\Delta_m\vec{x}$. If the number of elements and their interconnection is constant, the optimum size of an element is not known à priori, but depends on the condition of the material, coinciding with the element in that state. The requirements as to element shape may be incompatible with those affecting element size. In that case a compromise between the requirements must be sought.

One known procedure used to specify the nodal point displacements is the rezoning method (see Gelten & De Jong (1981)). In the first step, the rezoning, the free nodal point positions are determined at the beginning of the increment to reduce the average deviation of the optimum shape and size of elements to a minimum, this average being taken over all elements. The new nodal point positions can be

determined automatically by means of a mesh generator - for instance Triquamesh (Schoofs et al. (1979)) -. In the second, the deformation step, the set of vector equations (III.3.11) is solved, with $\Delta_g \vec{\underset{\sim}{x}}$ chosen equal to $\Delta_m \vec{\underset{\sim}{x}}$,thus employing a Lagrangian formulation. The total incremental nodal point displacements are the summation of the displacements during both the rezoning and the deformation steps.

Another procedure is presented in this thesis and used to specify the nodal point positions. By this method the nodal point displacements are understood to be the result of the deformation of a fictitious material to which the CRS is associated and which progresses simultaneously with the deformation of the real material with which the MRS is associated. To determine this deformation, each element is considered individually together with the fictitious material with which it is associated. In the current state τ, the stresses in this material are determined compared to a state τ_f, in which the material is stress-free and both shape and size of the element are optimal. The load needed to effect the deformation from state τ_f to state τ is determined so as to meet the requirement that the equilibrium equation has to be satisfied in state τ, at every point of the fictitious material. After assembling the elements, the total load on the fictitious material is replaced by equivalent nodal forces. Subsequently these forces are relaxed, after which the deformation of the fictitious material is effected by the internal stresses and the forces resulting from the coupling between CRS and MRS. Following the procedure described in the preceding chapters, a set of vector equations in the incremental nodal point displacements can be formulated. This set is simultaneous with the set (III.3.11) because of the relationship between CRS and MRS. Solving these simultaneous sets gives $\Delta_g \vec{\underset{\sim}{x}}$ and $\Delta_m \vec{\underset{\sim}{x}}$. The nodal point displacements, viz. the deformation of the fictitious material, will be so as to minimize the average deviation of the optimum element shape and size. When the above method is used, the number of elements and their interconnection does not change. This restriction is not essential, yet makes the method easier to describe and apply. In the next section the CRS determination process is described. Symbols of quantities, which refer to the fictitious material, are overlined.

IV.2 The CRS determination process as a deformation process

The fictitious material
The optimum geometry of an element
The element nodal forces
Relaxation of the nodal forces

The fictitious material

The CRS is assumed to be associated with a fictitious material. To describe the deformation of and the stresses in this material we use the same quantities as in section II.2. The material behaviour is assumed to be isotropic and elastic. On the analogy of (II.5.1) we can write

$$\hat{\underline{\sigma}} = {}^4\hat{\mathbb{C}} : \hat{\underline{D}} \qquad \text{(IV.2.1)}$$

where $\hat{\underline{\sigma}}$ and $\hat{\underline{D}}$ are the co-rotational Cauchy stress tensor and deformation rate tensor respectively. The fourth-order elastic material tensor ${}^4\hat{\mathbb{C}}$ is assumed to be constant.

The optimum geometry of an element

In every known state τ we can indicate the optimum shape and size of every element. This is described in detail in chapter V for one particular element. In the state τ_f, each element is successively isolated from the element mesh and has the optimum shape and size. The fictitious material associated with the element under consideration is stress-free (see figure IV.2.1). The deformation tensor, which maps state τ_f into state τ, is denoted as $\bar{\underline{F}}^f$. Without any restrictions to generality we may assume the co-rotational deformation rate tensor to be constant during this state transition. Then, on the analogy of (II.2.59), we can write

$$\hat{\underline{D}}^f = \frac{1}{\tau - \tau_f} \hat{\underline{C}}^f = \frac{1}{\tau - \tau_f} \frac{1}{2} \ln(\underline{I} + 2\bar{\underline{E}}^f) \qquad \text{(IV.2.2)}$$

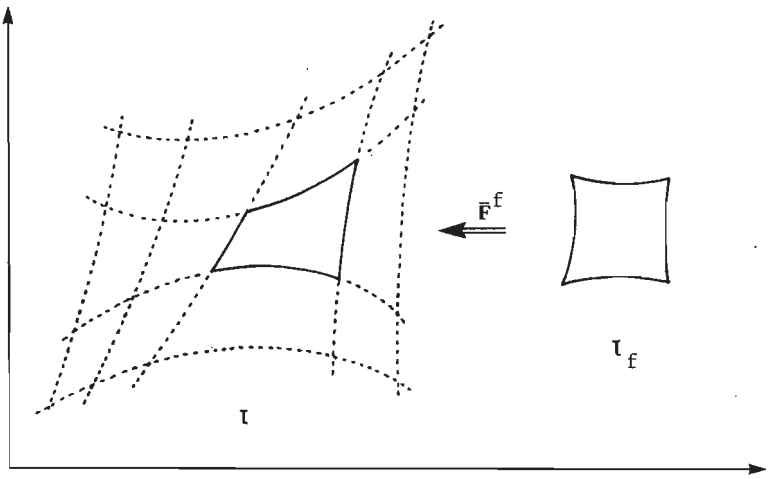

Fig. IV.2.1

Part of an element mesh in state τ and the optimum geometry of one isolated element in state τ_f

where $\hat{\bar{\mathbb{C}}}^f$ is the logarithmic and $\bar{\mathbb{E}}^f$ the Green-Lagrange strain tensor, both considered with respect to the state τ_f. Integrating (IV.2.1) results in the co-rotational Cauchy stress tensor at a point of the fictitious material in state τ

$$\hat{\bar{\boldsymbol{\sigma}}}^f = 4\hat{\mathbb{C}} : \frac{1}{2}\ln(\mathbb{I} + 2\bar{\mathbb{E}}^f) \qquad \text{(IV.2.3)}$$

If $\bar{\mathbb{R}}^f$ is the rotation tensor in the polar decomposition of $\bar{\mathbb{F}}^f$, the Cauchy stress tensor becomes

$$\bar{\boldsymbol{\sigma}}^f = \bar{\mathbb{R}}^f . \hat{\bar{\boldsymbol{\sigma}}}^f . \bar{\mathbb{R}}^{fc} \qquad \text{(IV.2.4)}$$

The element nodal forces

For the fictitious material associated with one isolated element, the deformation from state τ_f to state τ can be effected by means of a

volume load $\vec{\underset{\sim}{q}}$ and a boundary load $\vec{\underset{\sim}{p}}$, as is shown in figure IV.2.2a. These loads must be so as to satisfy in state τ, the equilibrium equation $(\vec{\nabla}.\bar{\sigma}^f) + \vec{\underset{\sim}{q}} = \vec{0}$ at every internal point of the element. The equation $\vec{\underset{\sim}{p}} = \bar{\sigma}^f.\vec{\nu}$ must be satisfied at every point of the element boundary. Assembling the thus loaded isolated elements produces the body of fictitious material with which the CRS is associated. It is obvious that this body has the same geometry as the body considered in the forming process. It is loaded with volume loads and surface loads as can be seen in figure IV.2.2b. These loads are replaced by equivalent nodal forces, denoted by $\vec{\underset{\sim}{\rho}}$, resulting in the situation shown in figure IV.2.2c. These forces are determined per element and those element nodal forces are denoted by $\vec{\underset{\sim e}{\rho}}$. Using the method of weighted residuals described in section II.4, and interpolating the relevant quantities in each element as described in section III.3, it is easily shown that the element nodal forces in state τ are given by expression

$$\vec{\underset{\sim e}{\rho}} = \int_{G_e} (\nabla \underset{\sim}{g} \underset{\sim}{\psi}^T)^T \vec{\underset{\sim e}{\gamma}}.\bar{\sigma}^f_e \, dG \qquad \text{(IV.2.5)}$$

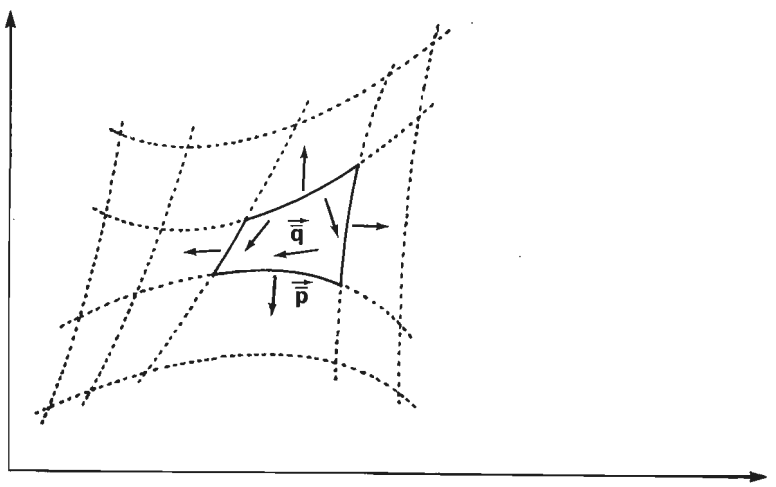

Fig. IV.2.2a

Volume load $\vec{q}$ and boundary load $\vec{p}$ on the fictitious material associated with one isolated element

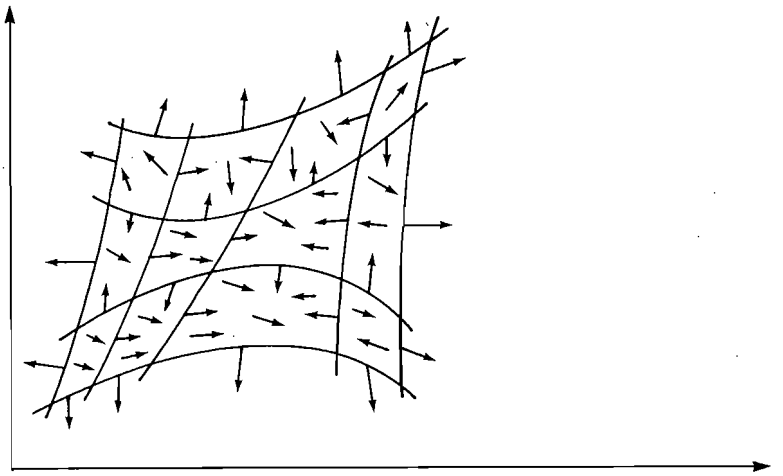

Fig. IV.2.2b

Volume and surface loads on the fictitious material associated with the element mesh

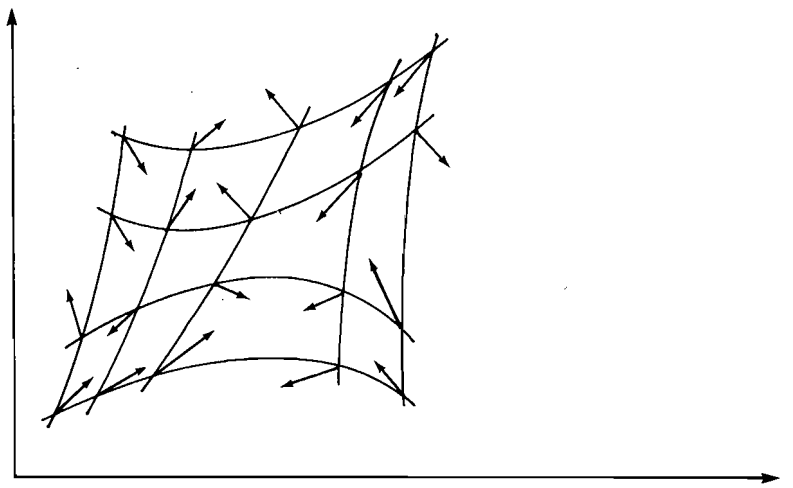

Fig. IV.2.2c

Nodal forces on the fictitious material in state τ

Relaxation of the nodal forces

Deformation of the fictitious material from state τ to state τ_e, the end of the increment, is effected by relaxing the nodal forces $\vec{\underset{\sim}{\varrho}}$. In state τ_e, the stresses resulting from this deformation, must satisfy the equilibrium equation $(\vec{\nabla}.\bar{\sigma}) = \vec{0}$ at every point of the material. In addition, the CRS boundary conditions must be satisfied. Using the method of weighted residuals and interpolating the relevant quantities in each element, results in the integral equation given below, which is equivalent to the equilibrium equation and has to be satisfied for every allowable weighting function

$$\sum_{e=1}^{n} \vec{\underset{\sim}{w}}_e^T \cdot \int_{G_e} (\nabla_g \underset{\sim}{\psi}^T)^T \vec{\underset{\sim}{\gamma}}_e . \bar{\sigma}_e \rfloor_e \, dG = \vec{\underset{\sim}{w}}^T . \vec{\underset{\sim}{r}}_2 \qquad \text{(IV.2.6)}$$

The nodal forces $\vec{\underset{\sim}{r}}_2$ result from the coupling between CRS and MRS and have a non-zero value only in those points where $d_g\vec{\chi} = d_m\vec{x}$ applies. According to (III.2.2) and (III.2.3), $\vec{\underset{\sim}{\gamma}}_e$ and $\rfloor_e$ are written as a function of the incremental displacements $\Delta_g\vec{\underset{\sim}{\chi}}_e$. Formally, the Cauchy stress tensor can also be written as a function of $\Delta_g\vec{\underset{\sim}{\chi}}_e$: $\bar{\sigma}_e = \bar{\underset{\sim}{f}}(\Delta_g\vec{\underset{\sim}{\chi}}_e)$. The incremental displacement $\Delta_g\vec{\underset{\sim}{\chi}}_e$ is interpolated within each element according to (III.3.3). Defining the vector column $\vec{\underset{\sim}{m}}_{2e}$ by

$$\vec{\underset{\sim}{m}}_{2e}(\Delta_g\vec{\underset{\sim}{\chi}}_e) = \int_{G_e} (\nabla_g \underset{\sim}{\psi}^T)^T \vec{\underset{\sim}{\gamma}}_e . \bar{\sigma}_e \rfloor_e \, dG \qquad \text{(IV.2.7)}$$

relation (IV.2.6) becomes

$$\sum_{e=1}^{n} \vec{\underset{\sim}{w}}_e^T . \vec{\underset{\sim}{m}}_{2e}(\Delta_g\vec{\underset{\sim}{\chi}}_e) = \vec{\underset{\sim}{w}}^T . \vec{\underset{\sim}{r}}_2 \qquad \text{(IV.2.8)}$$

Assembling the elements in the usual way gives

$$\vec{\underset{\sim}{w}}^T . \vec{\underset{\sim}{m}}_2(\Delta_g\vec{\underset{\sim}{\chi}}) = \vec{\underset{\sim}{w}}^T . \vec{\underset{\sim}{r}}_2 \qquad \text{(IV.2.9)}$$

The requirement that (IV.2.6) is satisfied for all weighting functions, interpolated in every element according to (III.3.5), implies that (IV.2.9) has to be satisfied for all possible nodal point values of $\vec{w}$, thus for every possible column $\underset{\sim}{\vec{w}}$. The incremental nodal point displacements $\Delta_g \underset{\sim}{\vec{x}}$ have thus to satisfy the set of vector equations

$$\underset{\sim 2}{\vec{m}}(\Delta_g \underset{\sim}{\vec{x}}) = \underset{\sim 2}{\vec{r}} \qquad \text{(IV.2.10)}$$

V The solution process

V.1 Introduction

The incremental nodal point displacements, $\Delta_g \vec{\underset{\sim}{x}}$, and the incremental displacement of the material in the nodal points, $\Delta_m \vec{\underset{\sim}{x}}$, must be determined in order to satisfy the following simultaneous sets of non-linear vector equations pertaining to the forming and CRS determination processes, respectively:

$$\vec{\underset{\sim}{m}}_1(\Delta_g \vec{\underset{\sim}{x}}, \Delta_m \vec{\underset{\sim}{x}}) = \vec{\underset{\sim}{r}}_1 \qquad \text{(V.1.1a)}$$

$$\vec{\underset{\sim}{m}}_2(\Delta_g \vec{\underset{\sim}{x}}) = \vec{\underset{\sim}{r}}_2 \qquad \text{(V.1.1b)}$$

Additional coupling of these sets is caused by certain requirements which the CRS and MRS displacements have to meet, including the requirement that the CRS and MRS boundaries must always coincide. The kinematic and dynamic boundary conditions must also be satisfied. It is not possible to solve (V.1.1) directly because of the non-linearity of the equations. The solution procedure described in this chapter, is known as the iterative method.

When the iterative method is used, a number of approximated solutions for (V.1.1) is determined. The approximation for the exact value of an incremental change $\Delta\alpha$, determined in iteration step i ($i \geq 0$), is

denoted by $\Delta\alpha^i$. The difference from the exact solution is denoted by $d\alpha$. Thus, for a CRS or an MRS change we write

$$\Delta_g\alpha = \Delta_g\alpha^i + d_g\alpha \qquad \text{(V.1.2a)}$$

$$\Delta_m\alpha = \Delta_m\alpha^i + d_m\alpha \qquad \text{(V.1.2b)}$$

An approximation for $d\alpha$ can be determined in iteration step i+1. If $d\alpha$ is sufficiently small, the incremental change $\Delta\alpha$ is considered to be accurate enough and the iteration process is stopped. The differences $d_g\alpha$ and $d_m\alpha$ are called the iterative CRS and MRS changes. In particular $d_g\vec{\chi}$ and $d_m\vec{x}$ are called the iterative displacement of a CRS and an MRS point, respectively.

To determine the approximated incremental nodal point displacements $\Delta_g\underset{\sim}{\vec{\chi}}^{i+1}$ and $\Delta_m\underset{\sim}{\vec{x}}^{i+1}$ we start from the incremental form of (III.3.6) and (IV.2.6). Expressions of the form (V.1.2a) are substituted for the incremental change of the reciprocal vector basis $\underset{\sim}{\vec{\gamma}}_e$, the Cauchy stress tensor $\bar{\sigma}_e$ and the Jacobians J_e and J_e^*. For $\bar{\sigma}_e$ we write

$$\bar{\sigma}_e = \bar{\sigma}^{fi} + d_g\bar{\sigma}_e \qquad \text{(V.1.3)}$$

where $\bar{\sigma}^{fi}$ is determined after iteration step i according to (IV.2.4). After these substitutions the two expressions are linearised with respect to the iterative changes $d_g(\ )$, as will be discussed in section V.2. Further processing of the linearised expressions demands the specification of the material behaviour of continuum and CRS, which is done in section V.3. The calculation of the stresses after iteration step i+1 is necessary to decide whether the approximated solution is accurate enough and, if necessary, to proceed with the solution process. The calculation method is discussed in section V.4. The differences $d_g\underset{\sim}{\vec{\gamma}}_e$, $d_g\bar{\sigma}_e$, d_gJ_e and $d_gJ_e^*$, which occur in the linearised expressions, are expressed in $d_g\vec{\chi}_e$. The CRS change $d_g\sigma_e$ can be replaced by an expression which contains the MRS change $d_m\sigma_e$. This quantity can be expressed in the iterative MRS displacement $d_m\vec{x}_e$ using the iterative constitutive equation which is formulated in section V.5.

V.2 The iterative method

The forming process
The CRS determination process
Two simultaneous linear vector equations

The forming process

After writing equation (III.3.6) in discretised form the incremental changes are replaced by expressions of the form (V.1.2a). Linearisation with respect to the iterative changes $d_g(\ )$ results in

$$\sum_{e=1}^{n} \vec{w}_e^T \cdot \int_{G_e} (\nabla_g \psi^T)^T [d_g \vec{\gamma}_e \cdot \varpi_e^i + \vec{\gamma}_e^i \cdot d_g \varpi_e + \vec{\gamma}_e^i \cdot \varpi_e^i \frac{d_g J_e}{J_e^i}] J_e^i \, dG$$

$$- \sum_{e=1}^{n} \vec{w}_e^T \cdot \int_{G_e} \psi \, \vec{q}_e \frac{d_g J_e}{J_e^i} J_e^i \, dG - \sum_{e=1}^{n} \vec{w}_e^T \cdot \int_{G_e^*} \psi \, \vec{t}_e^* \frac{d_g J_e^*}{J_e^{*i}} J_e^{*i} \, dG^* =$$

$$\sum_{e=1}^{n} \vec{w}_e^T \cdot \int_{G_e} \psi \, \vec{q}_e J_e^i \, dG + \sum_{e=1}^{n} \vec{w}_e^T \cdot \int_{G_e^*} \psi \, \vec{t}_e^* J_e^{*i} \, dG^*$$

$$- \sum_{e=1}^{n} \vec{w}_e^T \cdot \int_{G_e} (\nabla_g \psi^T)^T \vec{\gamma}_e^i \cdot \varpi_e^i J_e^i \, dG \qquad \text{(V.2.1)}$$

It follows from the CRS derivatives of the reciprocal vector basis $\vec{\gamma}$ and the Jacobians J and J^* presented in section II.2 - relations (II.2.72), (II.2.73) and (II.2.86) - that the iterative changes $d_g \vec{\gamma}_e$, $d_g J_e$ and $d_g J_e^*$ can be written as

$$d_g \vec{\gamma}_e = - \vec{\gamma}_e^i \cdot (\nabla_g d_g \vec{x}_e)^T \vec{\gamma}_e^i \qquad \text{(V.2.2)}$$

$$d_g J_e = J_e^i \vec{\gamma}_e^{iT} \cdot (\nabla_g d_g \vec{x}_e) \qquad \text{(V.2.3)}$$

$$d_g J_e^* = J_e^{*i} \vec{\gamma}_e^{*iT} \cdot (\nabla_g^* d_g \vec{x}_e) \qquad \text{(V.2.4)}$$

Thus, the iterative CRS changes of the geometrical quantities $\vec{\gamma}_e$, J_e and J_e^* are expressed in the iterative CRS point displacement $d_g\vec{x}_e$. The iterative CRS change of the Cauchy stress tensor, $d_g\sigma_e$, can be expressed in the iterative MRS change $d_m\sigma_e$ and the iterative displacements $d_g\vec{x}_e$ and $d_m\vec{x}_e$. On the analogy of (II.2.100) we can write

$$d_g\sigma_e = d_m\sigma_e + (d_g\vec{x}_e - d_m\vec{x}_e).\vec{\gamma}_e^{iT}(\nabla_g\sigma_e^i) \qquad (V.2.5)$$

In section V.5 a linear relationship between $d_m\sigma_e$ and $d_m\vec{x}_e$ is derived which, together with (V.2.5) allows us to write $d_g\sigma_e$ as a linear function of $d_g\vec{x}_e$ and $d_m\vec{x}_e$ only. This iterative constitutive equation and the expressions (V.2.2-4) are substituted in (V.2.1). Interpolation of $d_g\vec{x}_e$ and $d_m\vec{x}_e$ by analogy with (III.3.3) and (III.3.4), results in the contracted equation

$$\sum_{e=1}^{n} \vec{w}_e^T.\underline{A}_e^i.d_m\vec{x}_e + \sum_{e=1}^{n} \vec{w}_e^T.\underline{B}_e^i.d_g\vec{x}_e = \sum_{e=1}^{n} \vec{w}_e^T.\vec{R}_{1e}^i \qquad (V.2.6)$$

In appendix 1 the tensor matrices $\underline{A}_e$ and $\underline{B}_e$ are given integrally. On assembling the elements in the usual way this equation becomes

$$\vec{w}^T.\underline{A}^i.d_m\vec{x} + \vec{w}^T.\underline{B}^i.d_g\vec{x} = \vec{w}^T.\vec{R}_1^i \qquad (V.2.7)$$

According to the principle of weighted residuals this equation has to be satisfied for every $\vec{w}$. Hence the iterative displacements $d_m\vec{x}$ and $d_g\vec{x}$ have to satisfy the following set of linear vector equations

$$\underline{A}^i.d_m\vec{x} + \underline{B}^i.d_g\vec{x} = \vec{R}_1^i \qquad (V.2.8)$$

The CRS determination process

Writing (IV.2.6) in discretised form, substituting expressions of the form (V.1.2a) for the incremental changes, (V.1.3) for $\bar{\sigma}_e$ and

linearising with respect to the iterative changes $d_g(\ )$, gives

$$\sum_{e=1}^{n} \vec{w}_e^T \cdot \int_{G_e} (\nabla_g \psi^T)^T [d_g \vec{\gamma}_e \cdot \bar{\sigma}_e^{fi} + \vec{\gamma}_e^i \cdot d_g \bar{\sigma}_e + \vec{\gamma}_e^i \cdot \bar{\sigma}_e^{fi} \frac{d_g J_e}{J_e^i}] J_e^i \, dG =$$

$$+ \vec{w}^T \cdot \vec{r}_2 - \sum_{e=1}^{n} \vec{w}_e^T \cdot \int_{G_e} (\nabla_g \psi^T)^T \vec{\gamma}_e^i \cdot \bar{\sigma}_e^{fi} J_e^i \, dG \qquad (V.2.9)$$

The iterative changes $d_g \vec{\gamma}_e$ and $d_g J_e$ can be expressed in $d_g \vec{x}_e$, according to (V.2.2) and (V.2.3). Moreover, $d_g \bar{\sigma}_e$ can be written as a linear expression in $d_g \vec{x}_e$. Substitution of all this in (V.2.9) and intepolation of $d_g \vec{x}_e$, results in the contracted equation

$$\sum_{e=1}^{n} \vec{w}_e^T \cdot \underline{V}_e^i \cdot d_g \vec{x}_e = \sum_{e=1}^{n} \vec{w}_e^T \cdot \vec{R}_{2e}^i \qquad (V.2.10)$$

In appendix 1 the tensor matrix $\underline{V}_e$ is written integrally. Assembling the elements in the usual way results in

$$\vec{w}^T \cdot \underline{V}^i \cdot d_g \vec{x} = \vec{w}^T \cdot \vec{R}_2^i \qquad (V.2.11)$$

According to the principle of weighted residuals this equation has to be satisfied for every $\vec{w}$, which implies that the iterative nodal point displacements $d_g \vec{x}$ have to satisfy the following set of linear vector equations

$$\underline{V}^i \cdot d_g \vec{x} = \vec{R}_2^i \qquad (V.2.12)$$

Two simultaneous linear vector equations

The iterative displacements $d_m \vec{x}$ and $d_g \vec{x}$ have to satisfy the following simultaneous vector equations

$$\underline{A}^i \cdot d_m \vec{x} + \underline{B}^i \cdot d_g \vec{x} = \vec{R}_1^i \qquad (V.2.13a)$$

$$\underline{V}^i \cdot d_g \vec{x} = \vec{R}_2^i \qquad (V.2.13b)$$

The elastic material tensor

It is assumed that the elastic material behaviour of both the real material of the body and the fictitious material with which the CRS is associated, is isotropic and that the elastic material parameters remain constant. The fourth-order elastic material tensors $^4\hat{\mathbb{C}}$ and $^4\hat{\bar{\mathbb{C}}}$, belonging to the real and the fictive material respectively, are defined by:

$$^4\hat{\mathbb{C}} = K\,\mathbb{I}\,\mathbb{I} + 2G(^4\mathbb{I} - \frac{1}{3}\,\mathbb{I}\,\mathbb{I}) \qquad \text{(V.3.5a)}$$

$$^4\hat{\bar{\mathbb{C}}} = \bar{K}\,\mathbb{I}\,\mathbb{I} + 2\bar{G}(^4\mathbb{I} - \frac{1}{3}\,\mathbb{I}\,\mathbb{I}) \qquad \text{(V.3.5b)}$$

Here K and $\bar{K}$ are bulk moduli and G and $\bar{G}$ shear moduli. E being Young's modulus and ν Poisson's ratio, K and G are defined by

$$K = \frac{E}{3(1-2\nu)} \quad ; \quad G = \frac{E}{2(1+\nu)} \qquad \text{(V.3.6)}$$

The elasto-plastic material tensor

To describe the elasto-plastic material behaviour of the continuum, the Von Mises yield condition with isotropic hardening is used. According to this yield condition plastic deformation at a material point can occur only on satisfaction of equation

$$f(\hat{\sigma},\sigma_v) = \frac{1}{2}\,\hat{\sigma}^d:\hat{\sigma}^d - \frac{1}{3}\,\sigma_v^2 = 0 \qquad \text{(V.3.7)}$$

The tensor $\hat{\sigma}^d$ is the deviatoric part of the co-rotational Cauchy stress tensor and σ_v is the current yield stress, which is the one and only history parameter. It is assumed that σ_v is a function of the effective plastic strain $\tilde{\varepsilon}^p$ with respect to a reference state τ_o where $\sigma_v = \sigma_v^o$ and $\tilde{\varepsilon}^p = \tilde{\varepsilon}^{po}$. In state τ, $\tilde{\varepsilon}^p$ is defined by

$$\tilde{\varepsilon}^p = \tilde{\varepsilon}^{po} + \int_{\tau_o}^{\tau} \dot{\tilde{\varepsilon}}^p\,d\tau = \tilde{\varepsilon}^{po} + \int_{\tau_o}^{\tau} \sqrt{\frac{2}{3}\,\hat{\mathbb{D}}^p:\hat{\mathbb{D}}^p}\,d\tau \qquad \text{(V.3.8)}$$

According to (V.3.7) the associated flow rule reads as

$$\hat{\mathbb{D}}^p = \alpha \frac{\partial f}{\partial \boldsymbol{\sigma}} = \alpha \, \hat{\boldsymbol{\sigma}}^d \tag{V.3.9}$$

Using the definition of the effective strain rate $\dot{\tilde{\varepsilon}}^p$, it is easily shown that α can be written as

$$\alpha = \frac{3}{2} \frac{\dot{\tilde{\varepsilon}}^p}{\sigma_v} \tag{V.3.10}$$

According to (V.3.4) and the definition $\zeta = \alpha\beta$ we find for $\frac{1}{\beta} k(\mathbf{n})$

$$\frac{1}{\beta} k(\mathbf{n}) = \frac{1}{\alpha\beta^2} \dot{H} = \frac{1}{\alpha\beta^2} \dot{\sigma}_v = \frac{1}{\alpha\beta^2} \frac{d\sigma_v}{d\tilde{\varepsilon}^p} \dot{\tilde{\varepsilon}}^p \tag{V.3.11}$$

Using (V.3.10) and the hardening parameter $h = \dfrac{d\sigma_v}{d\tilde{\varepsilon}^p}$ we arrive at

$$\frac{1}{\beta} k(\mathbf{n}) = \frac{1}{\beta^2} \frac{2}{3} h \, \sigma_v \tag{V.3.12}$$

Employing (V.3.5) and $\mathbf{n} = \dfrac{\hat{\boldsymbol{\sigma}}^d}{\beta}$ it is easily shown that the relations

$$\hat{\mathbb{C}}^4 : \mathbf{n} \, \mathbf{n} : \hat{\mathbb{C}}^4 = \frac{1}{\beta^2} 4G^2 \hat{\boldsymbol{\sigma}}^d \hat{\boldsymbol{\sigma}}^d \tag{V.3.13}$$

$$\mathbf{n} : \hat{\mathbb{C}}^4 : \mathbf{n} = \frac{1}{\beta^2} 2G \, \hat{\boldsymbol{\sigma}}^d : \hat{\boldsymbol{\sigma}}^d = \frac{1}{\beta^2} \frac{4}{3} G \, \sigma_v^2 \tag{V.3.14}$$

hold. Substituting (V.3.12), (V.3.13) and (V.3.14) in (V.3.3) finally gives

$$\hat{\mathbb{L}}^4 = \hat{\mathbb{C}}^4 - \frac{3G}{1 + \frac{h}{3G}} \frac{\hat{\boldsymbol{\sigma}}^d \hat{\boldsymbol{\sigma}}^d}{\sigma_v^2} \tag{V.3.15}$$

V.4 Calculation of the stresses

The co-rotational Cauchy stress tensor
The effective plastic strain
The mean normal method with radial return
The implicit radial return method

The co-rotational Cauchy stress tensor

The change of the co-rotational Cauchy stress tensor at an MRS point $\underset{\sim}{m}$ during the state transition $\Delta\tau : \tau_o \rightarrow \tau$, can be determined by integrating the constitutive equation (V.3.2)

$$\Delta\hat{\sigma} = \int_{\tau_o}^{\tau} {}^4\hat{\mathbb{L}} : \hat{\mathbb{D}} \, d\tau \qquad (V.4.1)$$

If $\hat{\mathbb{D}}$ is assumed to be constant during the state transition $\Delta\tau$, we can use relation (II.2.59) and write

$$\Delta\hat{\sigma} = \frac{1}{\tau - \tau_o} \int_{\tau_o}^{\tau} {}^4\hat{\mathbb{L}} \, d\tau : \hat{\mathbb{C}} \qquad (V.4.2)$$

Here $\hat{\mathbb{C}}$ is the logarithmic strain tensor defined by

$$\hat{\mathbb{C}} = \frac{1}{2}\ln(\mathbb{I} + 2\mathbb{E}) \qquad (V.4.3)$$

where $\mathbb{E}$ is the Green-Lagrange strain tensor at point $\underset{\sim}{m}$ with respect to the state τ_o.

The effective plastic strain

The fourth-order tensor ${}^4\hat{\mathbb{L}}$ is a function of the current yield stress σ_y, which is assumed to be a function of the effective plastic strain $\hat{\varepsilon}^p$. Using the Von Mises yield condition the consistency relation (II.5.4) reads as

$$\hat{\sigma}^d : \dot{\hat{\sigma}}^d - \frac{2}{3}\sigma_v \dot{\sigma}_v = 0 \qquad (V.4.4)$$

With $\sigma_v = \sigma_v(\tilde{\varepsilon}^p)$ the next expression for $\dot{\tilde{\varepsilon}}^p$ is easily derived

$$\dot{\tilde{\varepsilon}}^p = \frac{\hat{\sigma}^d : \dot{\hat{\sigma}}^d}{\frac{2}{3}\sigma_v h} = \frac{\hat{\sigma}^d : \dot{\hat{\sigma}}}{\frac{2}{3}\sigma_v h} \qquad (V.4.5)$$

where $h = \frac{d\sigma_v}{d\tilde{\varepsilon}^p}$ is the hardening parameter. Using the constitutive relation we find

$$\dot{\tilde{\varepsilon}}^p = \frac{\hat{\sigma}^d : \hat{\mathbb{D}}}{(1 + \frac{h}{3G})\sigma_v} \qquad (V.4.6)$$

The change in effective plastic strain during the state transition $\Delta\tau : \tau_o \rightarrow \tau$ can be determined by integrating (V.4.6) and yields

$$\Delta\tilde{\varepsilon}^p = \int_{\tau_o}^{\tau} \frac{\hat{\sigma}^d : \hat{\mathbb{D}}}{(1 + \frac{h}{3G})\sigma_v} d\tau = \frac{1}{\tau - \tau_o} \int_{\tau_o}^{\tau} \frac{\hat{\sigma}^d}{(1 + \frac{h}{3G})\sigma_v} d\tau : \hat{\mathbb{C}} \qquad (V.4.7)$$

The stress tensor in state τ can be determined by simultaneously integrating (V.4.2) and (V.4.7). Several methods are known for carrying out this integration - for instance, see Krieg & Krieg (1977)-. Using the Von Mises yield condition with isotropic hardening, the so-called mean normal method is found to be very efficient and accurate.

The mean normal method with radial return

With the mean normal method a stress tensor $\hat{\sigma}_e$ is determined, this being the stress tensor if the material would show purely elastic behaviour during the state transition $\Delta\tau : \tau_o \rightarrow \tau$

$$\hat{\sigma}_e = \hat{\sigma}^o + {}^4\hat{\mathbb{C}} : \hat{\mathbb{C}} \qquad (V.4.8)$$

If $f(\hat{\sigma}_e, \sigma_v^o) \leq 0$, this tensor is equal to the co-rotational Cauchy stress tensor in state τ. If $f(\hat{\sigma}_e, \sigma_v^o) > 0$, two scalars (λ_1, λ_2) are determined from

$$f(\hat{\sigma}^o + \lambda \hat{\mathbb{C}}^4 : \hat{\mathbb{C}} \ , \ \sigma_v^o) = 0 \qquad (V.4.9)$$

and a stress tensor $\hat{\sigma}_m$ is defined by

$$\hat{\sigma}_m = \frac{1}{2}(\hat{\sigma}^o + \lambda \hat{\mathbb{C}}^4 : \hat{\mathbb{C}} + \hat{\sigma}_e) \quad ; \quad \lambda = \max(\lambda_1, \lambda_2) \qquad (V.4.10)$$

According to (V.4.7) the effective plastic strain is estimated as

$$\tilde{\varepsilon}^p = \tilde{\varepsilon}^{po} + \frac{(1-\lambda)\hat{\sigma}_m^d : \hat{\mathbb{C}}}{(1 + \frac{h}{3G})\sqrt{\frac{3}{2}\hat{\sigma}_m^d : \hat{\sigma}_m^d}} \qquad (V.4.11)$$

If the hardening parameter h is unknown, $\tilde{\varepsilon}^p$ cannot be calculated from the above expression. In that case an iterative procedure is followed. In the first step the hardening parameter h is chosen zero and in every following step it is calculated from

$$h = \frac{\sigma_v(\tilde{\varepsilon}^p) - \sigma_v^o}{\tilde{\varepsilon}^p - \tilde{\varepsilon}^{po}} \qquad (V.4.12)$$

Finally, when the iterative calculation of $\tilde{\varepsilon}^p$ and h has been carried out, the co-rotational Cauchy stress tensor $\hat{\sigma}$ in state τ is given by

$$\hat{\sigma} = \hat{\sigma}^o + \lambda \hat{\mathbb{C}}^4 : \hat{\mathbb{C}} + (1-\lambda)[\hat{\mathbb{C}}^4 - \frac{3G}{1 + \frac{h}{3G}} \frac{\hat{\sigma}_m^d \hat{\sigma}_m^d}{\frac{3}{2}\hat{\sigma}_m^d : \hat{\sigma}_m^d}] : \hat{\mathbb{C}} \qquad (V.4.13)$$

This stress tensor, together with the yield stress in state τ, which is determined as a function of $\tilde{\varepsilon}^p$, will generally not satisfy the yield condition (V.3.7). According to Brekelmans (1981) the yield condition will be satisfied only if the material behaviour is perfectly plastic (h = 0) or if $\hat{\sigma}^{do}$ and $\hat{\mathbb{C}}^d$ are similar. In all other cases the stress tensor $\hat{\sigma}$ is adjusted, using the so-called explicit radial return method.

When the co-rotational Cauchy stress tensor $\hat{\sigma}$ in state τ is determined, the deviatoric part of this tensor is multiplied by a scalar α given by

$$\alpha = \frac{\sigma_v(\tilde{\varepsilon}^p)}{\sqrt{\frac{3}{2}\,\hat{\sigma}^d : \hat{\sigma}^d}} \qquad (V.4.14)$$

The tensor $\alpha\,\hat{\sigma}^d$ and the yield stress σ_v satisfy the yield condition in state τ. Since the stress tensor is adjusted afterwards, this adjustment procedure is called the explicit radial return method.

The implicit radial return method

An implicit radial return method can also be employed. In that case the fourth-order elasto-plastic material tensor is assumed to be constant during the state transition $\Delta\tau : \tau_o \rightarrow \tau$, which results in the expression

$$\hat{\sigma} = \hat{\sigma}^o + {}^4\hat{\mathbb{L}} : \hat{\mathbb{C}} \qquad (V.4.15)$$

for $\hat{\sigma}$ in state τ. By means of (V.3.15) it is easily shown that the deviatoric part of $\hat{\sigma}$ is given by

$$\hat{\sigma}^d = \hat{\sigma}^{do} + 2G\,\hat{\mathbb{C}}^d - \frac{3G}{1 + \frac{h}{3G}}\,\frac{\hat{\sigma}^d\hat{\sigma}^d}{\sigma_v^2} : \hat{\mathbb{C}}^d \qquad (V.4.16)$$

If the scalar κ and the tensor $\hat{\sigma}_n$ are defined by

$$\kappa = \left[1 + \frac{3G}{1 + \frac{h}{3G}}\,\frac{\hat{\sigma}^d : \hat{\mathbb{C}}^d}{\sigma_v^2}\right]^{-1} \quad ; \quad \hat{\sigma}_n = \hat{\sigma}^{do} + 2G\,\hat{\mathbb{C}}^d \qquad (V.4.17)$$

expression (V.4.16) for $\hat{\sigma}^d$ results in

$$\hat{\sigma}^d = \kappa\,\hat{\sigma}_n \qquad (V.4.18)$$

The scalar κ is determined so as to make $\hat{\sigma}^d$ satisfy the yield condition in state τ. Substitution of (V.4.18) in the yield condition results in

$$\kappa = \frac{\sigma_v(\tilde{\varepsilon}^p)}{\sqrt{\frac{3}{2}\,\hat{\sigma}_n : \hat{\sigma}_n}} \qquad \text{(V.4.19)}$$

where $\tilde{\varepsilon}^p$ is determined according to the mean-normal method, described before. The following expression can be derived for the co-rotational Cauchy stress tensor in state τ

$$\hat{\sigma} = \kappa\,\hat{\sigma}_n + \frac{1}{3}\,\mathrm{tr}(\sigma^o)\,\mathbb{I} + K\,\mathrm{tr}(\hat{\mathbb{C}})\,\mathbb{I} \qquad \text{(V.4.20)}$$

which, together with σ_v, satisfies the yield condition. Starting from the above expression for $\hat{\sigma}$, an iterative constitutive relation between $d_m\hat{\sigma}$ and $d_m\vec{x}$ will be derived in the next section.

V.5 An iterative constitutive equation for time independent elasto-plastic material behaviour

The iterative constitutive equation for the material
The iterative constitutive equation for the CRS

The iterative constitutive equation for the material

The relation between the iterative MRS change of the Cauchy stress tensor, $d_m\sigma$, and the iterative MRS point displacement, $d_m\vec{x}$, has been presented by Nagtegaal & Veldpaus [21]. The derivation of this iterative constitutive equation is incorporated in this thesis as appendix 2. In the derivation presented here, it was necessary to assume the Green-Lagrange strain tensor with respect to the beginning of the increment, to be very small, i.e. $||E|| << 1$. If this assumption is not correct, the convergence rate of the iteration process will be affected, the final solution, however, will not. In appendix 2 some results of appendix 3, dealing with functions of a tensor, are used.

The derivation of the constitutive equation starts from the relation between the Cauchy stress tensor σ and the co-rotational Cauchy stress tensor $\hat{\sigma}$, reading

$$\sigma = R.\hat{\sigma}.R^c \tag{V.5.1}$$

Here R is the rotation tensor in the polar decomposition of the deformation tensor F. Employing the iterative solution procedure, (V.5.1) becomes

$$\sigma^i + d_m\sigma = (R^i + d_mR).(\hat{\sigma}^i + d_m\hat{\sigma}).(R^{ic} + d_mR^c) \tag{V.5.2}$$

and linearisation yields

$$d_m\sigma = d_mR.R^{ic}.\sigma^i + \sigma^i.R^i.d_mR^c + R^i.d_m\hat{\sigma}.R^{ic} \tag{V.5.3}$$

Closer examination of $d_m\mathbb{R}$ and $d_m\hat{\boldsymbol{\omega}}$ results in

$$d_m\boldsymbol{\omega} = \frac{1}{2}(d_m\mathbb{H} - d_m\mathbb{H}^C).\boldsymbol{\omega}^i + \boldsymbol{\omega}^i.\frac{1}{2}(d_m\mathbb{H} - d_m\mathbb{H}^C)^C$$

$$+ {}^4\mathbb{M}^i:\frac{1}{2}(d_m\mathbb{H} + d_m\mathbb{H}^C) \qquad (V.5.4)$$

where the tensor $d_m\mathbb{H}$ is defined by

$$d_m\mathbb{H} = d_m\mathbb{F}.(\mathbb{F}^i)^{-1} = d_m\vec{b}\,\underset{\sim}{}^T\vec{c}\,\underset{\sim}{}^i = (\underset{\sim}{v}_m d_m\vec{x})^T\vec{c}\,\underset{\sim}{}^i \qquad (V.5.5)$$

For the fourth-order elasto-plastic material tensor ${}^4\mathbb{M}^i$ the expression

$${}^4\mathbb{M}^i = K\,\mathbb{I}\,\mathbb{I} + 2\tilde{G}({}^4\mathbb{I} - \frac{1}{3}\,\mathbb{I}\,\mathbb{I} - \frac{3}{2}\,\tilde{\mu}\,\frac{\boldsymbol{\omega}_n^i\boldsymbol{\omega}_n^i}{\sigma_{n\,i2}}) \qquad (V.5.6)$$

holds, where K is the bulk modulus. The tensor $\boldsymbol{\omega}_n^i$ is defined analogous to (V.4.18) and σ_n^i by

$$\sigma_n^i = \sqrt{\frac{3}{2}\,\boldsymbol{\omega}_n^i:\boldsymbol{\omega}_n^i} \qquad (V.5.7)$$

while the quantities $\tilde{G}$ and $\tilde{\mu}$ are given by

$$\tilde{G} = G\,\frac{\sigma_v^i}{\sigma_n^i} \quad ; \quad \tilde{\mu} = 1 - \frac{h^i\sigma_n^i}{3G(1 + \frac{h^i}{3G})\sigma_v^i} \qquad (V.5.8)$$

where G is the shear modulus, σ_v^i the current yield stress and h^i the current hardening parameter.

The iterative constitutive equation for the CRS

The iterative constitutive equation for the fictitious material associated with the CRS is analogous to (V.5.4) and reads as

$$d_g\bar{\boldsymbol{\omega}} = \frac{1}{2}(d_g\bar{\mathbf{H}} - d_g\bar{\mathbf{H}}^c).\bar{\boldsymbol{\omega}}^i + \bar{\boldsymbol{\omega}}^i.\frac{1}{2}(d_g\bar{\mathbf{H}} - d_g\bar{\mathbf{H}}^c)^c + {}^4\bar{\mathbb{C}}:\frac{1}{2}(d_g\bar{\mathbf{H}} + d_g\bar{\mathbf{H}}^c) \quad ; \qquad (V.5.9)$$

$$d_g\bar{\mathbf{H}} = d_g\bar{\mathbf{F}}.(\bar{\mathbf{F}}^i)^{-1} = d_g\vec{\boldsymbol{\beta}}^{T\to i}_{\sim}\vec{\boldsymbol{\gamma}}^{\,i}_{\sim} = (\nabla_{\sim g}\, d_g\vec{\mathbf{x}})^{T\to i}_{\sim}\vec{\boldsymbol{\gamma}}^{\,i}_{\sim} \quad ; \qquad (V.5.10)$$

$${}^4\bar{\mathbb{C}} = \bar{K}\,\mathbb{I}\,\mathbb{I} + 2\bar{G}({}^4\mathbb{I} - \tfrac{1}{3}\,\mathbb{I}\,\mathbb{I}) \qquad (V.5.11)$$

Here, $\bar{K}$ and $\bar{G}$ are the bulk and shear modulus of the fictitious material.

VI Axisymmetric forming processes

VI.1 Introduction

In the preceding chapters the theoretical aspects of the simulation of metal forming processes are presented. This chapter deals with the application of this theory to axisymmetric forming processes, which occur frequently in practice.

To facilitate elaboration of various mathematical expressions, two spatial reference systems are introduced: the Cartesian and the cylindrical reference system. Using the Cartesian reference system, every point in space is identified by a set of three mutually independent Cartesian coordinates x, y and z. The vector basis at a point is denoted by $\underset{\sim}{\vec{e}}$ and defined by

$$\underset{\sim}{\vec{e}}^{T} = [\vec{e}_x \quad \vec{e}_y \quad \vec{e}_z] \qquad \text{(VI.1.1)}$$

This vector basis is orthonormal, i.e. $\underset{\sim}{\vec{e}}^{T}.\underset{\sim}{\vec{e}} = \underline{I}$. Using the cylindrical reference system, every spatial point is identified by a set of three mutually independent cylindrical coordinates r, φ and z. The vector basis at a point is denoted by $\underset{\sim}{\vec{\varepsilon}}$ and defined by

$$\underset{\sim}{\vec{\varepsilon}}^{T} = [\vec{\varepsilon}_r \quad \vec{\varepsilon}_\varphi \quad \vec{\varepsilon}_z] \qquad \text{(VI.1.2)}$$

This vector basis is orthonormal as well: $\underset{\sim}{\vec{\varepsilon}}^{T}.\underset{\sim}{\vec{\varepsilon}} = \underline{I}$. Both reference systems are shown in figure VI.1.1.

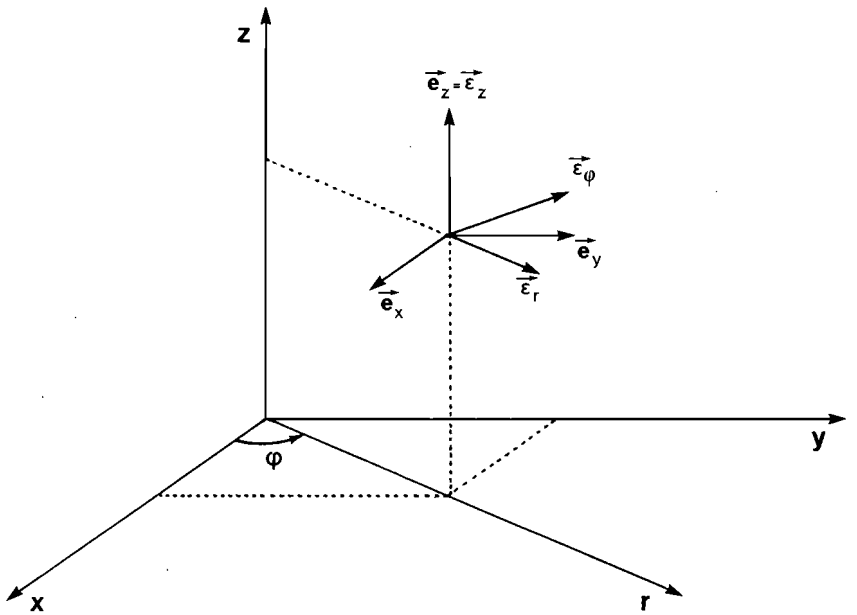

Fig. VI.1.1
The Cartesian and cylindrical reference systems

The following relationship exists between the Cartesian and cylindrical coordinates and vector bases:

$$x = r \cos \varphi \quad , \quad y = r \sin \varphi \quad , \quad z = z \tag{VI.1.3}$$

$$\begin{bmatrix} \vec{e}_x \\ \vec{e}_y \\ \vec{e}_z \end{bmatrix} = \begin{bmatrix} \cos \varphi & -\sin \varphi & 0 \\ \sin \varphi & \cos \varphi & 0 \\ 0 & 0 & 1 \end{bmatrix} \begin{bmatrix} \vec{\varepsilon}_r \\ \vec{\varepsilon}_\varphi \\ \vec{\varepsilon}_z \end{bmatrix} \tag{VI.1.4}$$

Every CRS point is identified unambiguously by a set of CRS coordinates $\underset{\sim}{g}$. Moreover, every CRS point can be identified by means of the Cartesian and cylindrical coordinates of that point in a state τ.

In section VI.2 an axisymmetric element is presented which is used for the simulation of the forming process. Various relevant quantities at a point of this element are considered. Vectors and tensors are written in components with respect to the cylindrical basis at that point. For a vector $\vec{a}$ we write

$$\vec{a} = \underset{\sim}{a}^{T}\vec{\underset{\sim}{e}} = \vec{\underset{\sim}{e}}^{T}\underset{\sim}{a} \qquad \text{(VI.1.5)}$$

where column $\underset{\sim}{a}$ contains the cylindrical components of $\vec{a}$.

The state in which the geometry of an element is optimal, is called τ_f. In this state, the fictitious material associated with the element is stress-free. In state τ, the Cauchy stress tensor at a point of the element, the value of which depends on the deformation of the fictitious material at this point with respect to state τ_f, is a measure for the deviation from the optimum geometry of the element. Rigid body movement of the fictitious material must not affect these stresses. For this reason the axisymmetric element is not appropriate for simulating the CRS determination process. The fictitious material is considered to be associated with a plain-strain element which is introduced in section VI.3. Various relevant quantities are considered at a point of this element. Vectors and tensors are being written in components with respect to the Cartesian basis at that point. For a vector $\vec{a}$ we write

$$\vec{a} = \underset{\sim}{a}^{T}\vec{\underset{\sim}{e}} = \vec{\underset{\sim}{e}}^{T}\underset{\sim}{a} \qquad \text{(VI.1.6)}$$

where column $\underset{\sim}{a}$ contains the Cartesian components of $\vec{a}$.

Some detailed aspects of the CRS determination process are discussed in section VI.4.

VI.2 An axisymmetric element

The axisymmetric element, used to simulate the forming process, is shown in figure VI.2.1.

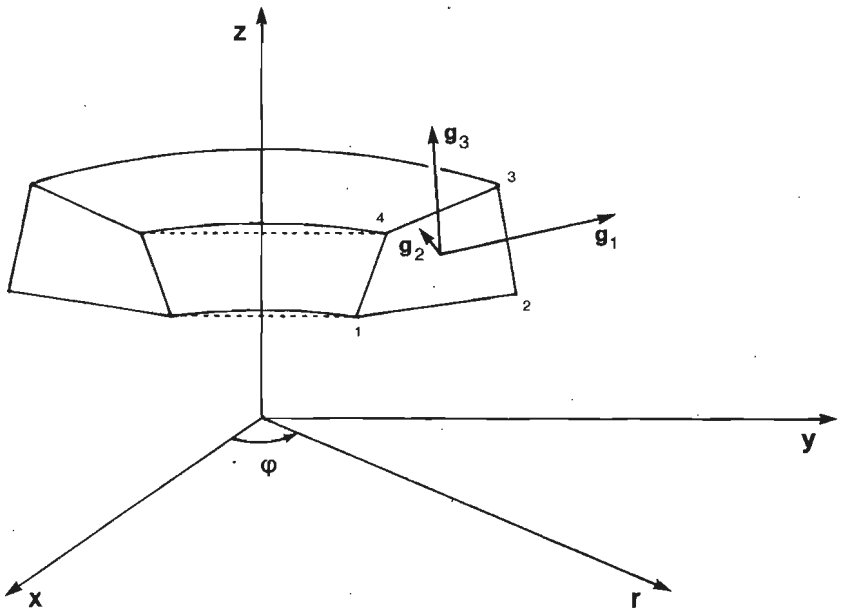

Fig. VI.2.1
The axisymmetric element

The cross-section is a quadrilateral with straight sides. For the local CRS coordinates we find

$$g_1 = g_1(r,z) \quad , \quad g_2 = g_2(\varphi) \quad , \quad g_3 = g_3(r,z) \qquad \text{(VI.2.1)}$$

Each local coordinate lies within the interval [-1,1]. It is assumed that $\frac{\partial \varphi}{\partial g_2} = \pi$ for every φ with $0 < \varphi \leq 2\pi$.

None of the relevant quantities in an axisymmetric forming process is a function of the φ- or g_2-coordinates. Thus attention can be fixed on one cross-section of the element, e.g. with $\varphi = 0$. The bilinear

interpolation functions used, are merely a function of the local CRS coordinates g_1 and g_3. The four vertices of the quadrilateral cross-section are the nodal points used for the interpolation. The four interpolation functions are contained in the column $\underset{\sim}{\psi}$:

$$\underset{\sim}{\psi} = \begin{bmatrix} \psi^1 \\ \psi^2 \\ \psi^3 \\ \psi^4 \end{bmatrix} = \begin{bmatrix} \frac{1}{4}(1-g_1)(1-g_3) \\ \frac{1}{4}(1+g_1)(1-g_3) \\ \frac{1}{4}(1+g_1)(1+g_3) \\ \frac{1}{4}(1-g_1)(1+g_3) \end{bmatrix} \qquad \text{(VI.2.2)}$$

A scalar quantity α at a point of the element is interpolated as follows

$$\alpha = \underset{\sim}{\psi}^T \underset{\sim}{\alpha} = [\psi^1 \ \psi^2 \ \psi^3 \ \psi^4] \begin{bmatrix} \alpha^1 \\ \alpha^2 \\ \alpha^3 \\ \alpha^4 \end{bmatrix} = \psi^1\alpha^1 + \psi^2\alpha^2 + \psi^3\alpha^3 + \psi^4\alpha^4 \qquad \text{(VI.2.3)}$$

where column $\underset{\sim}{\alpha}$ contains the values of α at the element nodal points. A vector $\vec{a}$ is interpolated as

$$\vec{a} = \underset{\sim}{\psi}^T \underset{\sim}{\vec{a}} \qquad \text{(VI.2.4)}$$

If the nodal point vectors $\underset{\sim}{\vec{a}}$ are written into components with respect to the cylindrical vector basis, we can write

$$\vec{a} = \underset{\sim}{\psi}^T \underline{a}^T \underset{\sim}{\vec{\varepsilon}} = [\psi^1 \ \psi^2 \ \psi^3 \ \psi^4] \begin{bmatrix} a_r^1 & a_\varphi^1 & a_z^1 \\ a_r^2 & a_\varphi^2 & a_z^2 \\ a_r^3 & a_\varphi^3 & a_z^3 \\ a_r^4 & a_\varphi^4 & a_z^4 \end{bmatrix} \begin{bmatrix} \vec{\varepsilon}_r \\ \vec{\varepsilon}_\varphi \\ \vec{\varepsilon}_z \end{bmatrix} \qquad \text{(VI.2.5)}$$

According to (II.2.61) the CRS vector basis $\vec{\beta}$ at CRS point g of the element is defined by

$$\vec{\beta} = \nabla_g \vec{x} = \nabla_g \vec{p} \quad ; \quad \nabla_g^T = [\frac{\partial}{\partial g_1} \frac{\partial}{\partial g_2} \frac{\partial}{\partial g_3}] \tag{VI.2.6}$$

Here $\vec{p}$ is the position vector of point g. In components with respect to the Cartesian vector basis $\vec{e}$ in g we can write

$$\vec{p} = p^T \vec{e} = [x \quad y \quad z] \begin{bmatrix} \vec{e}_x \\ \vec{e}_y \\ \vec{e}_z \end{bmatrix} \tag{VI.2.7}$$

and hence

$$\vec{\beta} = (\nabla_g p^T)\vec{e} = \beta_x \vec{e} \quad ; \quad \beta_x = \begin{bmatrix} \frac{\partial x}{\partial g_1} & \frac{\partial y}{\partial g_1} & \frac{\partial z}{\partial g_1} \\ \frac{\partial x}{\partial g_2} & \frac{\partial y}{\partial g_2} & \frac{\partial z}{\partial g_2} \\ \frac{\partial x}{\partial g_3} & \frac{\partial y}{\partial g_3} & \frac{\partial z}{\partial g_3} \end{bmatrix} \tag{VI.2.8}$$

With (VI.1.3), (VI.1.4) and (VI.2.1), $\vec{\beta}$ can be written in components with respect to the cylindrical basis $\vec{\varepsilon}$ in g as

$$\vec{\beta} = \beta_c \vec{\varepsilon} \quad ; \quad \beta_c = \begin{bmatrix} \frac{\partial r}{\partial g_1} & 0 & \frac{\partial z}{\partial g_1} \\ 0 & \pi r & 0 \\ \frac{\partial r}{\partial g_3} & 0 & \frac{\partial z}{\partial g_3} \end{bmatrix} \tag{VI.2.9}$$

Interpolating the cylindrical coordinates r and z according to (VI.2.3), the matrix $\underline{\beta}_C$ becomes

$$\underline{\beta}_C = \begin{bmatrix} \frac{\partial \underset{\sim}{\psi}^T}{\partial g_1} \underset{\sim}{r} & 0 & \frac{\partial \underset{\sim}{\psi}^T}{\partial g_1} \underset{\sim}{z} \\ 0 & \pi \underset{\sim}{\psi}^T \underset{\sim}{r} & 0 \\ \frac{\partial \underset{\sim}{\psi}^T}{\partial g_3} \underset{\sim}{r} & 0 & \frac{\partial \underset{\sim}{\psi}^T}{\partial g_3} \underset{\sim}{z} \end{bmatrix} \qquad \text{(VI.2.10)}$$

The Jacobian $\jmath$ of the mapping $\vec{\chi} : G \to V(\tau)$ is defined by

$$\jmath = \vec{\beta}_1 \cdot (\vec{\beta}_2 * \vec{\beta}_3) \qquad \text{(VI.2.11)}$$

If the basis vectors $\vec{\beta}_i$ (i = 1,2,3) are written in components with respect to the cylindrical basis $\vec{\underset{\sim}{\varepsilon}}$, it is easily shown that

$$\jmath = \det(\beta_C) \qquad \text{(VI.2.12)}$$

The reciprocal vector basis $\vec{\underset{\sim}{\gamma}}$ can be determined from

$$\vec{\underset{\sim}{\beta}} \cdot \vec{\underset{\sim}{\gamma}}^T = \underline{I} \qquad \text{(VI.2.13)}$$

If both $\vec{\underset{\sim}{\beta}}$ and $\vec{\underset{\sim}{\gamma}}$ are written in components with respect to $\vec{\underset{\sim}{\varepsilon}}$, this results in

$$\underline{\beta}_C \vec{\underset{\sim}{\varepsilon}} \cdot \vec{\underset{\sim}{\varepsilon}}^T \underline{\gamma}_C^T = \underline{I} \qquad \text{(VI.2.14)}$$

Because of the orthonormality of $\vec{\underset{\sim}{\varepsilon}}$ we find for $\underline{\gamma}_C$

$$\underline{\gamma}_C = \underline{\beta}_C^{-T} \qquad \text{(VI.2.15)}$$

According to (II.2.67) the gradient operator is defined by

$$\vec{\nabla} = \underset{\sim}{\vec{\gamma}}^{T} \nabla_{g} \tag{VI.2.16}$$

Using $\underset{\sim}{\vec{\gamma}}^{T} = \underset{\sim}{\vec{\varepsilon}}^{T} \underline{\gamma}_{c}^{T}$ this becomes

$$\vec{\nabla} = \underset{\sim}{\vec{\varepsilon}}^{T} \underline{\gamma}_{c}^{T} \nabla_{g} \tag{VI.2.17}$$

It is easily shown that the expression

$$\vec{\nabla} = \underset{\sim}{\vec{\varepsilon}}^{T} \nabla_{c} = \underset{\sim}{\vec{\varepsilon}}^{T} \underline{\gamma}_{c}^{T} \nabla_{g} \quad ; \quad \nabla_{c}^{T} = [\frac{\partial}{\partial r} \quad \frac{1}{r}\frac{\partial}{\partial \varphi} \quad \frac{\partial}{\partial z}] \tag{VI.2.18}$$

holds for $\vec{\nabla}$. The cylindrical vector basis $\underset{\sim}{\vec{\varepsilon}}$ is not independent of the φ- or g_2-coordinate:

$$\nabla_{c} \underset{\sim}{\vec{\varepsilon}}^{T} = \begin{bmatrix} 0 & 0 & 0 \\ \frac{1}{r}\vec{\varepsilon}_{\varphi} & -\frac{1}{r}\vec{\varepsilon}_{r} & 0 \\ 0 & 0 & 0 \end{bmatrix} \tag{VI.2.19}$$

and, using (VI.2.18)

$$\nabla_{g} \underset{\sim}{\vec{\varepsilon}}^{T} = \begin{bmatrix} 0 & 0 & 0 \\ \pi\vec{\varepsilon}_{\varphi} & -\pi\vec{\varepsilon}_{r} & 0 \\ 0 & 0 & 0 \end{bmatrix} \tag{VI.2.20}$$

For the gradient and the divergence of a vector $\vec{a}$ the following expressions hold - the quantity in brackets ( ) is affected by ∇_{g} -:

$$\begin{aligned} \vec{\nabla}\,\vec{a} &= \underset{\sim}{\vec{\varepsilon}}^{T} \underline{\gamma}_{c}^{T} \nabla_{g} \{(\underset{\sim}{a}^{T}) \underset{\sim}{\vec{\varepsilon}} + (\underset{\sim}{\vec{\varepsilon}}^{T}) \underset{\sim}{a}\} \\ &= \underset{\sim}{\vec{\varepsilon}}^{T} \underline{\gamma}_{c}^{T} \nabla_{g} \{(\underset{\sim}{\psi}^{T}) \underline{a}^{T} \underset{\sim}{\vec{\varepsilon}} + (\underset{\sim}{\vec{\varepsilon}}^{T}) \underline{a}\, \underset{\sim}{\psi}\} \end{aligned} \tag{VI.2.21}$$

$$\vec{\nabla}.\vec{a} = \underset{\sim}{\nabla}_g^T \underline{\gamma}_c(\underset{\sim}{a}) + \vec{\underset{\sim}{\varepsilon}}^T.\underline{\gamma}_c^T \underset{\sim}{\nabla}_g(\vec{\underset{\sim}{\varepsilon}}^T)\underset{\sim}{a}$$

$$= \underset{\sim}{\nabla}_g^T \underline{\gamma}_c \underline{a}(\underset{\sim}{\psi}) + \vec{\underset{\sim}{\varepsilon}}^T.\underline{\gamma}_c^T \underset{\sim}{\nabla}_g(\vec{\underset{\sim}{\varepsilon}}^T)\underline{a}\ \underset{\sim}{\psi} \qquad \text{(VI.2.22)}$$

For the gradient of a tensor $\mathbb{A}$ we can write

$$\vec{\nabla}\,\mathbb{A} = \vec{\nabla}(\vec{\underset{\sim}{\varepsilon}}^T \underline{A}\ \vec{\underset{\sim}{\varepsilon}})$$

$$= \vec{\underset{\sim}{\varepsilon}}^T \underline{\gamma}_c^T \underset{\sim}{\nabla}_g((\vec{\underset{\sim}{\varepsilon}}^T)\underline{A}\ \vec{\underset{\sim}{\varepsilon}} + \vec{\underset{\sim}{\varepsilon}}^T(\underline{A})\vec{\underset{\sim}{\varepsilon}} + \vec{\underset{\sim}{\varepsilon}}^T \underline{A}(\vec{\underset{\sim}{\varepsilon}})) \qquad \text{(VI.2.23)}$$

At MRS point $\underset{\sim}{m}$ the deformation of the material in state τ as compared with τ_o, is described by means of the deformation tensor $\mathbb{F}$. If the position vector of $\underset{\sim}{m}$ in state τ is denoted by $\vec{x}$, $\mathbb{F}$ can be written as

$$\mathbb{F} = (\vec{\nabla}^o\vec{x})^c = (\underset{\sim}{\nabla}_m \vec{x})^T \underset{\sim}{c}^o = \underset{\sim}{\vec{b}}^T \underset{\sim}{\vec{c}}^o \qquad \text{(VI.2.24)}$$

In components with respect to the cylindrical basis in $\underset{\sim}{m}$ this becomes

$$\mathbb{F} = \vec{\underset{\sim}{\varepsilon}}^T \underline{b}_c^T \underline{c}_c^o \vec{\underset{\sim}{\varepsilon}} = \vec{\underset{\sim}{\varepsilon}}^T \underline{F}\ \vec{\underset{\sim}{\varepsilon}} \qquad \text{(VI.2.25)}$$

with

$$\underline{b}_c = \begin{bmatrix} \frac{\partial r}{\partial m_1} & 0 & \frac{\partial z}{\partial m_1} \\ 0 & \pi r & 0 \\ \frac{\partial r}{\partial m_3} & 0 & \frac{\partial z}{\partial m_3} \end{bmatrix} \qquad \text{(VI.2.26)}$$

VI.3 A plain-strain element

A plain-strain element is used to simulate the CRS determination process, and is shown in figure VI.3.1.

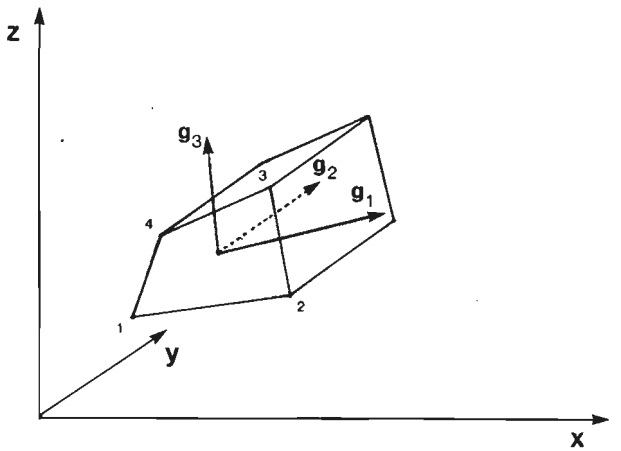

Fig. VI.3.1
The plain-strain element

With every axisymmetric element a plain-strain element having the same cross-section for $\varphi = 0$ is associated. The local CRS coordinates are such that

$$g_1 = g_1(x,z) \quad , \quad g_2 = g_2(y) \quad , \quad g_3 = g_3(x,z) \qquad \text{(VI.3.1)}$$

Each local coordinate lies within the interval [-1,1]. Moreover, $\frac{\partial y}{\partial g_2}$ has an arbitrary but equal value α for all y.

In the plain-strain CRS determination process none of the relevant quantities is a function of the y- or g_2-coordinates. The interpolation functions and nodal points used to interpolate these quantities are the same as those presented in section VI.2 for the axisymmetric element. For a vector $\vec{a}$ we write

$$\vec{a} = \underset{\sim}{\psi}^T \underline{a}^T \vec{\underset{\sim}{e}} = [\psi^1 \ \psi^2 \ \psi^3 \ \psi^4] \begin{bmatrix} a_x^1 & a_y^1 & a_z^1 \\ a_x^2 & a_y^2 & a_z^2 \\ a_x^3 & a_y^3 & a_z^3 \\ a_x^4 & a_y^4 & a_z^4 \end{bmatrix} \begin{bmatrix} \vec{e}_x \\ \vec{e}_y \\ \vec{e}_z \end{bmatrix} \qquad \text{(VI.3.2)}$$

In section VI.2 we found for the components of the vector basis $\vec{\underset{\sim}{\beta}}$ at CRS point $\underset{\sim}{g}$:

$$\vec{\underset{\sim}{\beta}} = \underline{\beta}_x \vec{\underset{\sim}{e}} \quad ; \quad \underline{\beta}_x = \begin{bmatrix} \frac{\partial x}{\partial g_1} & \frac{\partial y}{\partial g_1} & \frac{\partial z}{\partial g_1} \\ \frac{\partial x}{\partial g_2} & \frac{\partial y}{\partial g_2} & \frac{\partial z}{\partial g_2} \\ \frac{\partial x}{\partial g_3} & \frac{\partial y}{\partial g_3} & \frac{\partial z}{\partial g_3} \end{bmatrix} \qquad \text{(VI.3.3)}$$

On account of (VI.3.1) the matrix $\underline{\beta}_x$ becomes

$$\underline{\beta}_x = \begin{bmatrix} \frac{\partial x}{\partial g_1} & 0 & \frac{\partial z}{\partial g_1} \\ 0 & \alpha & 0 \\ \frac{\partial x}{\partial g_3} & 0 & \frac{\partial z}{\partial g_3} \end{bmatrix} \qquad \text{(VI.3.4)}$$

Interpolation of the Cartesian components x and y according to (VI.2.3) results in

$$\underline{\beta}_x = \begin{bmatrix} \frac{\partial \underset{\sim}{\psi}^T}{\partial g_1} \underset{\sim}{x} & 0 & \frac{\partial \underset{\sim}{\psi}^T}{\partial g_1} \underset{\sim}{z} \\ 0 & \alpha & 0 \\ \frac{\partial \underset{\sim}{\psi}^T}{\partial g_3} \underset{\sim}{x} & 0 & \frac{\partial \underset{\sim}{\psi}^T}{\partial g_3} \underset{\sim}{z} \end{bmatrix} \qquad \text{(VI.3.5)}$$

For the Jacobian J of the mapping $\vec{x} : G \to V(\tau)$, we find

$$J = \det(\underline{\beta}_x) \tag{VI.3.6}$$

and for the components of the reciprocal vector basis $\vec{\gamma}$

$$\vec{\gamma} = \underline{\gamma}_x \vec{e} = \underline{\beta}_x^{-T} \vec{e} \tag{VI.3.7}$$

The gradient operator can be written as

$$\vec{\nabla} = \vec{\gamma}^T \nabla_g = \vec{e}^T \underline{\gamma}_x^T \nabla_g = \vec{e}^T \nabla_x \quad ; \quad \nabla_x^T = \left[\frac{\partial}{\partial x} \quad \frac{\partial}{\partial y} \quad \frac{\partial}{\partial z}\right] \tag{VI.3.8}$$

Unlike the cylindrical vector basis $\vec{e}$, the Cartesian vector basis $\vec{e}$ is the same at every spatial point, hence

$$\nabla_x \vec{e}^T = \nabla_g \vec{e}^T = 0 \tag{VI.3.9}$$

For the gradient and the divergence of a vector $\vec{a}$ the following expressions hold - the quantity in brackets is affected by ∇_g -:

$$\vec{\nabla}\,\vec{a} = \vec{e}^T \underline{\gamma}_x^T \nabla_g (a^T) \vec{e} = \vec{e}^T \underline{\gamma}_x^T \nabla_g (\psi^T) \underline{a}^T \vec{e} \tag{VI.3.10}$$

$$\vec{\nabla} . \vec{a} = \nabla_g^T \underline{\gamma}_x (a) = \nabla_g^T \underline{\gamma}_x \underline{a}(\psi) \tag{VI.3.11}$$

At CRS point g the deformation tensor $\bar{F}$ describes the deformation of the fictitious material in state τ with respect to state τ_f. If the position vector of g in state τ is denoted by $\vec{\chi}$, we can write the following for $\bar{F}$

$$\bar{F} = (\vec{\nabla}^f \vec{\chi})^c = (\nabla_g \vec{\chi})^T \vec{\gamma}^f = \vec{\beta}^T \vec{\gamma}^f \tag{VI.3.12}$$

In components with respect to the Cartesian basis in g this becomes

$$\bar{F} = \vec{e}^T \underline{\beta}_x^T \underline{\gamma}_x^f \vec{e} = \vec{e}^T \underline{\bar{F}}\, \vec{e} \tag{VI.3.13}$$

If the cross-section of the element in state τ_f is a square with sides of length ℓ, the matrix $\underline{\gamma}_x^f$ becomes

$$\underline{\gamma}_x^f = \begin{bmatrix} \frac{2}{\ell} & 0 & 0 \\ 0 & \frac{1}{\alpha} & 0 \\ 0 & 0 & \frac{2}{\ell} \end{bmatrix} \qquad \text{(VI.3.14)}$$

and, thus, the matrix $\underline{\bar{F}}$ is

$$\underline{\bar{F}} = \begin{bmatrix} \frac{2}{\ell}\frac{\partial x}{\partial g_1} & 0 & \frac{2}{\ell}\frac{\partial x}{\partial g_3} \\ 0 & 1 & 0 \\ \frac{2}{\ell}\frac{\partial z}{\partial g_1} & 0 & \frac{2}{\ell}\frac{\partial z}{\partial g_3} \end{bmatrix} \qquad \text{(VI.3.15)}$$

VI.4 Aspects of the CRS determination process

The optimum element geometry
The coupling between CRS and MRS

The optimum element geometry

The axisymmetric element used to simulate the forming process is presented in section VI.2. The shape of its cross-section may affect the accuracy of the numerical integrations and the error, possibly introduced by the interpolation of the MRS displacement $\Delta_m \vec{x}_e$. We assume the accuracy of the numerical integration to be maximal and the error caused by interpolation to be minimal if the cross-section is a square. This shape is called the optimum shape.

Both the size and the shape of the cross-section may affect the interpolation error. In view of the size the error can be assumed to be minimal, if the area of the cross-section is a given function of the stress gradient within and in the neighbourhood of the element. Various ideas have been published in literature as to the optimum size of elements (see Turcke & McNeice (1974), Melosh & Marcal (1977), Chiou & Wang (1979), Babuska & Rheinboldt (1979, 1980), Dwyer et al. (1980), Zienkiewicz et al. (1981, [29]) and Bathe & Sussman (1983)). In the CRS determination process discussed in this thesis the optimum size of elements is not considered.

The length in y-direction of the plain-strain element in state τ_f is so chosen that the reciprocal vector basis $\underset{\sim}{\vec{\gamma}}^f$ at every CRS point is

$$\underset{\sim}{\vec{\gamma}}^f = \frac{2}{l^f} \underset{\sim}{\vec{e}} \qquad \text{(VI.4.1)}$$

In the current state τ the deformation tensor at CRS point $\underset{\sim}{q}$, which describes the deformation of the fictitious material at that point compared to state τ_f, is denoted by $\bar{\mathbf{F}}^f$ (see figure VI.4.1).

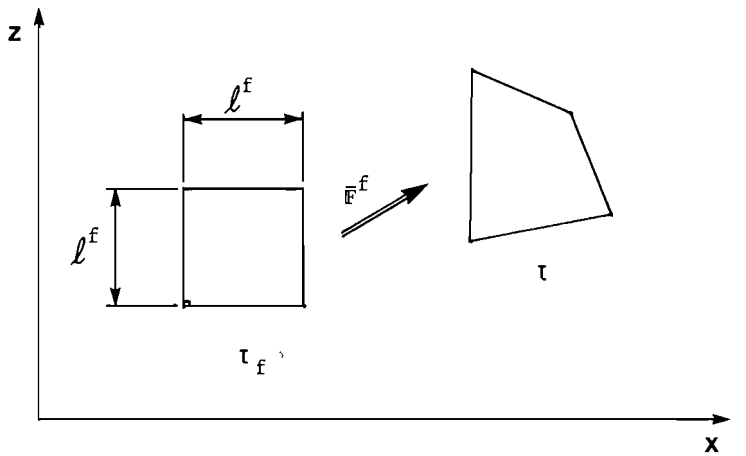

Fig. VI.4.1
The deformation of an element from state τ_f to state τ

On account of (VI.3.12) and using (VI.4.1) we can write

$$\bar{\mathbb{F}}^f = \vec{\underset{\sim}{\beta}}^T \vec{\underset{\sim}{\gamma}}^f = \frac{2}{\ell^f} \vec{\underset{\sim}{\beta}}^T \vec{\underset{\sim}{e}} \qquad \text{(VI.4.2)}$$

The Green-Lagrange strain tensor in $\underset{\sim}{g}$ in state τ compared to state τ_f becomes

$$\bar{\mathbb{E}}^f = \frac{1}{2}(\bar{\mathbb{F}}^{fc}.\bar{\mathbb{F}}^f - \mathbb{I}) = \frac{1}{2}\{(\frac{2}{\ell^f})^2 \vec{\underset{\sim}{e}}^T \vec{\underset{\sim}{\beta}}.\vec{\underset{\sim}{\beta}}^T \vec{\underset{\sim}{e}} - \mathbb{I}\} \qquad \text{(VI.4.3)}$$

Using $\bar{\mathbb{E}}^f$, the Cauchy stress tensor $\bar{\underset{\sim}{\sigma}}^f$ in $\underset{\sim}{g}$ can be determined as given in (IV.2.3) and (IV.2.4).

The coupling between CRS and MRS

During the simultaneous simulation of the forming process and the CRS determination process, there must always be an unambiguous relationship between CRS and MRS. This implies that the boundaries of both reference systems must always coincide. Hence, following (V.2.14),

if the iterative changes $d_g(\ )$ are assumed to be infinitesimal, the iterative displacements $d_g\vec{\chi}$ and $d_m\vec{x}$ at every boundary nodal point must satisfy

$$\vec{v}.d_g\vec{\chi} = \vec{n}.d_m\vec{x} \quad ; \quad \vec{v} = \vec{n} \tag{VI.4.4}$$

The unit outward normal vector $\vec{v}$ is defined as shown in figure VI.4.2.

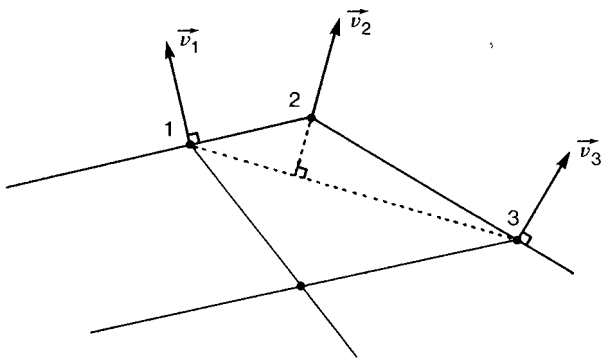

Fig. VI.4.2
The definition of the unit outward normal vector at boundary points

As discussed in section II.4 the external load on the material consists of a volume load $\vec{q}$ and a boundary load $\vec{t}^*$. After discretising the CRS, these loads must be transferred to consistent nodal forces and thus the material is loaded by concentrated forces. Nodal point positions are chosen so as to account for these forces in a straightforward manner. If $\vec{q}$, $\vec{t}^*$ or one or more concentrated forces are material-associated, the CRS must not move with respect to the MRS at the nodal points where the (consistent) nodal forces are applied. The iterative displacements at these nodal points must satisfy

$$d_g\vec{\chi} = d_m\vec{x} \tag{VI.4.5}$$

For a boundary point the above requirement is stronger than (VI.4.4)

VII Simulation of axisymmetric forming processes

VII.1 Introduction

A computer program is developed to test the method described in the preceding chapters. With this program numerical simulation of axisymmetric forming processes can be carried out, using either the Lagrangian or the AEL formulation. It is also possible to employ the rezoning technique. The program is written in Burroughs Extended Algol and implemented on the Burroughs B7700 computer of the Eindhoven University of Technology. Some program items concerning the simulation according to the AEL formulation are discussed in section VII.2. Results of some simulations are presented in section VII.3.

VII.2 A simulation program

For the simulation of a forming process according to the AEL formulation the following sequence of instructions is carried out by the program.

```
1:   define initial model;
     while increments-to-calculate do
     begin
2:      define new increment;
        while no-convergence do
        begin
3:         calculate CRS nodal point forces;
4:         make system of equations;
5:         introduce kinematic boundary conditions and coupling
           conditions for CRS and MRS;
6:         calculate iterative CRS and MRS displacements at nodal
           points;
7:         adjust CRS nodal point displacements;
8:         calculate material-associated quantities at follower
           points;
9:         update geometry and location;
10:        update material-associated data at follower points;
11:        transfer material-associated data from follower points to
           integration and nodal points;
12:        calculate residual nodal point forces;
13:        check convergence;
        end;
     end.
```

These instructions will be discussed shortly.

1: Data on geometry, connectivity, kinematic and dynamic boundary conditions and material behaviour are input data for the program. It is possible to interrupt the simulation and restart with the same or partly changed boundary conditions. In that case, the data on the deformation history must also be available as input data.

2: At the beginning of every increment the follower points are redefined, to be the MRS points, coinciding with the nodal points and the mid-points of element sides and elements. Defining the follower points determines the cells as well. For every nodal and integration point are stipulated the cell in which it is situated and its local MRS coordinates within this cell. Material-associated data at the nodal points are transferred to the new follower points by interpolation.

3: The nodal forces arising out of the deviation of optimum element shape, are determined according to the method described in chapter IV and section V.4.

4: The iterative CRS and MRS displacements $d_g\vec{\underset{\sim}{x}}$ and $d_m\vec{\underset{\sim}{x}}$ must satisfy the systems of linearised equations (V.2.13)

$$\begin{bmatrix} \underline{\underline{A}}^i & \underline{\underline{B}}^i \\ 0 & \underline{\underline{V}}^i \end{bmatrix} \begin{bmatrix} d_m\vec{\underset{\sim}{x}} \\ d_g\vec{\underset{\sim}{x}} \end{bmatrix} = \begin{bmatrix} \vec{\underset{\sim}{R}}_1^i \\ \vec{\underset{\sim}{R}}_2^i \end{bmatrix} \qquad \text{(VII.2.1)}$$

If the material is (nearly) incompressible, as is the case in some elasto-plastic forming processes, the axisymmetric element used, may behave much too stiffly, as is described by Nagtegaal et al. (1974) and Nagtegaal & De Jong (1981). To prevent this "locking", reduced numerical integration is employed for those terms in (VII.2.1), which characterize the hydrostatic material behaviour.

5: At a nodal point the two components of $d_g\vec{\underset{\sim}{x}}$ and $d_m\vec{\underset{\sim}{x}}$ are either suppressed, prescribed (nonzero) or unknown. At a boundary point we want to satisfy the coupling condition (V.2.14), that is

$$\vec{v}^i . d_g\vec{\underset{\sim}{x}} = \vec{n}^i . d_m\vec{\underset{\sim}{x}} \qquad \text{(VII.2.2)}$$

where $\vec{v}^i = \vec{n}^i$ is the unit outward normal vector at that point. At some points the coupling condition (VI.4.5) has to be satisfied, that is

$$d_g\vec{\chi} = d_m\vec{x} \qquad \text{(VII.2.3)}$$

Satisfying (VII.2.2) or (VII.2.3) means coupling one or both components of $d_g\vec{\chi}$ and $d_m\vec{x}$. The coupled components are denoted by an index c, the free but unknown components are denoted by an index $\bar{u}$ (for $d_g\vec{\chi}$) and u (for $d_m\vec{x}$). After dealing with the suppressed and prescribed components in the usual way, the system of equations (VII.2.1) can be written as follows

$$\begin{bmatrix} \underline{A}_{uu} & \underline{A}_{uc} & \underline{B}_{u\bar{u}} & \underline{B}_{uc} \\ \underline{A}_{cu} & \underline{A}_{cc} & \underline{B}_{c\bar{u}} & \underline{B}_{cc} \\ \underline{0} & \underline{0} & \underline{V}_{\bar{u}u} & \underline{V}_{\bar{u}c} \\ \underline{0} & \underline{0} & \underline{V}_{\bar{c}u} & \underline{V}_{\bar{c}c} \end{bmatrix} \begin{bmatrix} d_m\underset{\sim}{x}_u \\ d_m\underset{\sim}{x}_c \\ d_g\underset{\sim}{\chi}_{\bar{u}} \\ d_g\underset{\sim}{\chi}_c \end{bmatrix} = \begin{bmatrix} \underset{\sim}{R}_{1u} \\ \underset{\sim}{R}_{1c} \\ \underset{\sim}{R}_{2\bar{u}} \\ \underset{\sim}{R}_{2c} \end{bmatrix} \qquad \text{(VII.2.4)}$$

Taking $d_g\underset{\sim}{\chi}_c = d_m\underset{\sim}{x}_c$ into account and deleting the equations with the unknown right-hand vector $\underset{\sim}{R}_{2c}$ leaves us with

$$\begin{bmatrix} \underline{A}_{uu} & \underline{A}_{uc} + \underline{B}_{uc} & \underline{B}_{u\bar{u}} \\ \underline{A}_{cu} & \underline{A}_{cc} + \underline{B}_{cc} & \underline{B}_{c\bar{u}} \\ \underline{0} & \underline{V}_{\bar{u}c} & \underline{V}_{\bar{u}\bar{u}} \end{bmatrix} \begin{bmatrix} d_m\underset{\sim}{x}_u \\ d_m\underset{\sim}{x}_c \\ d_g\underset{\sim}{\chi}_{\bar{u}} \end{bmatrix} = \begin{bmatrix} \underset{\sim}{R}_{1u} \\ \underset{\sim}{R}_{1c} \\ \underset{\sim}{R}_{2\bar{u}} \end{bmatrix} \qquad \text{(VII.2.5)}$$

6: The iterative displacement components $d_m\underset{\sim}{x}_u$, $d_m\underset{\sim}{x}_c$ and $d_g\underset{\sim}{\chi}_{\bar{u}}$ are solved from (VII.2.5).

7: If the CRS and MRS boundaries coincide at the beginning of an iterative calculation, they will still approximately coincide after the iterative calculation, if (VII.2.2) is satisfied and if the iterative displacements $d_g\vec{\chi}$ and $d_m\vec{x}$ are infinitesimal. Since these displacements are finite the boundaries will move apart, as is shown in figure VII.2.1 for one nodal point.

To ensure that the CRS and MRS boundaries coincide as closely as possible at the end of the iterative calculation, the iterative boundary nodal point displacements $d_g\vec{\chi}$ are adjusted. This is done in such a way that every boundary nodal point will finally

be situated on the circular arc through the MRS points which, at the beginning of the iterative calculation, coincide with the boundary point and the two adjacent boundary points, as shown in figure VII.2.2.

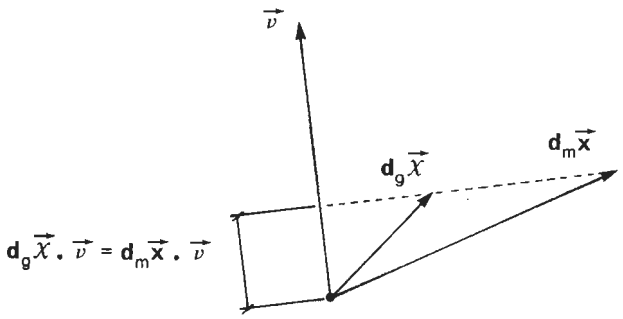

Fig. VII.2.1

Difference between iterative MRS and CRS displacements at a nodal point

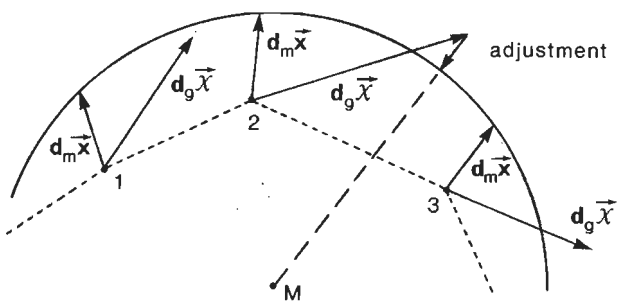

Fig. VII.2.2

Adjustment of the iterative CRS displacement at boundary nodal point 2

8: The material-associated quantities are determined at the follower points. After calculating the iterative change of the deformation tensor $\mathbf{F}$, according to

$$d_m\mathbf{F} = (\vec{v}\ d_m\vec{x})^c = (\underset{\sim}{v}_m d_m\vec{x})^{T\to o}_{\underset{\sim}{c}} \qquad \text{(VII.2.6)}$$

the iterative change of the Green-Lagrange strain tensor is calculated in accordance with

$$d_m\mathbf{E} = \frac{1}{2}(d_m\mathbf{F}^c.\mathbf{F}^i + \mathbf{F}^{ic}.d_m\mathbf{F} + d_m\mathbf{F}^c.d_m\mathbf{F}) \qquad \text{(VII.2.7)}$$

The Cauchy stress tensor and the current yield stress are determined according to the procedure described in section V.4. The hardening parameter is constant in value, as the hardening is supposed to be linear.

9: Calculating the new position of the nodal points is very straightforward. For every follower point it is determined in which element this point is situated and what its local CRS coordinates are within this element. The same applies, for every nodal point, to the cell in which this point is situated and what its local MRS coordinates are within this cell.

Although the iterative boundary nodal point displacements are adjusted, the CRS and MRS boundaries will not coincide exactly as is shown in figure VII.2.3. This deviation is unavoidable and in most cases very slight. However, follower points may fall outside the element mesh. This must be corrected for two reasons, the first being that one or more cells will not then be defined. Second, material-associated data must not be lost to the new element mesh. For every follower point, situated outside the element mesh, a new follower point is defined as shown in figure VII.2.4.

10: The material-associated data at the new follower points are calculated by interpolation between the data at points $\underset{\sim}{m}_1$ and $\underset{\sim}{m}_2$.

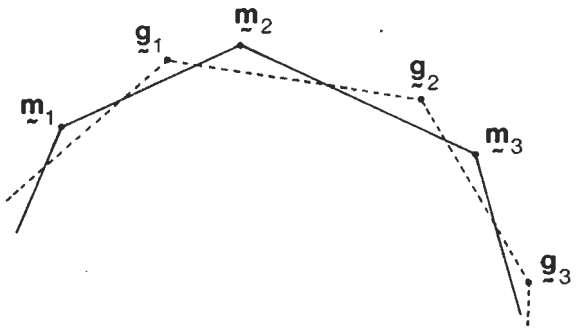

Fig. VII.2.3
Deviation of the CRS and MRS boundaries

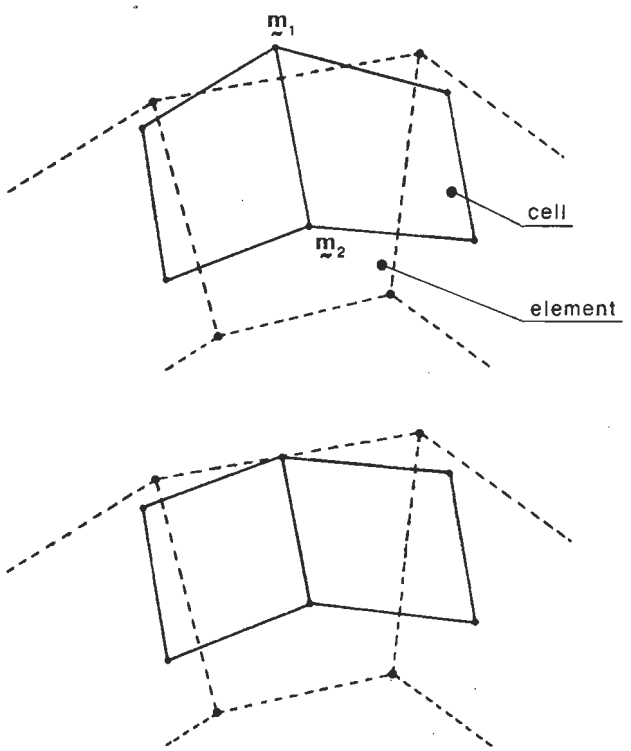

Fig. VII.2.4
Definition of a new follower point

11: Some material-associated quantities must be determined at the integration points. This is necessary for the calculation of the residual nodal point forces and, if a new iterative calculation has to be carried out, for the calculation of the left-hand matrix in (VII.2.1). All the material-associated quantities must be determined at the nodal points as well. At the beginning of the ensuing increment these data are transferred to the new follower points. The Cauchy stress tensor σ at the nodal points is used in every iterative calculation to determine $(\vec{v}\ \sigma)$ at the integration points. Material-associated data at an integration or nodal point are determined by linear interpolation between these data at those follower points, which are the vertices of the cell in which the integration or nodal point is situated (see figure VII.2.5).

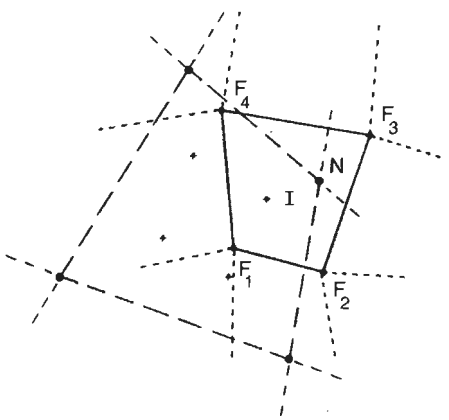

Fig. VII.2.5

Calculation of material-associated data at nodal point N *and integration point* I *by linear interpolation between data at follower points* F_1, F_2, F_3 *and* F_4

12: The residual nodal point forces are determined per element, following

$$\vec{R}^{i}_{\sim 1e} = \int_{G_e} \underset{\sim}{\psi}\, \vec{q}_e J_e^{i}\, dG + \int_{G_e^*} \underset{\sim}{\psi}\, \vec{t}^{*}_e J_e^{*i}\, dG^{*}$$

$$- \int_{G_e} (\nabla_{g\sim} \underset{\sim}{\psi}^{T})^{T} \vec{\gamma}^{i}_{\sim e} \cdot \sigma^{i}_e J^{i}_e\, dG \qquad \text{(VII.2.8)}$$

Volume loads $\vec{q}$ and surface loads $\vec{t}^{*}$ are taken into account by concentrated nodal point forces $\vec{r}^{k}$ which are applied after assembling the elements. The total residual nodal force vector then becomes

$$\vec{R}^{i}_{\sim 1} = \sum_{k=1}^{n_k} \vec{r}^{k}_{\sim} - \sum_{e=1}^{n} \int_{G_e} (\nabla_{g\sim} \underset{\sim}{\psi}^{T})^{T} \vec{\gamma}^{i}_{\sim e} \cdot \sigma^{i}_e J^{i}_e\, dG \qquad \text{(VII.2.9)}$$

When the iterative calculation is terminated, the equivalent nodal force vector $\vec{n}_{\sim 1}$, defined by

$$\vec{n}_{\sim 1} = - \sum_{e=1}^{n} \int_{G_e} (\nabla_{g\sim} \underset{\sim}{\psi}^{T})^{T} \vec{\gamma}_{\sim e} \cdot \sigma_e J_e\, dG \qquad \text{(VII.2.10)}$$

is taken into account in the first iteration step of the next increment, by adding it to the new external nodal force vector.

13: The accuracy of the current approximated solution for the incremental MRS displacement $\Delta_m \vec{x}_{\sim}$, is checked. A measure for this accuracy is a norm of $d_m \vec{x}_{\sim}$ or $\vec{R}_{\sim 1}$. If the "exact" solution for $\Delta_m \vec{x}_{\sim}$ is obtained, these norms are both zero. The approximation is considered to be accurate enough if one of these norms is smaller than an associated limit value. In that case the iteration process is converged and a new incremental calculation can be started.

If the Lagrangian formulation is used in the numerical simulation, the iterative nodal point displacements have to satisfy the system of linearised equations given below, resulting from (VII.2.1) with $d_g\vec{\chi} = d_m\vec{x}$, that is

$$(\underline{\underline{A}}^i + \underline{\underline{B}}^i).d_m\vec{x} = \vec{R}_1^i \qquad \text{(VII.2.11)}$$

The integration points act as follower points. The program steps 2, 3, 7, 10 and 11 are dropped completely, whereas others are carried out partly.

If the rezoning technique is employed in the simulation, the iterative displacements $d_g\vec{\chi}$ and $d_m\vec{x}$ are calculated in two steps. First the iterative nodal point displacements $d_g\vec{\chi}^{\blacktriangledown}$ are determined so as to satisfy the system of linearised equations

$$\underline{\underline{V}}^i.d_g\vec{\chi}^{\blacktriangledown} = \vec{R}_2^i \qquad \text{(VII.2.12)}$$

obtained from (VII.2.1) with $d_m\vec{x} = \vec{0}$. After defining the new element mesh resulting from these iterative nodal point displacements, material-associated data are transferred from follower points to integration points by interpolation as already described.

In the second step the simulation is continued using the new element mesh and the Lagrangian formulation. The nodal point displacements $d_m\vec{x}$ are determined so as to satisfy (VII.2.11). The total iterative nodal point displacements are

$$d_g\vec{\chi} = d_g\vec{\chi}^{\blacktriangledown} + d_m\vec{x} \qquad \text{(VII.2.13)}$$

The material-associated quantities are determined at the follower points. Finally these data are transferred to integration and nodal points in the usual way.

VII.3 Results of some simulations

The first process which is analysed, clearly shows the possibilities of the AEL formulation. We consider the circular disk, shown in figure VII.3.1. In five equal incremental steps the radial displacement of the outer edge is prescribed. The ultimate radial strain is 25%. The dashed area is considered in the simulation.

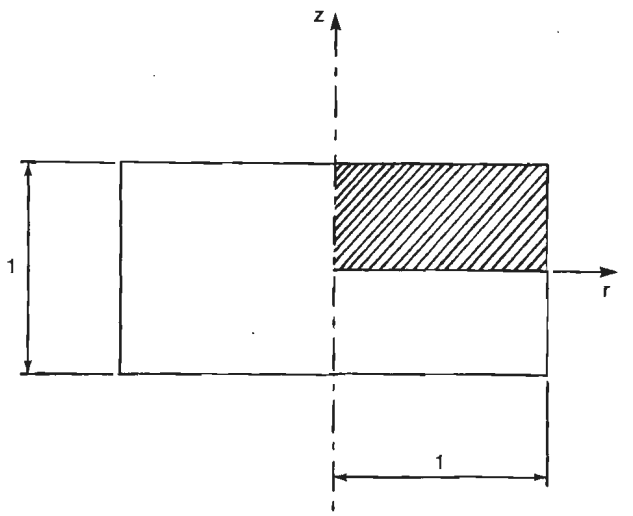

$E = 2.1 \cdot 10^5$ N/mm^2
$\nu = 0.3$
$h = 10^4$ N/mm^2
$\sigma_v^0 = 250$ N/mm^2
$\bar{E} = 100$ N/mm^2
$\bar{\nu} = 0.45$
measures in mm

Fig. VII.3.1
Circular disk: geometry and material parameters

If the material behaviour is elasto-plastic the analytical solution for the stress components is given by

$$\sigma_{rr} = \sigma_{\varphi\varphi} = \sigma_v^0 + \frac{2Eh}{E + 2h(1-\nu)} \left\{ \frac{1}{2} \ln(1 + 2E_{rr}) - \frac{\sigma_v^0 (1-\nu)}{E} \right\} ;$$

$$\sigma_{zz} = 0 \qquad \text{(VII.3.1)}$$

The use of the Lagrangian formulation leads to the result shown in figure VII.3.2a. Using the AEL formulation leads to the result which is shown in figure VII.3.2b.

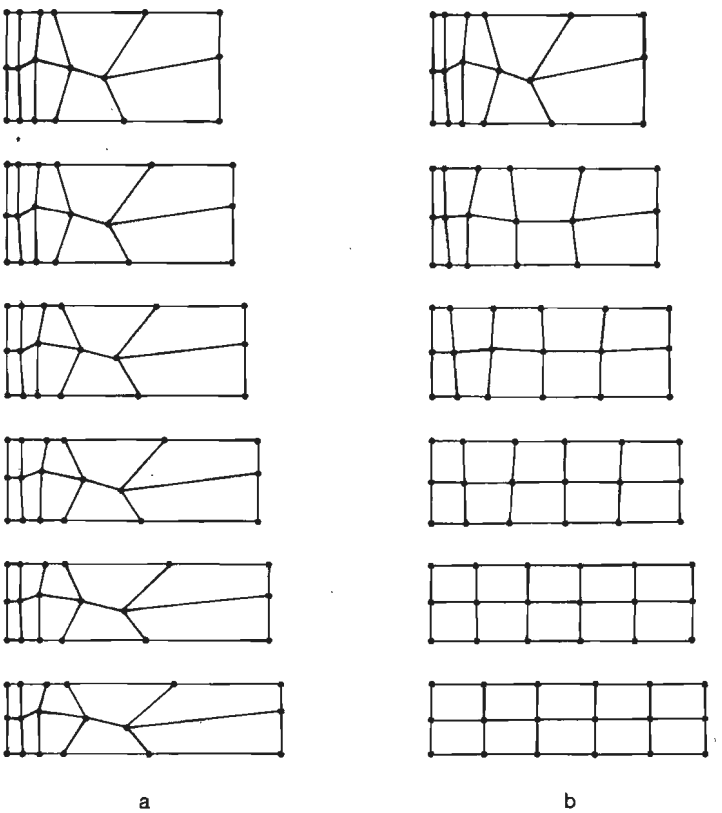

Fig. VII.3.2

Element mesh in various states of the deformation process, using the Lagrangian (a) *and the AEL* (b) *formulation*

As we can see all elements have the same geometry in the final state if the AEL formulation is used. Using the rezoning technique also leads to the result shown in figure VII.3.2b. In all cases and every increment, convergence was reached after the same number of iterative

calculations and then the stresses had the exact values given by (VII.3.1). The ratio of the total process time was (in seconds)

Lagrangian : rezoning : AEL = 137 : 195 : 207 (VII.3.2)

The use of the AEL formulation provides the possibility to suppress or prescribe nodal point displacements or nodal point forces in a straightforward manner, while at the same time the material displacement at those points is an unknown quantity, which can be determined. In figure VII.3.3 the undeformed (dotted) and the deformed state of the circular disk is shown both when the Lagrangian formulation (a) and the AEL formulation (b) is used. Using the AEL formulation the following conditions are chosen

$$d_g x_r = 0 \quad ; \; d_g x_z = d_m x_z \qquad \text{at points 1-9} \qquad \text{(VII.3.3a)}$$

$$d_g \vec{x} = d_m \vec{x} \qquad \text{at all other points} \qquad \text{(VII.3.3b)}$$

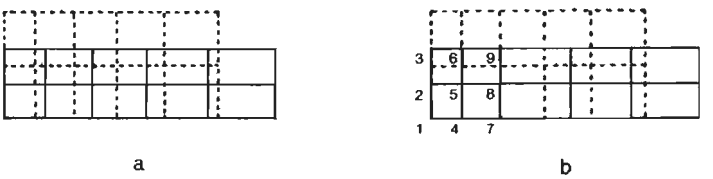

Fig. VII.3.3

Element mesh in undeformed and deformed state, using the Lagrangian (a) *and the AEL* (b) *formulation*

The following simulation is carried out merely to show the possibility of optimizing element geometries, even if all nodal points are situated on a curved boundary. We consider the body and initial element mesh, shown in figure VII.3.4.

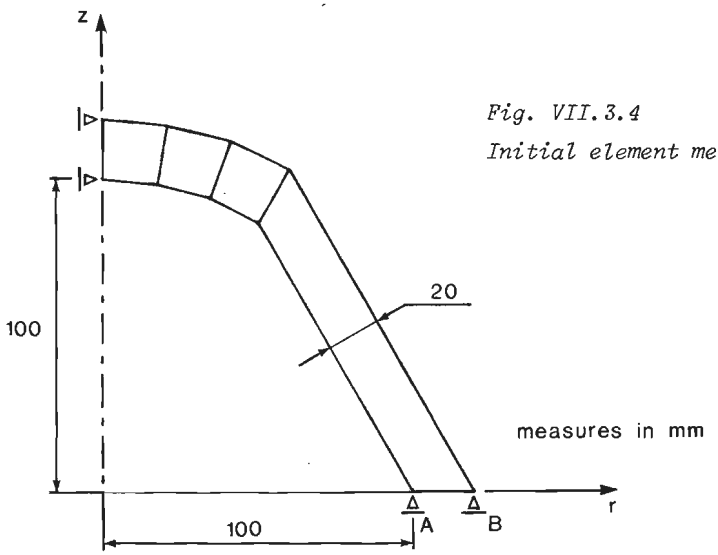

Fig. VII.3.4
Initial element mesh

If there is no prescribed material displacement the CRS determination process leads to the element mesh shown in figure VII.3.5.

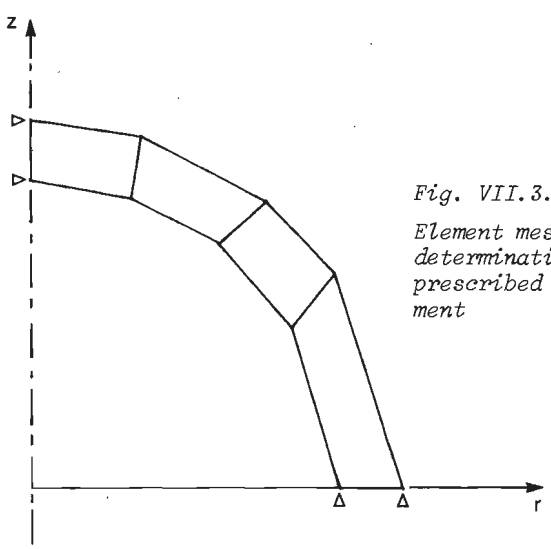

Fig. VII.3.5
Element mesh after CRS determination process with no prescribed material displacement

A consequence of this rather sweeping change of the element mesh is that the new geometry of the body is very much different from the initial geometry. Although this is almost certainly not allowable in a real simulation, this example clearly shows the possibility of mesh adaptation by the CRS determination process. If radial displacements of the points A and B are prescribed, we have a simultaneous forming and CRS determination process. The displacement is prescribed in 50 equal increments. The deformed state after 50 increments is shown in figure VII.3.6a. The same configuration, following from a Lagrangian formulation, is shown in figure VII.3.6b.

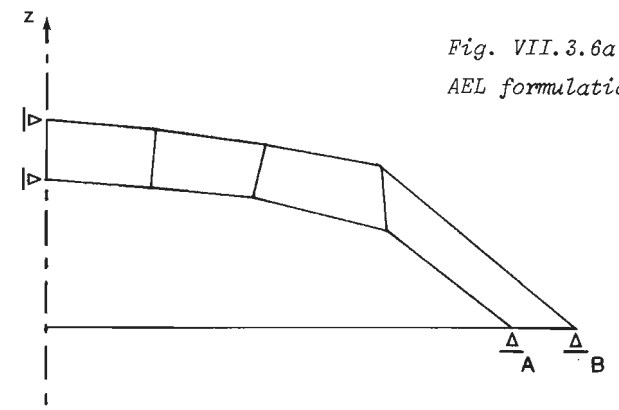

Fig. VII.3.6a
AEL formulation

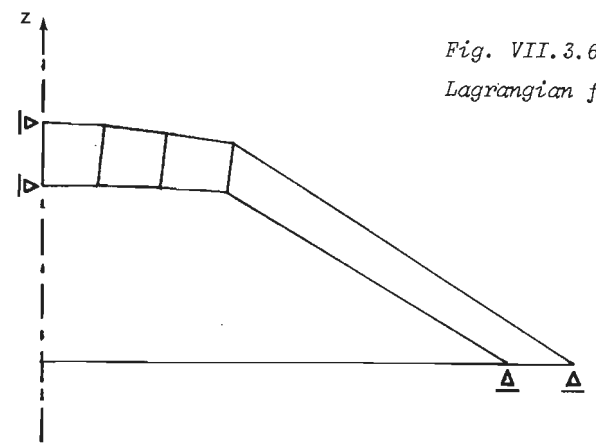

Fig. VII.3.6b
Lagrangian formulation

The deformation of a thick-walled cylinder under internal pressure represents a more realistic forming process. In the incremental simulation the pressure is realized by prescribing proper nodal forces at nodal points on the cylinder inner edge. The section of the cylinder to be analysed is shown in figure VII.3.7. Also the load history is shown.

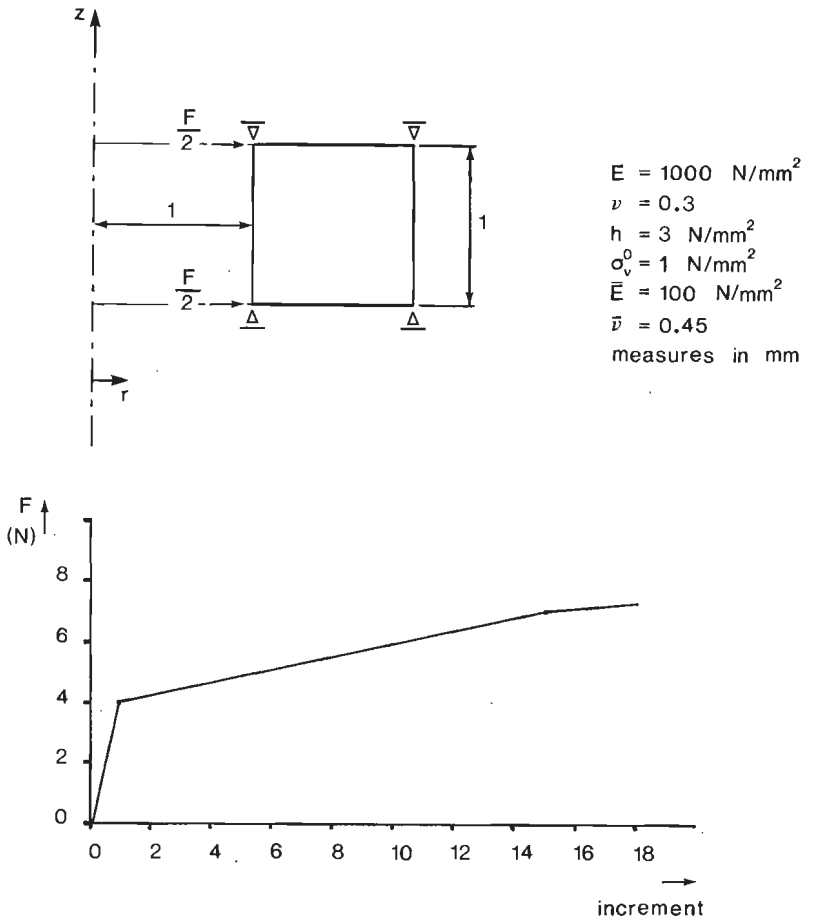

Fig. VII.3.7

Thick-walled cylinder under internal pressure: geometry of analysed section, material parameters and load history

To prevent "locking", reduced integration is employed. The simulation is carried out using a Lagrangian formulation and an element mesh with 5 elements, which are equally sized in the initial state. Because the radial displacement is a nonlinear function of the radius, the elements will not remain of equal size during the deformation process, as can be seen from figure VII.3.8a. However, if the AEL formulation is used, all elements have the same geometry, as is shown in figure VII.3.8b. The total prescribed internal radial force in the shown deformed state is 7.1 N.

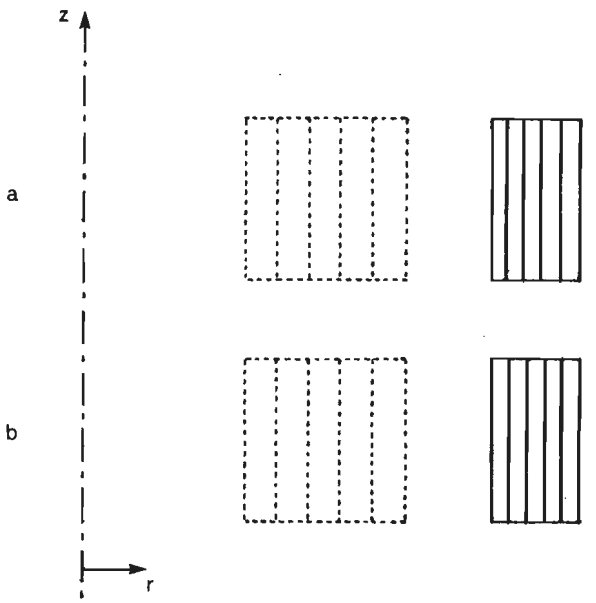

Fig. VII.3.8

Element mesh in undeformed and deformed state, using the Lagrangian (a) *and the AEL* (b) *formulation*

Figure VII.3.9 shows the internal pressure as a function of the inner radius, which is almost the same for both of the above mentioned simulations. It is found that the simulation with the AEL formulation leads to the same result as the Lagrangian simulation using 10 elements, while the Lagrangian simulation, using 5 elements, differs slightly from this.

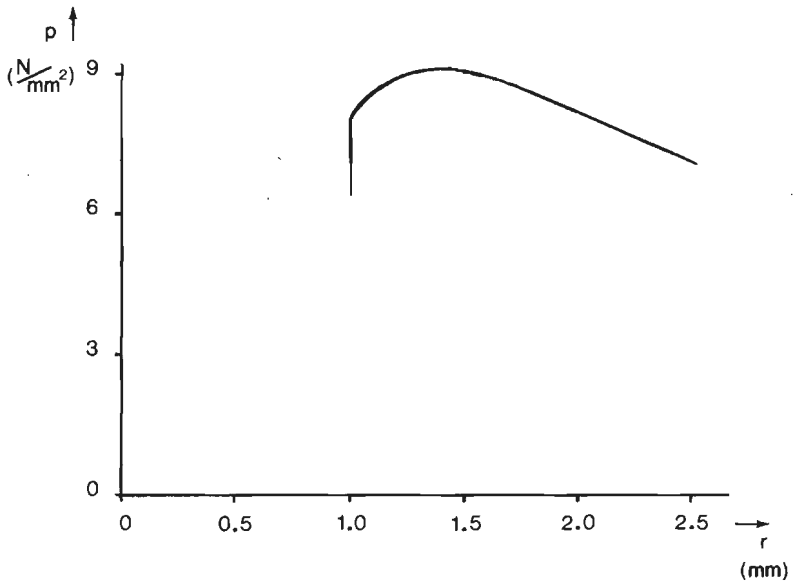

Fig. VII.3.9
Internal pressure as a function of the inner radius

The simulation of the coining process clearly shows the merits of the AEL formulation when prescribing certain boundary conditions. Figure VII.3.10 shows the geometry, the initial element mesh and the material parameters of the body to be deformed. All contact areas are assumed to be frictionless. The tool is rigid and its displacement is prescribed, as shown in the figure, to give a maximum height reduction of 25%.

Using the Lagrangian formulation the contact area between tool and specimen will not be constant during the simulation. This is because the prescribed tool displacement is taken into account by prescribing the displacement of nodal points which are material points having also a displacement in r-direction. The use of the AEL formulation provides the possibility to suppress the displacement in r-direction of those nodal points which are situated under the tool. The following conditions are satisfied.

$$d_g x_r = 0 \quad ; \quad d_g x_z = d_m x_z \qquad \text{for } 0 \leq r^o \leq 9$$

$$d_g \vec{x} = d_m \vec{x} \qquad \text{for } 9 < r^o \leq 18 \qquad \text{(VII.3.4)}$$

The deformed geometry is shown in figure VII.3.11a. The same simulation is carried out with more nodal point displacements suppressed in r-direction, according to the conditions

$$d_g x_r = 0 \quad ; \quad d_g x_z = d_m x_z \qquad \text{for } 0 \leq r^o \leq 13.5$$

$$d_g \vec{x} = d_m \vec{x} \qquad \text{for } 13.5 < r^o \leq 18 \qquad \text{(VII.3.5)}$$

The deformed geometry is shown in figure VII.3.11b. The stress component σ_{zz} in the contact area between tool and specimen for both the conditions (VII.3.4) and (VII.3.5) is shown in figure VII.3.12. It is obvious that the simulation according to (VII.3.5) leads to a more realistic deformation and that the tool-specimen stress is smoother.

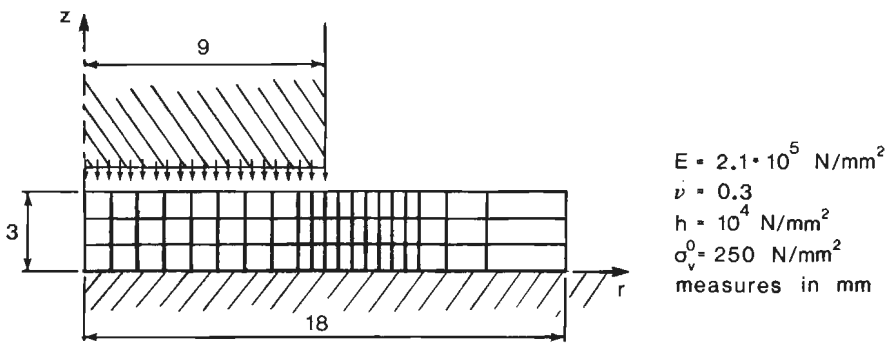

Fig. VII.3.10

Geometry, initial element mesh and material parameters for the coining process

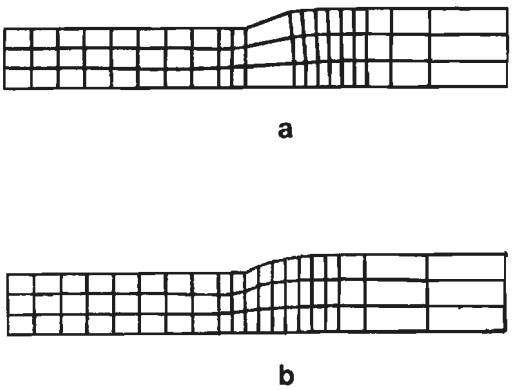

Fig. VII.3.11

Deformed geometry and element mesh after 25% height reduction

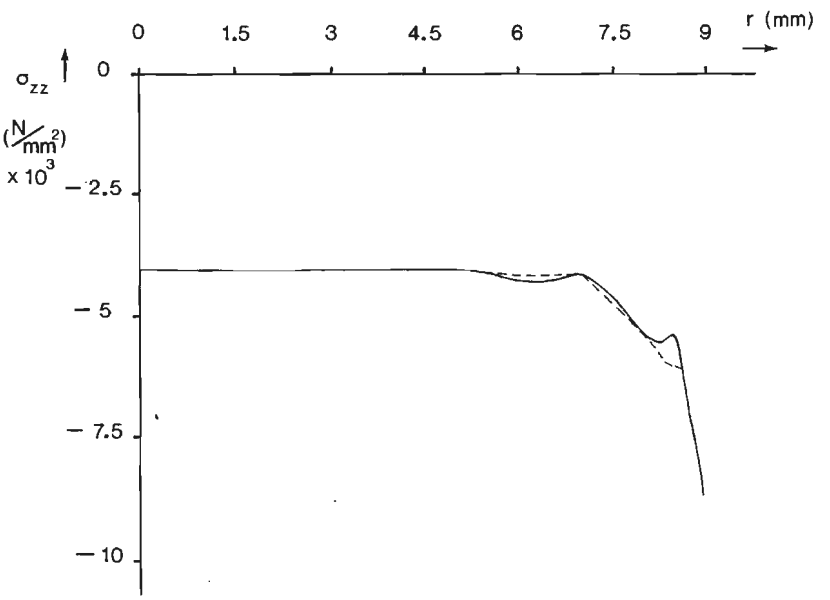

Fig. VII.3.12

Stress component σ_{zz} in the contact area between tool and specimen; simulations with conditions (VII.3.4): ——, and (VII.3.5): -----

VIII Concluding remarks

If the finite element method and the Lagrangian formulation is used to simulate forming processes, the elements are associated with the material. Large local deformations may cause excessively distorted elements which may give rize to numerical difficulties. To prevent this problem a number of ad hoc solutions is known, such as the rezoning technique, where, if necessary, the simulation is interrupted and restarted with a new element mesh.

This thesis describes the results of research on the application of the Arbitrary-Eulerian-Lagrangian (AEL) formulation for the simulation of forming processes. Using this formulation the element mesh is not associated with the material to be deformed. However, it is necessary that there is an unambiguous relationship between the points of element mesh and material. The theoretical background of the AEL formulation is presented and some new conceptions are introduced. In the mathematical formulations a vector-tensor notation is used.

The flexibility, provided by the AEL formulation concerning the choice of the element mesh, can be used to optimize the shape of individual elements. The optimization described in this thesis is a continuous and automatic process. The position and geometry of the elements result from the deformation of a fictitious, isotropic, elastic material - Young's modulus $\bar{E}$, Poisson's ratio $\bar{\nu}$ -, which is associated with the element mesh.

The method is applied to the simulation of axisymmetric forming processes. The elastic material behaviour is isotropic and linear, while isotropic hardening is assumed in the elasto-plastic range. The automatic optimization of the element shape leads to good results for the simulation of the considered forming processes. It appears that the Young's modulus $\bar{E}$ does not affect the optimization, whereas this is less apparent if a higher value of $\bar{\nu}$ ($0 \leq \bar{\nu} < 0.5$) is chosen. The AEL formulation is very appropriate not only to generate a suitable element mesh but also to take certain boundary conditions into account.

As the element mesh is not associated with the material to be deformed, material-associated quantities are calculated at follower points, being material points, which are redefined several times during the simulation. Subsequently the material-associated data are transferred to the integration points by interpolation. This provokes inaccuracies, which disturb the nodal point equilibrium, causing the convergence rate of the iterative procedure to decrease.

Because of the fact that, besides the forming process, the deformation of the fictitious material is considered and because of the necessary use of follower points, a relatively large amount of data in the analysis occurs. Moreover, the computer time needed for an analysis is rather long. This is partly caused by the low efficiency of the program, which aspect did not receive to much attention.

Resuming we can conclude that the use of the AEL formulation and the finite element method to simulate forming processes is very advantageous for automatically optimizing element shape and accounting for certain boundary conditions. The merits of the formulation will increase if further investigation is done concerning the possibilities of the presented method.

It is possible to adapt the element size to, for instance, the stress gradient within and in the neighbourhood of an element. For a real optimization of the element mesh it will generally be also necessary to adapt the number of elements. Further research on automatic optimization of element size and number of elements is required.

Combining the AEL formulation with the use of gap-elements offers the possibility to simulate processes where contact phenomena occur, even if the contact surfaces show large relative displacements. Further theoretical investigation of the contact phenomena and the coupling between the boundaries of the element mesh and the material is necessary.

It is recommendable to explore possibilities to adapt the presented method in such a way that the convergence rate of the iterative

procedure increases. Also, attention must be given to improve the efficiency of the program.

IX References

1 Babuška I., Rheinboldt W.C. (1979)
Adaptive approaches and reliability estimations in finite element analysis. Computer methods in applied mechanics and engineering, Vol. 17/18, pp. 519-540.

2 Babuška I., Rheinboldt W.C. (1980)
Reliable error estimation and mesh adaptation for the finite element method. Computational methods in nonlinear mechanics (ed. J.T. Oden), North-Holland Publishing Company, pp. 67-108.

3 Bathe K.-J., Sussman T.D. (1983)
An algorithm for the construction of optimal finite element meshes in linear elasticity. Recent developments in computing methods for nonlinear solid and structure mechanics, ASME meeting, Houston, Ta., USA, june.

4 Belytschko T.B., Kennedy J.M. (1978)
Computer models for subassembly simulation. Nuclear engineering and design, Vol. 49, pp. 17-38.

5 Brekelmans W.A.M. (1982)
Over het integreren van de elasto-plastische constitutieve vergelijkingen voor een drie-dimensionale spanningstoestand bij Von Mises vloeicriterium, isotrope versteviging en geen beïnvloeding door de temperatuur. Personal notes.

6 Chiou S.-I., Wang C.-C. (1979)
Error estimates of finite element approximations for problems in linear elasticity; part 1: Problems in elastostatics. Archive for rational mechanics and analysis, Vol. 72, pp. 41-60.

7 Donea J. (1978)
Finite element analysis of transient dynamic fluid-structure interaction. Advanced structural dynamics (course), Commission of the European Communities joint research centre, Ispra, Italy, oktober.

8 Donea J., Giuliani S., Halleux J.P. (1982)
An Arbitrary Lagrangian-Eulerian finite element method for transient dynamic fluid-structure interactions. Computer methods in applied mechanics and engineering, Vol. 33, pp. 689-723.

9 Dwyer H.A., Kee R.J., Sanders B.R. (1980)
Adaptive grid method for problems in fluid mechanics and heat transfer. AIAA journal, Vol. 18, pp. 1205-1212.

10 Gelten C.J.M., De Jong J.E. (1981)
A method to redefine a finite element mesh and its application to metal forming and crack growth analysis. European conference on nonlinear finite element analysis, The Hague, The Netherlands, november.

11 Hirt C.W., Amsden A.A., Cook J.L. (1974)
An Arbitrary Lagrangian-Eulerian computing method for all flow speeds. Journal of computational physics, Vol. 14, pp. 227-253.

12 Huetink J. (1981)
Analysis of metal forming processes based on a combined Eulerian-Lagrangian finite element formulation. European conference on nonlinear finite element analysis, The Hague, The Netherlands, november.

13 Hughes T.J.R., Liu W.K., Zimmermann T.K. (1981)
Lagrangian-Eulerian finite element formulation for incompressible viscous flows. Computer methods in applied mechanics and engineering, Vol. 29, pp. 329-349.

14 Hutchinson J.W. (1973)
Finite strain analysis of elastic-plastic solids and structures. Numerical solution of nonlinear structural problems (ed. R.F. Hartung), ASME, N.Y., USA, Vol. 17, pp. 17-29.

15 Kennedy J.M., Belytschko T.B. (1981)
Theory and application of a finite element method for Arbitrary Lagrangian-Eulerian fluids and structures. Nuclear engineering and design, Vol. 68, pp. 129-146.

16 Krieg R.D., Krieg D.B. (1977)
Accuracies of numerical solution methods for the elastic-perfectly plastic model. Journal of pressure vessel technology, pp. 510-515.

17 Lai W.H., Rubin D., Krempl E. (1978)
Introduction to continuum mechanics. 4th. Edition (1979), Pergamon Press.

18 Melosh R.J., Marcal P.V. (1977)
An energy basis for mesh refinement of structural continua. International journal for numerical methods in engineering, Vol. 17, pp. 1083-1091.

19 Nagtegaal J.C., Parks D.H., Rice J.R. (1974)
On numerically accurate finite element solutions in the fully plastic range. Computer methods in applied mechanics and engineering, Vol. 4, pp. 153-177.

20 Nagtegaal J.C., De Jong J.E. (1980)
Some computational aspects of elastic-plastic large strain analysis. Computational methods in nonlinear mechanics (ed. J.T. Oden), North-Holland Publishing Company, pp. 303-339.

21 Nagtegaal J.C., Veldpaus F.E.
On the implementation of finite strain plasticity equations in a numerical model. To be published.

22 Pracht W.E. (1975)
Calculating three-dimensional fluid flows at all speeds with an Eulerian-Lagrangian computing mesh. Journal of computational physics, Vol. 17, pp. 132-159.

23 Roll K., Neitzert T. (1982)
On the application of different numerical methods to calculate cold forming processes. Numerical methods in industrial forming processes, Swansea, U.K., june.

24 Schoofs A.J.G., Van Beukering L.H.T.M., Sluiter M.L.C. (1979)
A general purpose two-dimensional mesh generator. Advances in engineering software, Vol. 1, pp. 131-136.

25 Stein L.R., Gentry R.A., Hirt C.W. (1977)
Computational simulation of transient blast loading on three-dimensional structures. Computer methods in applied mechanics and engineering, Vol. 11, pp. 57-74.

26 Turcke D.J., McNeice G.M. (1974)
Guidelines for selecting finite element grids based on an optimization study. Computers and structures, Vol. 4, pp. 499-519.

27 Zienkiewicz O.C. (1977)
The finite element method. 3rd. Edition (1977), McGraw Hill Book Company.

28 Zienkiewicz O.C., Kelly D.W., Gago J.P. de S., Babuška I. (1981)
Hierarchical finite element approaches, error estimates and adaptive refinement. The mathematics of finite elements and applications MAFELAP 1981, Brunel University.

29 Zienkiewicz O.C., Gago J.P. de S., Kelly D.W.
The hierarchical concept in finite element analysis. To be published.

Appendix 1: The iterative weighted residual equation for forming process and CRS determination process

The contribution of one element to the left- and right-hand side of (V.2.1), the discretised iterative weighted residual equation for the forming process, is - dropping the indices i and e -:

$$\vec{\underset{\sim}{w}}^T . \int_G (\underset{\sim}{\nabla}_g \underset{\sim}{\psi}^T)^T [d_g \vec{\underset{\sim}{\gamma}} . \underset{\sim}{\sigma} + \vec{\underset{\sim}{\gamma}} . d_g \underset{\sim}{\sigma} + \vec{\underset{\sim}{\gamma}} . \underset{\sim}{\sigma} \frac{d_g J}{J}] J \, dG - \vec{\underset{\sim}{w}}^T . \int_G \underset{\sim}{\psi} \vec{q} \frac{d_g J}{J} J \, dG$$

$$- \vec{\underset{\sim}{w}}^T . \int_{G^*} \underset{\sim}{\psi} \vec{t}^* \frac{d_g J^*}{J^*} J^* \, dG^* \quad ; \qquad \text{(A1.1a)}$$

$$\vec{\underset{\sim}{w}}^T . \int_G \underset{\sim}{\psi} \vec{q} J \, dG + \vec{\underset{\sim}{w}}^T . \int_{G^*} \underset{\sim}{\psi} \vec{t}^* J^* \, dG^* - \vec{\underset{\sim}{w}}^T . \int_G (\underset{\sim}{\nabla}_g \underset{\sim}{\psi}^T)^T \vec{\underset{\sim}{\gamma}} . \underset{\sim}{\sigma} J \, dG$$

$$\text{(A1.1b)}$$

The iterative changes $d_g \vec{\underset{\sim}{\gamma}}$, $d_g J$ and $d_g J^*$ can be written as

$$d_g \vec{\underset{\sim}{\gamma}} = - \vec{\underset{\sim}{\gamma}} . (\underset{\sim}{\nabla}_g d_g \vec{\chi})^T \vec{\underset{\sim}{\gamma}} \qquad \text{(A1.2)}$$

$$d_g J = J \vec{\underset{\sim}{\gamma}}^T . (\underset{\sim}{\nabla}_g d_g \vec{\chi}) \qquad \text{(A1.3)}$$

$$d_g J^* = J^* \vec{\underset{\sim}{\gamma}}^{*T} . (\underset{\sim}{\nabla}_g^* d_g \vec{\chi}) \qquad \text{(A1.4)}$$

On the analogy of (II.2.100), we can write for $d_g \underset{\sim}{\sigma}$

$$d_g \underset{\sim}{\sigma} = d_m \underset{\sim}{\sigma} + (d_g \vec{\chi} - d_m \vec{x}) . \vec{\underset{\sim}{\gamma}}^T (\underset{\sim}{\nabla}_g \underset{\sim}{\sigma}) \qquad \text{(A1.5)}$$

Using the fact that the fourth-order material tensor $^4\underset{\sim}{M}$ is right-symmetrical, the iterative constitutive equation (V.5.4) becomes

$$d_m \underset{\sim}{\sigma} = \frac{1}{2}(d_m \underset{\sim}{H} - d_m \underset{\sim}{H}^C) . \underset{\sim}{\sigma} + \underset{\sim}{\sigma} . \frac{1}{2}(d_m \underset{\sim}{H} - d_m \underset{\sim}{H}^C)^C + {}^4\underset{\sim}{M} : d_m \underset{\sim}{H}^C \quad ; \qquad \text{(A1.6)}$$

$$d_m \underset{\sim}{H} = (\underset{\sim}{\nabla}_m d_m \vec{x})^T \underset{\sim}{C} \qquad \text{(A1.7)}$$

Substituting (A1.2-7) in (A1.1) results in the following compact expressions for the left- and right-hand side, respectively:

$$A + B \quad ; \quad R_1 \tag{A1.8}$$

For A, B and R_1 we can write

$$A = A_1 + A_2 + A_3 + A_4 + A_5 + A_6 \tag{A1.9a}$$

$$B = B_1 + B_2 + B_3 + B_4 + B_5 \tag{A1.9b}$$

$$R_1 = R_{11} + R_{12} + R_{13} \tag{A1.9c}$$

The individual terms are given by

$$A_1 = \frac{1}{2} \int_G (\vec{v}\ \vec{w})^c : \{(\vec{v}\ d_m\vec{x})^c . \varpi\} \rfloor\ dG \tag{A1.10a}$$

$$A_2 = -\frac{1}{2} \int_G (\vec{v}\ \vec{w})^c : \{(\vec{v}\ d_m\vec{x}) . \varpi\} \rfloor\ dG \tag{A1.10b}$$

$$A_3 = \frac{1}{2} \int_G (\vec{v}\ \vec{w})^c : \{\varpi . (\vec{v}\ d_m\vec{x})\} \rfloor\ dG \tag{A1.10c}$$

$$A_4 = -\frac{1}{2} \int_G (\vec{v}\ \vec{w})^c : \{\varpi . (\vec{v}\ d_m\vec{x})^c\} \rfloor\ dG \tag{A1.10d}$$

$$A_5 = \int_G (\vec{v}\ \vec{w})^c : {}^4\mathbb{M} : (\vec{v}\ d_m\vec{x}) \rfloor\ dG \tag{A1.10e}$$

$$A_6 = -\int_G (\vec{v}\ \vec{w})^c : \{d_m\vec{x} . (\vec{v}\ \varpi)\} \rfloor\ dG \tag{A1.10f}$$

$$B_1 = -\int_G (\vec{v}\ \vec{w})^c : \{(\vec{v}\ d_g\vec{\chi})^c . \varpi\} \rfloor\ dG \tag{A1.10g}$$

$$B_2 = \int_G (\vec{v}\ \vec{w})^c : \{d_g\vec{\chi} . (\vec{v}\ \varpi)\} \rfloor\ dG \tag{A1.10h}$$

$$B_3 = \int_G (\vec{v}\ \vec{w})^c : \varpi\ (\vec{v} . d_g\vec{\chi}) \rfloor\ dG \tag{A1.10i}$$

$$B_4 = -\int_G \vec{w} . \vec{q}\ (\vec{v} . d_g\vec{\chi}) \rfloor\ dG \tag{A1.10j}$$

$$B_5 = -\int_{G^*} \vec{w} . \vec{t}^*\ (\vec{v}^* . d_g\vec{\chi}) \rfloor^*\ dG^* \tag{A1.10k}$$

$$R_{11} = \int_G \vec{w}.\vec{q}\ \jmath\ dG \qquad \text{(A1.10l)}$$

$$R_{12} = \int_{G^*} \vec{w}.\vec{t}^*\ \jmath^*\ dG^* \qquad \text{(A1.10m)}$$

$$R_{13} = -\int_G (\vec{v}\ \vec{w})^c : \bar{\sigma}\ \jmath\ dG \qquad \text{(A1.10n)}$$

Since all terms are linear, instead of (A1.8) we can write

$$\vec{w}.\bar{A}.d_m\vec{x} + \vec{w}.\bar{B}.d_g\vec{\chi} \quad ; \quad \vec{w}.\vec{R}_1 \qquad \text{(A1.11)}$$

or, with interpolation of $\vec{w}$, $d_m\vec{x}$ and $d_g\vec{\chi}$,

$$\underset{\sim}{\vec{w}}^T.\underline{\bar{A}}.d_{m\sim}\vec{x} + \underset{\sim}{\vec{w}}^T.\underline{\bar{B}}.d_{g\sim}\vec{\chi} \quad ; \quad \underset{\sim}{\vec{w}}^T.\underset{\sim}{\vec{R}}_1 \qquad \text{(A1.12)}$$

The contribution of one element to the left- and right-hand side of (V.2.9), the discretised iterative weighted residual equation for the CRS determination process is

$$\underset{\sim}{\vec{w}}^T.\int_G (\underset{\sim g}{\nabla}\underset{\sim}{\psi}^T)^T[d_{g\sim}\vec{\gamma}.\bar{\sigma}^f + \underset{\sim}{\vec{\gamma}}.d_g\bar{\sigma} + \underset{\sim}{\vec{\gamma}}.\bar{\sigma}^f\frac{d_g\jmath}{\jmath}]\jmath\ dG \quad ; \qquad \text{(A1.13a)}$$

$$-\underset{\sim}{\vec{w}}^T.\int_G (\underset{\sim g}{\nabla}\underset{\sim}{\psi}^T)^T\underset{\sim}{\vec{\gamma}}.\bar{\sigma}^f\ \jmath\ dG \qquad \text{(A1.13b)}$$

Using the fact that the fourth-order material tensor ${}^4\bar{C}$ is right-symmetrical, the iterative constitutive equation (V.5.9) becomes

$$d_g\bar{\sigma} = \tfrac{1}{2}(d_g\bar{H} - d_g\bar{H}^c).\bar{\sigma} + \bar{\sigma}.\tfrac{1}{2}(d_g\bar{H} - d_g\bar{H}^c)^c + {}^4\bar{C}:d_g\bar{H}^c \quad ; \qquad \text{(A1.14)}$$

$$d_g\bar{H} = (\underset{\sim g}{\nabla}d_g\vec{\chi})^T\underset{\sim}{\vec{\gamma}} \qquad \text{(A1.15)}$$

Substituting (A1.2), (A1.3), (A1.14) and (A1.15) in (A1.13) results in the following compact expressions for the left- and right-hand side, respectively:

$$V \quad ; \quad R_2 \qquad \text{(A1.16)}$$

For V we can write

$$V = V_1 + V_2 + V_3 + V_4 + V_5 + V_6 + V_7 \qquad \text{(A1.17)}$$

The individual terms are given by

$$V_1 = - \int_G (\vec{v}\,\vec{w})^C : \{(\vec{v}\, d_g\vec{\chi})^C . \bar{\varpi}\}\, dG \qquad \text{(A1.18a)}$$

$$V_2 = \frac{1}{2} \int_G (\vec{v}\,\vec{w})^C : \{(\vec{v}\, d_g\vec{\chi})^C . \bar{\varpi}\}\, dG \qquad \text{(A1.18b)}$$

$$V_3 = - \frac{1}{2} \int_G (\vec{v}\,\vec{w})^C : \{(\vec{v}\, d_g\vec{\chi}) . \bar{\varpi}\}\, dG \qquad \text{(A1.18c)}$$

$$V_4 = \frac{1}{2} \int_G (\vec{v}\,\vec{w})^C : \{\bar{\varpi} . (\vec{v}\, d_g\vec{\chi})\}\, dG \qquad \text{(A1.18d)}$$

$$V_5 = - \frac{1}{2} \int_G (\vec{v}\,\vec{w})^C : \{\bar{\varpi} . (\vec{v}\, d_g\vec{\chi})^C\}\, dG \qquad \text{(A1.18e)}$$

$$V_6 = \int_G (\vec{v}\,\vec{w})^C : {}^4\bar{\mathbb{C}} : (\vec{v}\, d_g\vec{\chi})\, dG \qquad \text{(A1.18f)}$$

$$V_7 = \int_G (\vec{v}\,\vec{w})^C : \bar{\varpi}\, (\vec{v} . d_g\vec{\chi})\, dG \qquad \text{(A1.18g)}$$

$$R_2 = - \int_G (\vec{v}\,\vec{w})^C : \bar{\varpi}\, dG \qquad \text{(A1.18h)}$$

As all terms are linear in $\vec{w}$ and $d_g\vec{\chi}$, instead of (A1.16) we can write

$$\vec{w} . \mathbf{V} . d_g\vec{\chi} \quad ; \quad \vec{w} . \vec{R}_2 \qquad \text{(A1.19)}$$

or, with interpolation of $\vec{w}$ and $d_g\vec{\chi}$,

$$\underset{\sim}{\vec{w}}^T . \underline{\mathbf{V}} . d_g\underset{\sim}{\vec{\chi}} \quad ; \quad \underset{\sim}{\vec{w}}^T . \underset{\sim}{\vec{R}}_2 \qquad \text{(A1.20)}$$

Appendix 2: An iterative constitutive equation for time-independent elasto-plastic material behaviour

The derivation of the constitutive equation starts from the relationship between the Cauchy stress tensor $\boldsymbol{\sigma}$ and the co-rotational Cauchy stress tensor $\hat{\boldsymbol{\sigma}}$, that is

$$\boldsymbol{\sigma} = \mathbf{R}.\hat{\boldsymbol{\sigma}}.\mathbf{R}^{c} \tag{A2.1}$$

where $\mathbf{R}$ is the rotation tensor in the polar decomposition of the deformation tensor $\mathbf{F}$. It is easily shown that the linearised expression for the iterative MRS change of $\boldsymbol{\sigma}$ is given by

$$d_m\boldsymbol{\sigma} = d_m\mathbf{R}.\mathbf{R}^{ic}.\boldsymbol{\sigma}^{i} + \boldsymbol{\sigma}^{i}.\mathbf{R}^{i}.d_m\mathbf{R}^{c} + \mathbf{R}^{i}.d_m\hat{\boldsymbol{\sigma}}.\mathbf{R}^{ic} \tag{A2.2}$$

From the definition (II.2.44) of the Green-Lagrange strain tensor and the definition (II.2.43) of the polar decomposition of the deformation tensor $\mathbf{F}$, it follows that

$$\mathbf{R} = \mathbf{F}.(\mathbf{I} + 2\mathbf{E})^{-\frac{1}{2}} \tag{A2.3}$$

Using the Cayley-Hamilton theorem it is shown in appendix 3 that

$$(\mathbf{I} + 2\mathbf{E})^{-\frac{1}{2}} = c_2\mathbf{E}.\mathbf{E} + c_1\mathbf{E} + c_0\mathbf{I} \tag{A2.4}$$

where the scalar quantities c_0, c_1 and c_2 will depend on the invariants of $\mathbf{E}$. Now it is assumed that $\mathbf{E}$ is small compared to the unit tensor $\mathbf{I}$

$$||\mathbf{E}|| \ll 1 \tag{A2.5}$$

In that case we can write

$$(\mathbf{I} + 2\mathbf{E})^{-\frac{1}{2}} \approx \mathbf{I} - \mathbf{E} = \frac{3}{2}\mathbf{I} - \frac{1}{2}\mathbf{F}^{c}.\mathbf{F} \tag{A2.6}$$

and thus for $\mathbb{R}$

$$\mathbb{R} = \frac{3}{2}\,\mathbb{F} - \frac{1}{2}\,\mathbb{F}.\mathbb{F}^{C}.\mathbb{F} \tag{A2.7}$$

Some simple manipulation results in

$$d_m\mathbb{R}.\mathbb{R}^{iC} = \frac{1}{2}(d_m\mathbb{H} - d_m\mathbb{H}^{C}) \quad ; \quad d_m\mathbb{H} = d_m\mathbb{F}.(\mathbb{F}^{i})^{-1} \tag{A2.8}$$

In section V.4 for $\hat{\boldsymbol{\sigma}}$ in state τ the following expression has been derived

$$\hat{\boldsymbol{\sigma}} = \kappa\,\hat{\boldsymbol{\sigma}}_n + \frac{1}{3}\,\mathrm{tr}(\boldsymbol{\sigma}(\tau_o))\,\mathbb{I} + K\,\mathrm{tr}(\hat{\mathbb{C}})\,\mathbb{I} \tag{A2.9}$$

Hence

$$d_m\hat{\boldsymbol{\sigma}} = d_m\kappa\,\hat{\boldsymbol{\sigma}}^{i}_n + \kappa^{i} d_m\hat{\boldsymbol{\sigma}}_n + K\,\mathrm{tr}(d_m\hat{\mathbb{C}})\,\mathbb{I} \tag{A2.10}$$

From the definition (V.4.19) of the scalar quantity κ we find

$$\kappa = \frac{\sigma_v}{\hat{\sigma}_n} \quad ; \quad \hat{\sigma}_n = \sqrt{\frac{3}{2}\,\hat{\boldsymbol{\sigma}}_n : \hat{\boldsymbol{\sigma}}_n}\ , \tag{A2.11}$$

it follows after linearisation that

$$d_m\kappa = \frac{\sigma^{i}_v}{\hat{\sigma}^{i}_n}\left(\frac{d_m\sigma_v}{\sigma^{i}_v} - \frac{d_m\hat{\sigma}_n}{\hat{\sigma}^{i}_n}\right) \tag{A2.12}$$

Using (V.4.6) the MRS change of the current yield stress σ_v is given by

$$\dot{\sigma}_v = \frac{h\hat{\boldsymbol{\sigma}}^{d}}{(1 + \frac{h}{3G})\sigma_v} : \hat{\mathbb{D}} \tag{A2.13}$$

and from this, for the first term on the right-hand side of (A2.12), we arrive at

$$d_m\sigma_v = \frac{h^i \hat{\sigma}^i d}{(1 + \frac{h^i}{3G})\sigma_v^i} : d_m\hat{\mathbb{C}} = \frac{h^i \hat{\sigma}_n^i}{(1 + \frac{h^i}{3G})\hat{\sigma}_n^i} : d_m\hat{\mathbb{C}} \qquad \text{(A2.14)}$$

For the second term on the right-hand side of (A2.12) we note that from the definition (V.4.17) of $\hat{\sigma}_n$, it follows that

$$\dot{\hat{\sigma}}_n = 2G\,\hat{\mathbb{D}}^d \qquad \text{(A2.15)}$$

and therefore the MRS change of $\hat{\sigma}_n$ becomes

$$d_m\dot{\hat{\sigma}}_n = 2G\, d_m\hat{\mathbb{C}}^d \qquad \text{(A2.16)}$$

With the definition (A2.11) of $\hat{\sigma}_n$ and (A2.15) it is seen that

$$\dot{\hat{\sigma}}_n = \frac{3G\hat{\sigma}_n}{\hat{\sigma}_n} : \hat{\mathbb{D}}^d \qquad \text{(A2.17)}$$

From this we arrive at

$$d_m\dot{\hat{\sigma}}_n = \frac{3G\hat{\sigma}_n^i}{\hat{\sigma}_n^i} : d_m\hat{\mathbb{C}}^d \qquad \text{(A2.18)}$$

Substituting (A2.14) and (A2.18) in (A2.12) results in

$$d_m\dot{\kappa} = \frac{h^i \hat{\sigma}_n^i}{(1 + \frac{h^i}{3G})\hat{\sigma}_n^{i2}} : d_m\hat{\mathbb{C}} - \frac{\sigma_v^i}{\hat{\sigma}_n^i}\frac{3G\hat{\sigma}_n^i}{\hat{\sigma}_n^{i2}} : d_m\hat{\mathbb{C}}^d \qquad \text{(A2.19)}$$

and, using (A2.10) leaves us with

$$d_m\hat{\sigma} = \frac{h^i \hat{\sigma}^i_n \hat{\sigma}^i_n}{(1 + \frac{h^i}{3G})\hat{\sigma}^{i2}_n} : d_m\hat{\mathbb{C}} + \frac{\sigma^i_v}{\hat{\sigma}^i_n} 2G(\mathbb{I}^4 - \frac{3}{2}\frac{\hat{\sigma}^i_n \hat{\sigma}^i_n}{\hat{\sigma}^{i2}_n}) : d_m\hat{\mathbb{C}}^d$$

$$+ K\, \mathbb{I}\,\mathbb{I} : d_m\hat{\mathbb{C}} \qquad \text{(A2.20)}$$

Replacing $d_m\hat{\mathbb{C}}^d$ by $d_m\hat{\mathbb{C}} - \frac{1}{3}\,\mathrm{tr}(d_m\hat{\mathbb{C}})\mathbb{I}$, we finally arrive at

$$d_m\hat{\sigma} = {}^4\hat{\mathbb{M}}^i : d_m\hat{\mathbb{C}} \qquad \text{(A2.21)}$$

where the fourth-order tensor ${}^4\hat{\mathbb{M}}^i$ is defined by

$${}^4\hat{\mathbb{M}}^i = K\,\mathbb{I}\,\mathbb{I} + 2\hat{\tilde{G}}({}^4\mathbb{I} - \frac{1}{3}\,\mathbb{I}\,\mathbb{I} - \frac{3}{2}\hat{\tilde{\mu}}\frac{\hat{\sigma}^i_n \hat{\sigma}^i_n}{\hat{\sigma}^{i2}_n}) \qquad \text{(A2.22)}$$

with the quantities $\hat{\tilde{G}}$ and $\hat{\tilde{\mu}}$ as

$$\hat{\tilde{G}} = G\frac{\sigma^i_v}{\hat{\sigma}^i_n} \quad ; \quad \hat{\tilde{\mu}} = 1 - \frac{h^i \hat{\sigma}^i_n}{3G(1 + \frac{h^i}{3G})\sigma^i_v} \qquad \text{(A2.23)}$$

The last term to be considered is the MRS change of the logarithmic strain tensor $\hat{\mathbb{C}}$, defined by

$$\hat{\mathbb{C}} = \frac{1}{2}\ln(\mathbb{I} + 2\mathbb{E}) \qquad \text{(A2.24)}$$

In appendix 3 it is shown that

$$\hat{\mathbb{C}} = b_2\mathbb{E}.\mathbb{E} + b_1\mathbb{E} + b_0\mathbb{I} \qquad \text{(A2.25)}$$

Assuming $||\mathbb{E}|| \ll 1$ we find

$$\hat{\mathbb{C}} \approx \mathbb{E} \qquad \text{(A2.26)}$$

Therefore, $d_m\hat{\mathbb{C}} = d_m\mathbb{E}$, that is

$$d_m\hat{\mathbb{C}} = \frac{1}{2}(\mathbb{F}^{ic}.d_m\mathbb{F} + d_m\mathbb{F}^c.\mathbb{F}^i) \tag{A2.27}$$

and, because $\mathbb{F}^i \approx \mathbb{R}^i$ if $||\mathbb{E}|| \ll 1$, also

$$d_m\hat{\mathbb{C}} = \frac{1}{2}\,\mathbb{R}^{ic}.(d_m\mathbb{H} + d_m\mathbb{H}^c).\mathbb{R}^i \tag{A2.28}$$

Substituting (A2.28) in (A2.21) we find

$$d_m\hat{\boldsymbol{\sigma}} = \frac{1}{2}\,{}^4\hat{\mathbb{M}}^i:\{\mathbb{R}^{ic}.(d_m\mathbb{H} + d_m\mathbb{H}^c).\mathbb{R}^i\} \tag{A2.29}$$

Premultiplying by $\mathbb{R}^i$ and postmultiplying by $\mathbb{R}^{ic}$ gives

$$\begin{aligned}\mathbb{R}^i.d_m\hat{\boldsymbol{\sigma}}.\mathbb{R}^{ic} &= \frac{1}{2}\,\mathbb{R}^i.{}^4\hat{\mathbb{M}}^i:\{\mathbb{R}^{ic}.(d_m\mathbb{H} + d_m\mathbb{H}^c).\mathbb{R}^i\}.\mathbb{R}^{ic} \\ &= {}^4\mathbb{M}^i:\frac{1}{2}(d_m\mathbb{H} + d_m\mathbb{H}^c)\end{aligned} \tag{A2.30}$$

where ${}^4\mathbb{M}^i$ is defined by

$${}^4\mathbb{M}^i = K\,\mathbb{I}\,\mathbb{I} + 2G^*\left({}^4\mathbb{I} - \frac{1}{3}\,\mathbb{I}\,\mathbb{I} - \frac{3}{2}\,\mu^*\,\frac{\boldsymbol{\sigma}^i_n\boldsymbol{\sigma}^i_n}{\sigma^{i2}_n}\right) \tag{A2.31}$$

Substituting (A2.8) and (A2.30) in (A2.2) finally results in the desired iterative constitutive equation

$$\begin{aligned}d_m\boldsymbol{\sigma} = {} & \frac{1}{2}(d_m\mathbb{H} - d_m\mathbb{H}^c).\boldsymbol{\sigma}^i + \boldsymbol{\sigma}^i.\frac{1}{2}(d_m\mathbb{H} - d_m\mathbb{H}^c)^c \\ & + {}^4\mathbb{M}^i:\frac{1}{2}(d_m\mathbb{H} + d_m\mathbb{H}^c)\end{aligned} \tag{A2.32}$$

Appendix 3: Functions of a tensor

In some cases the value of the function f(𝔸), where 𝔸 is a second-order tensor, can be determined fairly easily by employing the Cayley-Hamilton theorem

$$\mathbb{A}^3 = J_1\mathbb{A}^2 - J_2\mathbb{A} + J_3\mathbb{I} \tag{A3.1}$$

Here, J_1, J_2 and J_3 are the invariants of 𝔸, defined by

$$J_1 = \mathrm{tr}(\mathbb{A}) \; ; \quad J_2 = \tfrac{1}{2}[J_1^2 - \mathrm{tr}(\mathbb{A}^2)] \; ; \quad J_3 = \det(\mathbb{A}) \tag{A3.2}$$

Repeated use of (A3.1) results in

$$\mathbb{A}^n = \alpha_n\mathbb{A}^2 + \beta_n\mathbb{A} + \gamma_n\mathbb{I} \tag{A3.3}$$

where the coefficients α_n, β_n and γ_n are given by

$$\begin{aligned}
&\alpha_0 = 0 \quad \beta_0 = 0 \quad \gamma_0 = 1\\
&\alpha_1 = 0 \quad \beta_1 = 1 \quad \gamma_1 = 0\\
&\alpha_2 = 1 \quad \beta_2 = 0 \quad \gamma_2 = 0\\
&\alpha_3 = J_1 \quad \beta_3 = -J_2 \quad \gamma_3 = J_3\\
&\text{----------}\\
&\alpha_n = \alpha_{n-1}J_1 - \alpha_{n-2}J_2 + \alpha_{n-3}J_3\\
&\beta_n = -\alpha_{n-1}J_2 + \alpha_{n-2}J_3\\
&\gamma_n = \alpha_{n-1}J_3
\end{aligned} \tag{A3.4}$$

If 𝔸 is symmetrical, we can determine the coefficients a_0, a_1 and a_2 in such a way that, for f(𝔸), the expression

$$f(\mathbb{A}) = a_2\mathbb{A}^2 + a_1\mathbb{A} + a_0\mathbb{I} \tag{A3.5}$$

applies. On account of its symmetry, 𝔸 can be written as

$$\mathbb{A} = \sum_{i=1}^{3} A_i\vec{n}_i\vec{n}_i \tag{A3.6}$$

where A_i (i = 1,2,3) are the eigenvalues of $\mathbb{A}$ and $\vec{n}_i$ the normalized eigenvectors pertaining to them. For $f(\mathbb{A})$ we can write

$$f(\mathbb{A}) = \sum_{i=1}^{3} f(A_i)\vec{n}_i\vec{n}_i = a_2 \sum_{i=1}^{3} A_i^2\vec{n}_i\vec{n}_i + a_1 \sum_{i=1}^{3} A_i\vec{n}_i\vec{n}_i$$

$$+ a_0 \sum_{i=1}^{3} \vec{n}_i\vec{n}_i \qquad \text{(A3.7)}$$

Writing out the summations, we have

$$(a_0 + a_1A_1 + a_2A_1^2 - f(A_1))\vec{n}_1\vec{n}_1 +$$

$$(a_0 + a_1A_2 + a_2A_2^2 - f(A_2))\vec{n}_2\vec{n}_2 +$$

$$(a_0 + a_1A_3 + a_2A_3^2 - f(A_3))\vec{n}_3\vec{n}_3 = 0 \qquad \text{(A3.8)}$$

Hence, a_0, a_1 and a_2 must satisfy the next system of equations

$$\begin{bmatrix} 1 & A_1 & A_1^2 \\ 1 & A_2 & A_2^2 \\ 1 & A_3 & A_3^2 \end{bmatrix} \begin{bmatrix} a_0 \\ a_1 \\ a_2 \end{bmatrix} = \begin{bmatrix} f(A_1) \\ f(A_2) \\ f(A_3) \end{bmatrix} = \begin{bmatrix} r_1 \\ r_2 \\ r_3 \end{bmatrix} \qquad \text{(A3.9)}$$

Depending on the function $f(\mathbb{A})$ it may be possible to determine a_0, a_1 and a_2 in such a way that (A3.9) is satisfied, even if two or more eigenvalues of $\mathbb{A}$ have the same value. If, for instance, $f(\mathbb{A}) = \mathbb{A}^{-\frac{1}{2}}$, simple, but rather wearisome calculations result in

$$a_0 = \frac{r_1^3(r_2+r_3) + r_2^3(r_3+r_1) + r_3^3(r_1+r_2) + (r_1r_2 + r_2r_3 + r_3r_1)^2}{(r_1+r_2)(r_2+r_3)(r_3+r_1)}$$

(A3.10a)

$$a_1 = \frac{-(r_1^2r_2^2 + r_2^2r_3^2 + r_3^2r_1^2)(r_1r_2 + r_2r_3 + r_3r_1) - r_1^2r_2^2r_3^2}{(r_1+r_2)(r_2+r_3)(r_3+r_1)} \qquad \text{(A3.10b)}$$

$$a_2 = \frac{(r_1r_2 + r_2r_3 + r_3r_1)r_1^2r_2^2r_3^2}{(r_1+r_2)(r_2+r_3)(r_3+r_1)} \qquad \text{(A3.10c)}$$

It is easily shown that

$$(\mathbb{I} + 2\mathbb{E})^{-\frac{1}{2}} = c_2\mathbb{E}^2 + c_1\mathbb{E} + c_0\mathbb{I} \quad ; \qquad \text{(A3.11a)}$$

$$c_2 = 4a_2 \quad ; \quad c_1 = 2a_1 + 4a_2 \quad ; \quad c_0 = a_0 + a_1 + a_2 \qquad \text{(A3.11b)}$$

If $\mathbb{A}$ is not symmetrical or if a general valid solution for (A3.9) cannot be determined, the following method for calculating $f(\mathbb{A})$ can be used, if $f(\mathbb{A})$ is the sum of an infinite, convergent series, that is, if

$$f(\mathbb{A}) = \sum_{n=0}^{\infty} s_n\mathbb{A}^n \qquad \text{(A3.12)}$$

Using (A3.3) this results in

$$f(\mathbb{A}) = b_2\mathbb{A}^2 + b_1\mathbb{A} + b_0\mathbb{A} \qquad \text{(A3.13)}$$

where, on account of (A3.4) the coefficients b_0, b_1 and b_2 are given by

$$b_0 = s_0 + \sum_{n=3}^{\infty} s_n\gamma_n \qquad \text{(A3.14a)}$$

$$b_1 = s_1 + \sum_{n=3}^{\infty} s_n\beta_n \qquad \text{(A3.14b)}$$

$$b_2 = s_2 + \sum_{n=3}^{\infty} s_n\alpha_n \qquad \text{(A3.14c)}$$

In practice we take into account a finite though sufficient number of terms of the summation in (A3.14).

If $||2\mathbb{E}|| < 1$, we can write

$$\frac{1}{2}\ln(\mathbb{I} + 2\mathbb{E}) = \mathbb{E} - \mathbb{E}^2 + \frac{4}{3}\mathbb{E}^3 - 2\mathbb{E}^4 + \frac{16}{5}\mathbb{E}^5 - \frac{16}{3}\mathbb{E}^6 + \ldots$$

$$= \mathbb{E} - \mathbb{E}^2 + \sum_{n=3}^{\infty} (-1)^{n-1} \frac{2^{n-1}}{n} \mathbb{E}^n$$

$$= b_2\mathbb{E}^2 + b_1\mathbb{E} + b_0\mathbb{I} \qquad \text{(A3.15)}$$

where b_0, b_1 and b_2 are determined according to (A3.14), using

$$s_0 = 0 \quad ; \; s_1 = 1 \quad ; \quad s_2 = -1 \; ; \quad s_n = (-1)^{n-1} \frac{2^{n-1}}{n} \qquad \text{(A3.16)}$$

Samenvatting

De eindige elementen methode wordt veelvuldig toegepast voor de numerieke simulatie van omvormprocessen met het doel om voorspellingen te doen over de kwaliteit van het eindprodukt en de belasting op het gereedschap. Het wiskundig model dat aan de simulatie ten grondslag ligt, werd tot voor kort geformuleerd, gebruikmakend van ofwel de Euler ofwel de Lagrange beschrijvingswijze. De gevolgen hiervan zijn dat sommige numerieke simulaties moeizaam verlopen of zelfs onmogelijk zijn. Dit is niet het geval bij gebruik van de Arbitraire-Euler-Lagrange (AEL) beschrijvingswijze. In dit proefschrift wordt de theoretische achtergrond van deze beschrijvingswijze beschreven. Zij wordt toegepast bij enkele numerieke simulaties.

Ten grondslag aan de AEL beschrijvingswijze ligt het gebruik van een referentiesysteem dat niet gekoppeld is aan de om te vormen materie (Lagrange beschrijvingswijze) en ook geen vaste ruimtelijke positie inneemt (Euler beschrijvingswijze). De relevante grootheden worden opgevat als functie van de coördinaten die in dit referentiesysteem gedefinieerd zijn. Deze grootheden worden besproken en het wiskundig model wordt geformuleerd, waarbij gebruik wordt gemaakt van de methode der gewogen residuen.

Om het wiskundig model voor numerieke simulatie geschikt te maken, wordt het gediscretiseerd, zowel wat betreft het verloop van het proces (de incrementele methode) als wat betreft het referentiesysteem (de elementen methode). Een speciale werkwijze wordt toegepast om materiegebonden grootheden te bepalen.

De momentane positie van het referentiesysteem, m.a.w. de momentane positie en geometrie van de elementen, wordt opgevat als zijnde het resultaat van de vervorming van een fictief materiaal dat met het referentiesysteem verbonden wordt gedacht. De belasting die deze vervorming veroorzaakt en de bijbehorende kinematische randvoorwaarden worden zodanig bepaald dat voldaan wordt aan bepaalde wensen met betrekking tot de geometrie van de elementen en zodanig dat bepaalde randvoorwaarden eenvoudig in rekening kunnen worden

gebracht. De vervorming van reëel en fictief materiaal vindt gelijktijdig plaats.

Het gediscretiseerd wiskundig model bestaat uit een stelsel niet-lineaire algebraïsche vergelijkingen. De onbekende grootheden worden bepaald volgens een iteratieve methode. Daarbij wordt een aantal benaderingen van de uiteindelijke oplossing bepaald door herhaald oplossen van de gelineariseerde versie van bovengenoemd stelsel.

De AEL beschrijvingswijze is met succes toegepast voor de simulatie van enkele axi-symmetrische omvormprocessen.

Nawoord

Het in dit proefschrift beschreven onderzoek is van februari 1979 tot augustus 1983 uitgevoerd binnen de vakgroep Fundamentele Werktuigbouwkunde (voorheen Technische Mechanica) van de Technische Hogeschool Eindhoven.

De initiator van het onderzoek was Joop Nagtegaal. In de beginfase had ik in hem een enthousiast en deskundig begeleider. Toen Joop de TH verliet, werd zijn begeleidende taak overgenomen door Frans Veldpaus en Marcel Brekelmans. De vanzelfsprekendheid waarmee en de manier waarop dit gebeurde verdient bewondering. Het resultaat van de vele gesprekken die we samen gevoerd hebben is in het proefschrift aanwijsbaar aanwezig in de vorm van ideeën en formuleringen. Bij veel van deze besprekingen was de regulerende invloed van Jan Janssen van groot belang.

Van groot nut is het afstudeerwerk van Martien Hulsen geweest. Hij paste de AEL beschrijvingswijze toe voor de simulatie van hyperelastische vervormingsprocessen.

Het proefschrift is getypt door Lia Neervoort en Els Scheepens. Vooral Els heeft bereidwillig vele uren doorgebracht achter de terminal van het tekstverwerkingsysteem om op zeer accurate wijze de vele wijzigingen in de tekst aan te brengen. Marcel Brekelmans heeft het uiteindelijke manuscript grondig bekeken, hetgeen nog een aantal verbeteringen tot gevolg had.

Bovengenoemde personen wil ik hartelijk bedanken voor de bijdrage aan het onderzoek en de totstandkoming van het proefschrift en vooral ook voor de plezierige wijze waarop de samenwerking plaatsvond.

Behalve de hierboven met name genoemde personen, wil ik alle leden van de vakgroep Fundamentele Werktuigbouwkunde bedanken voor de prettige contacten. Mede als gevolg hiervan heb ik binnen deze vakgroep een aantal jaren fijn gewerkt

Eindhoven, augustus 1983

Piet Schreurs

STELLINGEN

behorende bij het proefschrift

NUMERICAL SIMULATION OF FORMING PROCESSES

1. De in dit proefschrift beschreven Arbitraire-Euler-Lagrange formulering is een geschikt uitgangspunt om bij gebruik van de eindige elementen methode (automatisch) de elementverdeling te optimaliseren en om zowel materiegebonden als niet-materiegebonden randvoorwaarden eenvoudig in rekening te brengen.

   Hoofdstuk VII van dit proefschrift.

2. Bij simulatie van omvormprocessen met behulp van de eindige elementen methode is optimaliseren van de elementverdeling in veel gevallen alleen goed mogelijk als het aantal elementen tijdens de simulatie kan worden veranderd.

3. De in dit proefschrift beschreven methode voor de berekening van materiegebonden grootheden in een niet-materiegebonden element-verdeling leidt, in vergelijking met de gebruikelijke werkwijze bij de Lagrange formulering, in het algemeen tot een lagere convergentiesnelheid.

   Hoofdstuk VII van dit proefschrift.

4. Voor de simulatie van vloeistofstromingsprocessen met behulp van de eindige elementen methode is de beschrijving van het proces in termen van stroomsnelheid en (eventueel) hydrostatische druk te prefereren boven de beschrijving in termen van stroomfunctie en wervelsterkte.

5. Bij de beschrijving van de stroming van incompressibele vloeistoffen in termen van stroomsnelheid en hydrostatische druk blijkt de Lagrange multiplicator, waarmee de incompressibiliteitseis meestal in rekening wordt gebracht, geïdentificeerd te kunnen worden met de hydrostatische druk. Dit impliceert dat, als bij toepassing van de elementen methode de druk in een knooppunt wordt voorgeschreven, lokaal niet meer kan worden voldaan aan de continuïteitsvergelijking.

   Gresho P.M., Lee R.L., Sani R.L.: *On the time-dependent solution of the incompressible Newton-Stokes equations in two and three dimensions.* Recent advances in numerical methods in fluids (ed. C. Taylor and K. Morgan), Pineridge Press Ltd., Swansea, U.K., pp. 27-79, 1980.

6. Roll en Neitzert negeren de mogelijkheid om de eindige elementen methode af te leiden met behulp van de methode der gewogen residuën.

   Roll K., Neitzert T.: *On the application of different numerical methods to calculate cold forming processes.* Numerical methods in industrial forming processes, Swansea, U.K., juni 1982.

7. Het begrip initiële rek is fysisch niet zinvol. Gebruik van dit begrip is verwarrend en moet vermeden worden.

8. De uit militaire kringen voortkomende, ongegronde verdachtmakingen aan het adres van de vredesbeweging vormen de beste propaganda die deze beweging zich wensen kan.

9. Het toenemend aanbod van voedingsmiddelen in voordeelverpakking zal de noodzakelijke gevarieerdheid in de voeding verminderen.

10. Door automatisering gaat werk naar de knoppen.

Eindhoven, 12 september 1983 Piet Schreurs